4

AD-A218 742

RD&E CENTER

Technical Report

No. 13394

AN INVESTIGATION OF CONVECTION COOLING OF SMALL GAS TURBINE BLADES USING INTERMITTENT COOLING AIR

AUGUST 1988

By Richard E. McClelland
U.S. Army Tank-Automotive Command
ATTN: AMSTA-RG
Warren, MI 48397-5000

APPROVED FOR PUBLIC RELEASE:
DISTRIBUTION IS UNLIMITED

U.S. ARMY TANK-AUTOMOTIVE COMMAND
RESEARCH, DEVELOPMENT & ENGINEERING CENTER
Warren, Michigan 48397-5000

NOTICES

This report is not to be construed as an official Department of the Army position.

Mention of any trade names or manufacturers in this report shall not be construed as an official endorsement or approval of such products or companies by the U.S. Government.

Destroy this report when it is no longer needed. Do not return it to the originator.

REPORT DOCUMENTATION PAGE

Form Approved
OMB No 0704-0188
Exp Date Jun 30 1986

1a REPORT SECURITY CLASSIFICATION UNCLASSIFIED	1b RESTRICTIVE MARKINGS NONE
2a SECURITY CLASSIFICATION AUTHORITY	3 DISTRIBUTION / AVAILABILITY OF REPORT Unclassified/Unlimited
2b DECLASSIFICATION / DOWNGRADING SCHEDULE	
4 PERFORMING ORGANIZATION REPORT NUMBER(S)	5 MONITORING ORGANIZATION REPORT NUMBER(S) 13394
6a NAME OF PERFORMING ORGANIZATION U.S. Army Tank-Automotive Command 6b OFFICE SYMBOL (If applicable) AMSTA-RG	7a NAME OF MONITORING ORGANIZATION
6c. ADDRESS (City, State, and ZIP Code) Warren, MI 48397-5000	7b ADDRESS (City, State, and ZIP Code)
8a. NAME OF FUNDING / SPONSORING ORGANIZATION U.S. Army Tank-Automotive Command 8b. OFFICE SYMBOL (If applicable) AMSTA-RG	9. PROCUREMENT INSTRUMENT IDENTIFICATION NUMBER N/A
8c. ADDRESS (City, State, and ZIP Code) Warren, MI 48397-5000	10 SOURCE OF FUNDING NUMBERS PROGRAM ELEMENT NO. 61101A PROJECT NO A91A TASK NO WORK UNIT ACCESSION NO DA300107

11 TITLE (Include Security Classification)
(U) An Investigation of Convection Cooling of Small Gas Turbine Blades Using Intermittent Cooling Air

12 PERSONAL AUTHOR(S)
Dr. Richard E. McClelland

13a TYPE OF REPORT	13b TIME COVERED	14 DATE OF REPORT (Year, Month, Day)	15 PAGE COUNT
Final	FROM Aug 83 TO Aug 88	1988, August 29	147

16 SUPPLEMENTARY NOTATION

17 COSATI CODES			18. SUBJECT TERMS (Continue on reverse if necessary and identify by block number)
FIELD	GROUP	SUB-GROUP	Heat Transfer; Gas Turbines; Turbines; Turbine Blades; Intermittent Flow

19. ABSTRACT (Continue on reverse if necessary and identify by block number)

This paper demonstrates that a pulsed or intermittent flow has the potential to substantially increase the convective heat transfer coefficient. The application to convection cooling of gas turbine blades and vanes is demonstrated in a test facility designed to simulate the first-stage turbine blade of the AGT 1500 gas turbine engine which powers the Army's M1 Abrams Main Battle Tank.

A cylindrical test section is convectively cooled while the flow is interrupted by a rotating chopper in the range 0 to 720 Hz. Heat transfer is measured as a function of the frequency of the disturbance.

The data shows an increase in heat transfer as high as thirty percent over the steady-flow case when air flow is held constant. The change in heat transfer increases with increasing frequency. The magnitude of change increases and decreases due to harmonics in the system.

20 DISTRIBUTION / AVAILABILITY OF ABSTRACT ☒ UNCLASSIFIED/UNLIMITED ☐ SAME AS RPT ☐ DTIC USERS	21 ABSTRACT SECURITY CLASSIFICATION UNCLASSIFIED
22a NAME OF RESPONSIBLE INDIVIDUAL Dr. Richard E. McClelland	22b TELEPHONE (Include Area Code) (313) 574-6411 22c OFFICE SYMBOL AMSTA-RG

DD FORM 1473, 84 MAR — 83 APR edition may be used until exhausted. All other editions are obsolete

PREFACE

The author wishes to express his appreciation to Dr. Richard W. Munt and the U.S. Army Tank Automotive Command for sponsorship and the support of the engineering and technical staff and facilities; to the faculty of the University of Detroit, Department of Mechanical Engineering, Dr. Juinn P. Chiou, Dr. Eugene S. Kordyban, Dr. Yogendra S. Chadda (Chairman); and, to Dr. Robert A. Piccirelli of the Department of Mechanical Engineering, Wayne State University.

TABLE OF CONTENTS

LIST OF ILLUSTRATIONS

LIST OF TABLES

1.0. INTRODUCTION

This work was conducted at the U.S. Army Tank Automotive Command, Propulsion Systems Division. The objective of the research is to demonstrate that a pulsed or intermittant flow has the potential to increase the convective heat transfer coefficient to the extent that a practical engineering application may result. In particular, the application to convective cooling of gas turbine blades and vanes is demonstrated in a test facility designed to simulate the first-stage turbine blade of the AGT-1500 gas turbine engine which powers the Army's Ml Abrams Main Battle Tank.

The use of higher turbine inlet temperatures in advanced gas turbines for higher engine efficiency has necessitated increasingly sophisticated cooling schemes for turbine blades and vanes. The general method of cooling is to direct relatively cool air, bled from the compressor, through the turbine blades and vanes. The cooling air is then injected into the primary gas stream. Increased cooling flow will reduce metal temperatures at primary gas flow temperatures well in excess of typical present day engine temperatures. It is not practical, however, because the cost in overall engine efficiency due to the increased compressor bleed exceeds the increase in overall efficiency due to the higher operating temperature.

Cooling schemes include convection as shown in Figure 1-1, film as shown in Figure 1-2, impingement as shown in Figure 1-3, transpiration and combinations as shown in Figure 1-3. Experimental data indicates that cooling air thermal effectiveness for transpiration-cooled blades approach 1.0. Typical numbers are 0.8. Data for full-coverage film cooling are in the 0.6-0.7 range. For pure convection, thermal effectiveness as high as 0.7 has only been achieved in experimental configurations. (3)

From the cost-of-manufacturing standpoint, convection cooling of small blades is attractive. Cost is increased as schemes to promote turbulence and increase cooling air-to-wall heat transfer coefficient are applied, complicating the casting. Manufacturing operations required for transpiration, impingement, and film cooling are usually complex.

Local film cooling and full-coverage film cooling are effective ways to maintain acceptable metal temperatures. Cooling air is brought through the hub to the blade interior. The air exits through small holes placed in arrays on both suction and pressure side, as needed. The air cools the metal as it passes through and forms a protective film barrier as it flows along the blade exterior. The air then reenters the cycle. The number and placement of holes is critical to ensure adequate cooling with minimum cooling airflow and least disruption of the aerodynamic design of the blade.

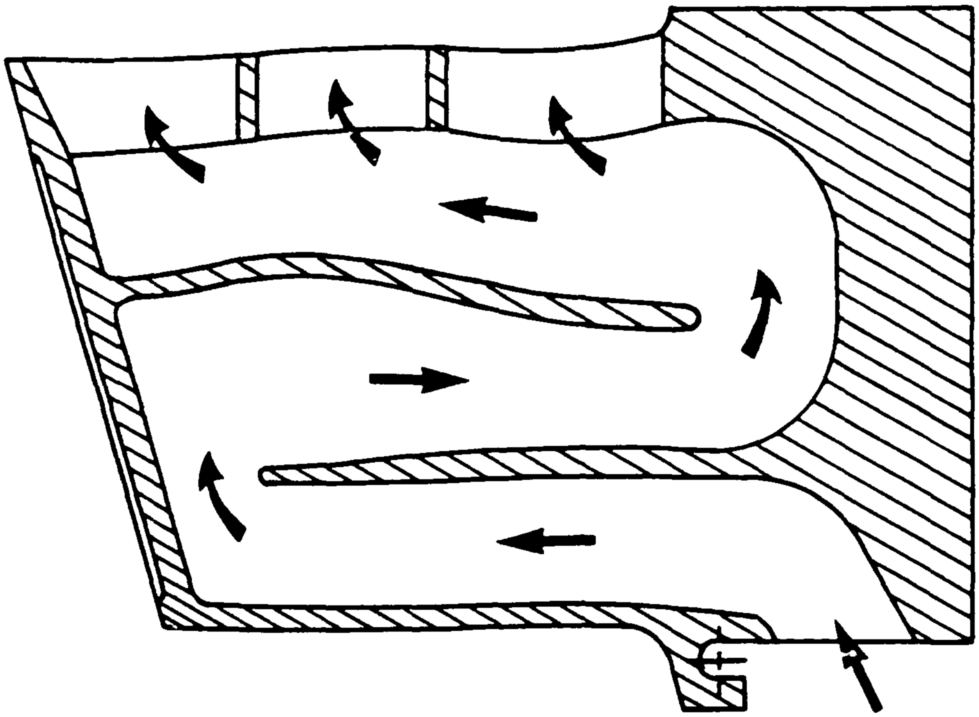

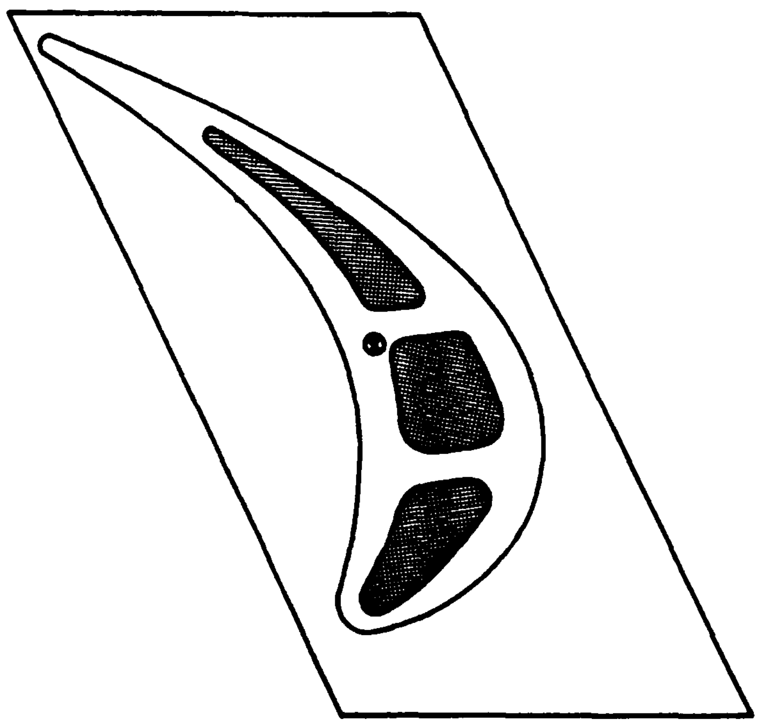

Figure 1-1 AGT 1500 High Pressure Turbine Blade

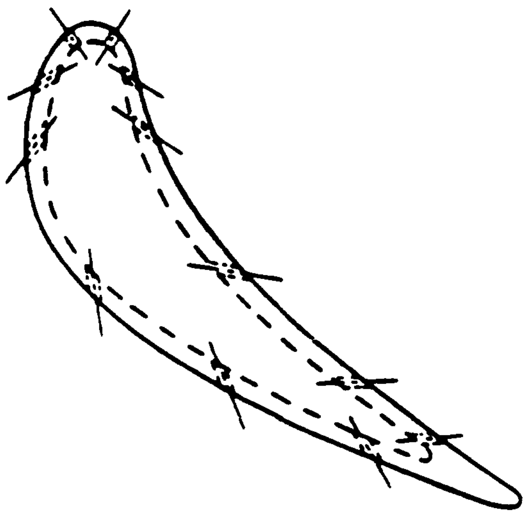

Figure 1-2, Film Cooling

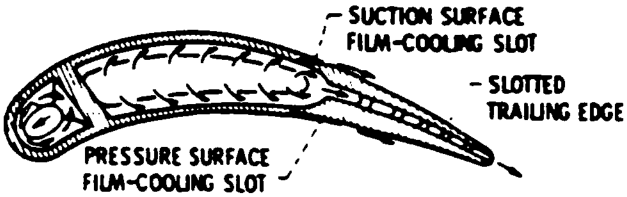

(a) Impingement Cooling

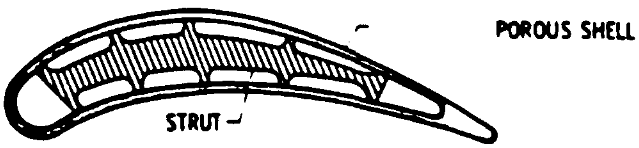

(b) Transpiration Cooling

Figure 1-3, Cooling

In impingement-cooled blades, an inner liner contains the high-pressure cooling air. Holes in the liner direct streams of relatively cold air onto the inner side of the blade skin. The cooling air then flows to the trailing edge of the blade where it reenters the cycle.

Combinations of local film cooling, convection cooling and impingement cooling on the inner blade surface are popular in more complex blade designs.

Porous metals have long been advocated for transpiration-cooled blades. The effusion of air through a permeable wall has two advantages over an internal air-cooled system. First, the contact between the cooling air and the wall through which it passes will be sufficient that the cooling air can be brought to nearly the metal-surface temperature. This minimizes the demand for cooling air. Second, as with the film-cooled design, the effusion of cooling air into the boundary layer between the hot gases and the blade surface can produce a substantial reduction in the gas-side heat transfer coefficient. Transpiration cooling of a surface using a porous wall consisting of a multitude of closely-spaced minute holes is more effective than full coverage film cooling that uses arrays of discrete holes in the surface. Relatively low structural strength of the porous walls, potential oxidation of the material, and the plugging of the very small holes after extended usage have precluded the use of transpiration cooling in production gas turbines.

Simple convection cooling of small (less than 2-inch height) axial gas turbine blades provides a generally cost-effective means of cooling. Because of the size of the blades and the cost goals of small (particularly automotive) gas turbine engines, impingement and full-coverage film cooling are generally avoided. The "as cast" internal cooling passages provide effective cooling without extensive machining operations. The cooling passages may be single or multiple pass. There may be "posts" or other devices to promote turbulence in an effort to enhance the heat transfer from the metal.

Forced convection heat transfer, as shown by McAdams (4), is commonly represented by the equation:

$$dq = h\ dA\ dT \qquad (1)$$

where q is heat flux , h is the proportionality constant or convective heat transfer coefficient , A is the heat transfer area , dT is the temperature difference between the wall and the fluid. The numerical value of h can vary greatly depending on the surface, fluid properties and on the flow conditions. It represents a combination of forced convection, free convection, and conduction in the moving fluid. In the case of flow of a gas inside a tube with well-developed turbulent flow, there are three distinct zones:

- A turbulent zone in the central portion or core

with many eddies.
- A transition (buffer) zone.
- A laminar sublayer next to the wall with zero velocity at the wall.

In the laminar sublayer, heat transfer is by conduction, while in the turbulent and transition zones, the mechanical mixing (convection) dominates heat transfer. McAdams (4) also represented the convection heat transfer by the sum of the conduction and mechanical diffusivity, Eh. In the laminar sublayer, Eh is zero.

$$q/A = (k + \rho c_p E_h) {}^{dT}\!/_{dY} \qquad (2)$$

The heat transfer is influenced by the material properties that determine conduction and the forced or induced movements that physically transfer heat along with the fluid particles. The physical (mechanical) properties lend themselves to manipulation.

Velocity pulsations are a part of many physical systems. Reciprocating pumps, acoustic vibrations, and flow instabilities are examples which result in pressure or velocity fluctuations in a flow system. In many instances, it is apparent that these fluctuations cause an increase in heat transfer in the system. One notable example is acoustic vibrations set up in rocket engines which increase heat transfer from combustion gases to the wall. (5)

Readings in the area of pulsed or intermittent flow convective heat transfer lead to the following conclusions:

- The findings of research to date are not conclusive and at times contradictory. The heat transfer coefficient may increase dramatically, decrease or remain the same.
- Differences in conflicting data often appear to result from flow reversals or standing waves such as Helmholtz type phenomenon.

This is an area that could be controlled by design. Research in this area, except to acknowledge its existence, seems to be non-existent. The present research investigates the effects of flow pulsation under controlled conditions on the heat transfer coefficient. These results may have application potential in the air cooling of gas turbine blades and vanes.

Analytical and empirical methods of predicting the convective heat transfer coefficient have been used successfully on steady flows to include nonlinear heat transfer. A number of investigators have developed analytical methods to predict overall heat transfer coefficients under various conditions. Since all models were generated with assumptions, there are limited ranges of Prandtl Numbers, Reynolds

Numbers and other conditions in which acceptable accuracy is obtained.

For moderate temperature differences and evaluating physical properties at the bulk temperature, Dittus (6) presents:

$$\frac{h_b D}{K_b} = 0.023\left(\frac{DG}{\mu_b}\right)^{.8}\left(\frac{c_p\mu}{k}\right)_b^{.4} \tag{3}$$

For evaluating physical properties, except cp in the Stanton number at the film temperature, Colburn (7) presented:

$$\frac{h_b}{c_{pb}G}\left(\frac{c_p\mu}{k}\right)_f^{2/3} = \frac{0.023}{\left(DG/\mu_f\right)^{.2}} \tag{4}$$

Evaluating physical properties at the bulk temperature, Sieder (8) presented:

$$\frac{h_b}{c_{pb}G}\left(\frac{c_p\mu}{k}\right)_b^{2/3}\left(\frac{\mu_w}{\mu_b}\right)^{.14} = \frac{0.023}{\left(DG/\mu_b\right)^{.2}} \tag{5}$$

These are reported to be accurate for fully developed turbulent flow inside tubes at Reynolds numbers from 10000 to 120000 and for Prandtl numbers from 0.7 to 120.

Martinelli (9) developed an analogy for uniform heat flux for incompressible fluid where physical properties are not dependent on temperature.

$$\frac{h}{c_pG} = \frac{\sqrt{f/2}}{\frac{T_w - T_b}{T_w - T_c}(5)\left[P_r + \ln(1 + 5P_r) + .5DR\ln\frac{Re}{60}\sqrt{f/2}\right]} \tag{6}$$

Where DR (Diffusion Ratio) = Eh/(Eh + k/ρcp)
f is friction factor

For small Prandtl numbers (Pr< 0.1), Lyon (10) presented this equation:

$$\frac{hD}{k} = 7 + 0.025\left(\frac{Dv\rho c_p}{k}\right)^{.8} \tag{7}$$

For uniform wall temperatures, this has been modified by Seban (11) for Prandtl numbers of 0.1 or less.

$$\frac{hD}{k} = 5.0 + 0.025\left(\frac{DGc_p}{k}\right)^{.8} \tag{8}$$

To predict the effects of length to diameter ratio at Reynolds numbers above 10000 and Prandtl numbers from 0.7 to 120, the following equations were suggested by Seban (11):

$$\frac{h_b}{c_pG}\left(\frac{c_p\mu}{k}\right)\left(\frac{\mu_w}{\mu_b}\right)^{.14} = \frac{0.023\left(1 + \left(D/L\right)^{.7}\right)}{\left(DG/\mu_b\right)^{.2}} \tag{9}$$

and McAdams (4):

$$\frac{h_b}{c_pG}\left(\frac{c_p\mu}{k}\right)_f^{2/3} = \frac{0.023\left(1 + \left(D/L\right)^{.7}\right)}{\left(DG/\mu_f\right)^{.2}} \tag{10}$$

From the literature survey, it appears that approximate solutions show more promise than finite difference techniques for expansion to include non-steady-state conditions. None of the references have attempted to use finite-difference techniques to solve the heat transfer problem in the turbulent regime. The nonsteady nature of the pulsatile flow certainly exacerbates the difficulty.

Some of the test data generated in earlier research is conflicting. In some prior literature, higher frequency is shown to have a moderate negative effect on convective heat transfer (12) while in others the frequency effect is positive. (13)

The data in the present research shows that for frequencies up to the shaft frequency of the engine at rated speed, the effects of the pulsations are not negatively influenced by high frequency. A cylindrical test section is used to investigate pulsating-flow heat transfer versus the baseline steady-flow case. The baseline data is generated at several Reynolds Numbers and steady flow. Particular attention is paid to the effects of harmonics. Heat is applied to the outer surface while the test section cooling air flows through the cylinder. Thermocouples monitor air temperatures and allow calculation of the convective heat transfer coefficient, h. The test section is geometrically similar to the turbine cooling passage and the cylindrical cross section assists analytical comparison. Pulsating flow is created with a chopper-type apparatus with controlled frequency. Amplitude is controlled by regulating the inlet air pressure. Inlet air temperature is controlled by an electric heater with temperature control.

The test apparatus allows verification of previously published data which validates the test rig. Much of the data presented here is believed to be new and previously unpublished.

2.0 Objectives

The objectives of the present investigation are:

- Generate test data that describes the influence of pulsed (intermittent) flow of air on the convective heat transfer coefficient. This data concentrates on higher frequency effects, both the general trend and the effects of harmonics due to flow passage geometry.
- Expand empirical methods of convective heat transfer prediction to include the effects of intermittent flow.
- Investigate the effects of intermittent flow with harmonic effects with the aim of reducing the cooling air taken from the gas turbine cycle for blade cooling.

3.0 RESULTS OF PRIOR INVESTIGATIONS

Investigations into the effects of periodically induced flow turbulence on convective heat transfer are neither new nor rare. There are a number of fine papers published, starting in the early 1950's. Several of these are synopsized here. The purpose of this chapter is to review the earlier work upon which this investigation is based, demonstrate the conflict of reported inconsistencies, and show that this work does offer a different approach than previous work and provides original data and a unique application of a known phenomenon.

Wang (14) presented experimental results of unsteady turbulent flows. The fundamental structure of unsteady turbulent flow was studied in a specially designed wind tunnel in which a fully developed turbulent pipe flow was accelerated or decelerated. Measurements of turbulence were made with hot-wire anemometers. It was found that the radial mean velocity is zero, the structure of the radial turbulence intensity is not affected by the unsteady process, but the structure of longitudinal turbulence intensity and Reynolds stress are highly affected by the unsteady process characterized by a generalized Strouhal Number. Wang showed, by developing an equation for unsteady flow potential, that the flow resistance due to friction has much more of an influence on unsteady flow than inertia effects. The inertia effects are an order of magnitude smaller than the resistance effects. In the experimental work, either acceleration or deceleration always had an effect of increasing the longitudinal turbulent intensity. The magnitude increased up to 1.2 times the equivalent steady state. Wang gave the generalized Strouhal Number as

$$STR = \left(R / u_0^2\right) {du_0}/_{dt} \tag{11}$$

For longitudinal turbulent intensity profiles, the curve of equivalent steady-state serves as the lower bound for both the accelerated and decelerated flow. The deviation from the steady state became large as the magnitude of the acceleration or deceleration increased.

Hwu (13) conducted an experimental investigation of the effects of vibration on forced convective heat transfer using a horizontal double-pipe steam-to-air heat exchanger. Vibration was induced acoustically and superimposed directly onto the air stream. The independent variables studied were flow rate of air, frequency and amplitude of vibration. The induced vibration was found to have appreciable effect only when it was at such frequencies that standing waves with appreciable amplitude were set up in the heat exchanger tube. Under these conditions, increase in h (heat transfer coefficient) up to 50% in the laminar region and 27% in the turbulent region were observed. The value of h increased with increasing amplitude of vibration, other variables remaining constant. h increased with decreasing wave length of the standing wave. For a given vibrational mode, improvement in h increased with flow rate up to Re=2080 and then decreased as flow rate increased further. The improvement in heat transfer was greater for flow in the laminar region than in the turbulent region. For a given intensity and resonant frequency, greater relative disturbance is created in laminar flows than in turbulent flows. Keeping other variables constant, improvement in the heat transfer coefficient increases with resonant frequency. This increase is greater for Re > 2590. Holding other variables constant, improvement in the heat transfer coefficient increases with pressure amplitude. This increase is at a greater rate with Re < 2080.

Forbes (15) studied the effect of vibration on natural convective heat transfer in a rectangular enclosure consisting of vertical, isothermal, heated and cooled plates and four adiabatic walls which contained water between the plates. Laminar and transition regimes were considered. The enclosure was subjected to a vertical sinusoidal motion with frequencies from 20 to 4000 Hz. Resonant frequency was determined by pressure transducers mounted to the bottom of the enclosure. Vibration had little effect on heat transfer when the flow was laminar prior to the vibration. Noticeable increases in the average heat transfer coefficient were measured when a flow transition occured. The increase in heat transfer appeared to be directly proportional to the level of turbulence. Increases in heat transfer coefficient up to 50% were noted. The maximum increases were noted at the resonance frequency.

Wendland (16) reported the effects of periodic pressure and temperature oscillations in a closed gas system on the heat transfer between the gas and the metal wall. A piston-cylinder-compression chamber was used to generate the periodic fluctuations. He found the heat transfer from the gas to the cylinder wall to be frequency dependent. The magnitude of the heat flux increased with frequency, from 52400 Btu/hr-ft2 at 25.21 Hz to 93900 Btu/hr- ft2 at 57.53 Hz. Charts of gas temperature spatial profile from the wall as a function of driving frequency clearly show the change in boundary layer thickness as the frequency is increased.

Cheng and Chang (17) studied the structure of nonstationary turbulent flow in a wind tunnel. A periodic turbulent boundary layer was generated by imposing a slowly-varying periodic motion on a fully-developed turbulent pipe flow. The frequencies were 1.88 Hz, 3.78 Hz and 7.08 Hz, and the variation of amplitude was +/- 50% with respect to mean velocity. It was found that internal flow structure, either with acceleration or deceleration, showed remarkable difference from the equivalent steady flow. The turbulent kinetic energy and Reynolds stress of an unsteady flow can increase up to one order of magnitude greater than those of an equivalent steady flow.

Bayle, Edwards and Singh (12) reported experiments conducted to compare heat transfer between a heated plate and a cooling surface flow under steady- and pulsed-flow conditions.

No effect upon the heat transfer rates was found until the amplitude of the pressure pulse reached a "critical" level. Above this, the heat transfer rate was increased for the pulsed flow over the steady flow, with the effect of the pulsations increasing with amplitude and decreasing slightly with frequency.

It appeared to the authors that flow reversal perhaps is the principal cause of enhanced rates of heat transfer. In all tests, the effect of flow pulsations was either to have no effect or to increase the rate of heat transfer over the steady-flow situation. No attempt was made to evaluate the standing wave effects. The "critical amplitude" was believed by the authors to be the amplitude necessary to cause flow reversal which produces an enhanced separation effect and an increase in turbulence in the boundary layer.

Data presented for two different frequencies of the pulsating flow shows that the heat transfer coefficient does not change from essentially steady flow to pulsating flow of a pressure amplitude equal to about 12 dynamic heads. At the "critical" point, the effect is pronounced and varies approximately as the amplitude to the Ø.23 power.

Frequency is expressed by Strouhal Number, fL/V, where L is the length of the flat plate used in the experiment, in the direction of flow; V is the mean fluid velocity; f is the frequency. The result represented, for this experiment, is that the heat transfer coefficient varied as the frequency to the -Ø.1 power.

Baxi and Ramachandran (18) reported the effect of vibration on the free- and forced-convection heat transfer from copper spheres subjected to a sinusoidal vibration. The vibration was normal to the airstream, when present. In the free-convection experiments, the frequency was varied from 2.5 Hz to 15.5 Hz. For low vibration amplitude, the effect on the Nusselt Number was negligible. For values of equivalent Reynolds Numbers greater than 2ØØ, the vibration increased the heat transfer coefficient, with both amplitude and frequency, as high as seven times the free convection values without vibration. The following relationships were presented: Free convection without vibration

$$Nu = 2 + 0.401\, Gr^{.25} \qquad (12)$$

Free convection with vibration

$$\frac{h_v}{h_0} = 0.83\left(\frac{Re^{.5}\left(a/D\right)^{.1}}{Gr^{.25}}\right)^{1.28} \qquad (13)$$

In the case of forced convection, frequency was varied from 3.3 Hz to 26.7 Hz. The flow velocity was varied from 24.5 ft/sec to 84 ft/sec. In the forced-convection regime, no effect was found on the Nusselt Number. The vibration amounted to a variation of 19.6 percent of the flow velocity at maximum.

Bergles (19,2Ø) was interested in the effect of incidental vibration on industrial boilers. Prior reports had been found inconclusive. The test section was almost identical to the test section used in the present investigation. The section was placed in a beaker of water and vibrated. Frequency ranged from 20 Hz to 80 Hz. Heat transfer was improved by a factor of two with vibration up to the point where boiling was fully established. Once boiling was fully established, there was no significant effect of the vibration.

Blair (21,22) reported on an experimental research program to determine the influence of free-stream turbulence on fully turbulent boundary layer flow. In his introduction, he also commented on the highly contradictory previous data for the impact of free-stream turbulence on boundary layer heat transfer. He commented that in accordance with the classic two-dimensional turbulent boundary layer correlations (Reynolds Analogy), the increases in skin friction require that heat transfer increase as well. The results of this flat-plate test rig show that for fully turbulent boundary layer flow, both the skin friction and heat transfer were substantially increased for increased levels of free-stream turbulence. For a free-stream intensity increase of six percent, an increase of 18 percent was recorded for heat transfer.

Bayley and Priddy (23) reported on an experimental program which represented a turbine blade cascade with a rotating squirrel cage turbulator simulating the turbulence of the gas turbine main-stream flow. The disturbance frequency was as high as 10000 Hz. Turbulence intensity was varied by the diameter of the bars and the position of the turbulator. The effects of the turbulence generator were striking. The convective heat transfer increase varied over the position on the blade (pressure or suction side) but at even intermediate locations heat transfer more than tripled. The effect of frequency variation was more modest, however, it is reported to increase with frequency to the maximum frequency .

Ishegaki (5) reported the effects of frequency on heat transfer in the turbulent-flow regime. To acknowledge the effects of increasing velocity, he created the parameter:

$$\left(\frac{u'}{u_0}\right)^2 \left(\frac{f_b C}{u_0}\right)^{1/2} \qquad (14)$$

u' is rms velocity fluctuation, uo is free stream velocity, fb is frequency of disturbance, C is characteristic length.

Di Cicco and Schoenhals (24) investigated the heat transfer rate when a pulsating pressure was applied to a stable film boiling system. Periodic pressure pulses of 90 psi were applied at frequencies of 11.3 Hz to 25.8 Hz. The improvement was reported to be from 59.5 to 103 percent. There was a general increase with frequency.

Faircloth and Schaetzle (25) conducted an experimental investigation vibrating a wire exposed to a forced air current. They compared the results to an equation published by McAdams (4):

$$Nu = 0.32 + 0.43(Re^{.52}) \qquad (15)$$

They calculated an effective Reynolds Number and correlated the results with the McAdams equation. This gave an analysis that is equivalent to Nusselt Number versus frequency. The results are:
For Re<.45 (free convection)

$$Nu = 0.48 \qquad (16)$$

For .45<Re<2.5 (forced convection, laminar)

$$Nu = 0.63(Re^{.288}) \qquad (17)$$

For Re>2.5 (forced convection with thermal acoustical streaming)

$$Nu = 0.82(Re^{.407}) \qquad (18)$$

Fand, et al (26,27,28) investigated heat transfer from a heated horizontal cylinder in the presense of sound waves. The results demonstrate that intense transverse sound vibrations strongly influence the rate of free convective heat transfer. They showed, as did others, that there is a sound intensity below which essentially no change to the heat transfer occurs. Then, after some critical level, the heat transfer rapidly increases with intensity.
The increases in free convective heat transfer were as high as 1200 percent.

In all of the studies, increase in the heat transfer coefficient was attributed to a reduction in the boundary layer. In an investigation by Hagge and Junkhan (29) and Junkhan (30), the boundary layer was mechanically stripped by a rotating blade passing close to a flat plate. The convective heat transfer from the plate was increased up to eleven times. The blade scrapes away the boundary layer. This is a gross representation of what each of the researchers was trying to achieve with sound, vibration, or in the present investigation, flow interruption.

Holman (31) described the effect on heat transfer by the sound field reported by others as acoustic streaming. This is described as regions of lower and higher pressure causing flow eddies, which do not otherwise exist, enhancing heat transfer much as would forced convection.

In a paper, referenced in many succeeding studies, Jackson, Harrison, and Boteler (32) were among the first to document the critical intensity below which heat transfer was not affected. Using acoustic vibrations in a constant temperature vertical tube, free convection was dominant below 118 decibels. Above 118 decibels, free convection was negligible and effect of sound was dominant. The effects of varying frequency were not investigated. The series of experiments were conducted to study the effects of resonant acoustic vibrations on convective heat transfer in a horizontal tube. Average heat transfer and local heat transfer rates for various portions of the tube were determined while the flow of air was excited by acoustic vibrations at varying frequencies. For resonant conditions, it was found that the acoustic waves produced a periodic effect on the local heat transfer coefficient. These were maximum at the pressure nodes of the standing waves. At standing antinodes, the reverse effect was noted. Therefore, overall, the increase in heat transfer was small. In this case, the length of the tube and frequency were such that numerous periods were present. When a short section was considered, the increase in heat transfer was as much as 150 percent. It was noted that at low decibels, there was no noticable effect.

Some years later, Jackson, with Purdy (33) and with Purdy and Oliver (34), reported similar data, this time superimposing a resonant sound field on the throughflow of a 10 foot-long pipe. Condensing steam on the outer surface of the pipe measured the heat transfer. The size of the pipe allowed Jackson to investigate the heat transfer along the pipe as a function of the position in a standing wave. Maxima of the local heat transfer coefficient occured at 0, 1/2, 1, 3/2 wavelengths. Again, Jackson mentioned the minimum intensity below which no change in heat transfer occurs. Of particular interest in this paper was that at resonant, standing wave frequencies, at the anti-nodes, where flow induced by the resonant condition is minimum, no vortex or eddy flow is induced and heat transfer actually decreased.

June and Baker (35) reported an experiment of acoustic vibration on a flat plate using a siren. The equipment was interesting because the chopper designed for the present research bears great resemblance to a siren. No pulsed flow was allowed to reach the flat plate, however. The intense sound field (up to 163 dB, reference .0002 microbar) had a significant effect on heat transfer. The maximum increase was 220 percent at 163 dB and 200 Hz. The heat transfer increased with sound intensity.

Another mechanical variation of the varying pressure flow was the investigation by Mendes, Souza and Sparrow (36). Periodically converging and diverging tubes forced systematic variations in Reynolds Number, and flow visualizations were performed. As might be expected, for the same flow, pressure drops were greater for the converging-diverging sections, but at the same pumping power, the heat transfer was increased 30-60 percent. The direct application of the geometric configuration is suggested but similarly it can be inferred that the flow-generated analogy, produced by velocity fluctuations in a duct of constant cross section, will also produce higher pressure drops but quite possibly higher heat transfer for the same pumping power.

Sparrow and Tao (37) performed a similar task by placing rings periodically in an otherwise smooth duct. The resulting influence on heat transfer when compared to the smooth duct is comparable to Mendes and Sparrow's converging-diverging duct.

Nevins and Ball (38) demonstrated the effect of pulsed air on a 1/4 inch flat copper plate. Interestingly the heat transfer, for the range of variables tested, was found to be independent of pulsation frequency and amplitude. Frequency was very low, up to 18 Hz.

Although laminar flow only is represented, Siegal and Perlmutter (39,40) demonstrated flow fluctuations similar to that of this investigation. Two flat plates were kept at constant temperature and laminar flow was pulsed between the plates by a sinusoidal pumping pressure. It was found that the oscillations did not produce an increase in the average heat transfer from the walls. Frequency was not given in these papers.

Seban (41) made a here to fore unmentioned point that the transition from laminar to turbulent flow is earlier in the presense of induced turbulence. This, combined with the fact that boundary layers will be reduced for turbulent flow, will render for those systems approaching transition flow, a likelihood of increased heat transfer.

Simonich and Bradshaw (42) commented on the conflicting reports by earlier researchers. In fact, they list prior work and whether the work reports an increase in Nusselt Number or not. The title "Effect of Free-Stream Turbulence on Heat Transfer through a Turbulent Boundary Layer" is descriptive of the work. They conclude that it is not possible for the temperature field to be completely unaffected by free-stream turbulence.

Mathewson (43) studied the effects of sonic pulsations on forced convective heat transfer to air, and on the film condensation of alcohol. The frequency range was 50 to 330 Hz. Reynolds Numbers were varied from 1600 to 4000. In the experiments with air, a maximum improvement in heat transfer was obtained with a pulse frequency of 330 Hz and a Reynolds Number of 2300. At higher Reynolds Numbers, the improvement in heat transfer over steady flow decreased rapidly and at lower Reynolds Numbers the improvement became independent of Reynolds Number. At any given Reynolds Number, the improvement decreased as pulse frequency was reduced and was nearly independent of amplitude. In the runs with the film condensation of alcohol, the Reynolds number was always below 1500, but turbulent. A maximum improvement in heat transfer coefficient of 57 percent was achieved. The inprovement was relatively insensitive to pulse frequency but depended on the pulse amplitude. There was a critical pulse amplitude below which the pulsation had no effect on heat transfer. The studies with air showed that there was little improvement in heat transfer in a pulsed gas with high Reynolds Number. Mathewson presented an empirical relationship for the convective heat transfer coefficient that was taken from Hanratty (44). This is based on the concept that the unsteady state heat transfer process is a "two-phase system." The flow of fluid in the immediate vicinity of the wall is not continuous. Masses of fluid move to and from the wall, continually changing the fluid in contact with the wall. The maximum rate of heat transfer occurs at the earliest instant when the temperature differential is greatest. The rate of heat transfer decreases with time. Eventually the mass of fluid is replaced and the process is repeated. The equation for heat transfer is:

$$h = 2c\rho\rho\sqrt{\frac{\alpha}{\pi\theta}} \qquad (19)$$

Where is the thermal diffusivity and is the contact time of the elements. This analysis suggests that as the contact time increases, the heat transfer coefficient would approach the steady state film theory, h = k/d, where k is the thermal conductivity of the film and d is the thickness of the laminar sublayer. He presented the heat transfer coefficient as

$$h = 2\sqrt{\frac{3600}{\pi}\rho c_p k f} \qquad (20)$$

f in this equation for the steady state condition must be obtained with at least one measured value of h.

Table 3-1 shows a brief synopsis of the research reviewed in this chapter. Figure 3-1 charts the percentage improvement in heat transfer versus frequency for that research dealing with free convection and

Table 3-1 Review of Previous Research

Reference	% Improve	Re	Freq	Free/Forced
Hwu (13)	27	2080	322	forced
Forbes,Carley,Bell (15)	50	4000		free
Cheng,Chang (17)	100		7	free
Bayle.Edwards,Singh (12)	35	176000	30	forced
Baxi,Ramachandran (18)	0	30000	27	forced
Bergles (19,20)	200	80		water
Bayle,Priddy (23)	400	750000	10000	forced
DiCicco,Schoenhals (24)	100	0	26	free
Faircloth,Schaetzle (25)	30	15	40	forced
Fand,Kaye (26)	300	1500		free
Fand,Roos,Cheng,Kaye (27)	1200	1500		free
Hagge,Junkham (29)	1100	700000	30	forced
Jackson,Harrison,Boteler (32)	150	2300	520	forced
Jackson,Purdy,Oliver (34)	13	11600	216	forced
	20	2100	221	forced
June,Baker (35)	220	200		free
Souza Mendes,Sparrow (36)	60	70000	NA	forced
Nevins,Ball (38)	0	8000	18	forced
Mathewson (43)	57	2300	330	forced

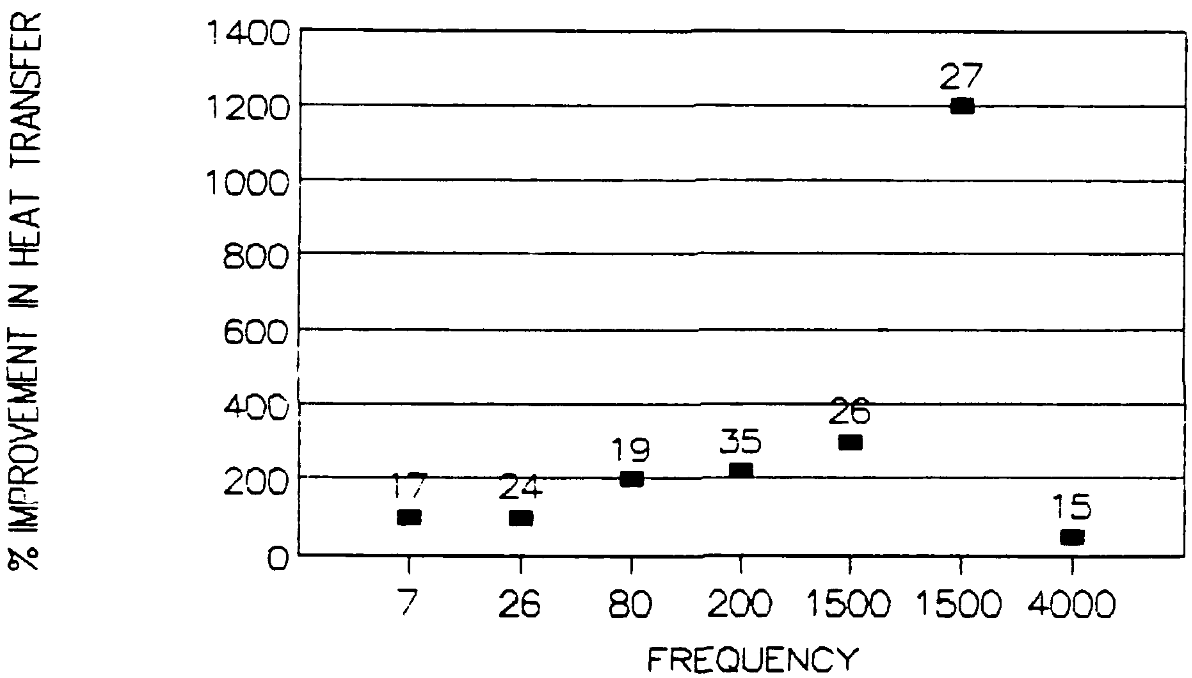

Figure 3-1, Prior Research Free Convection
References Labeled

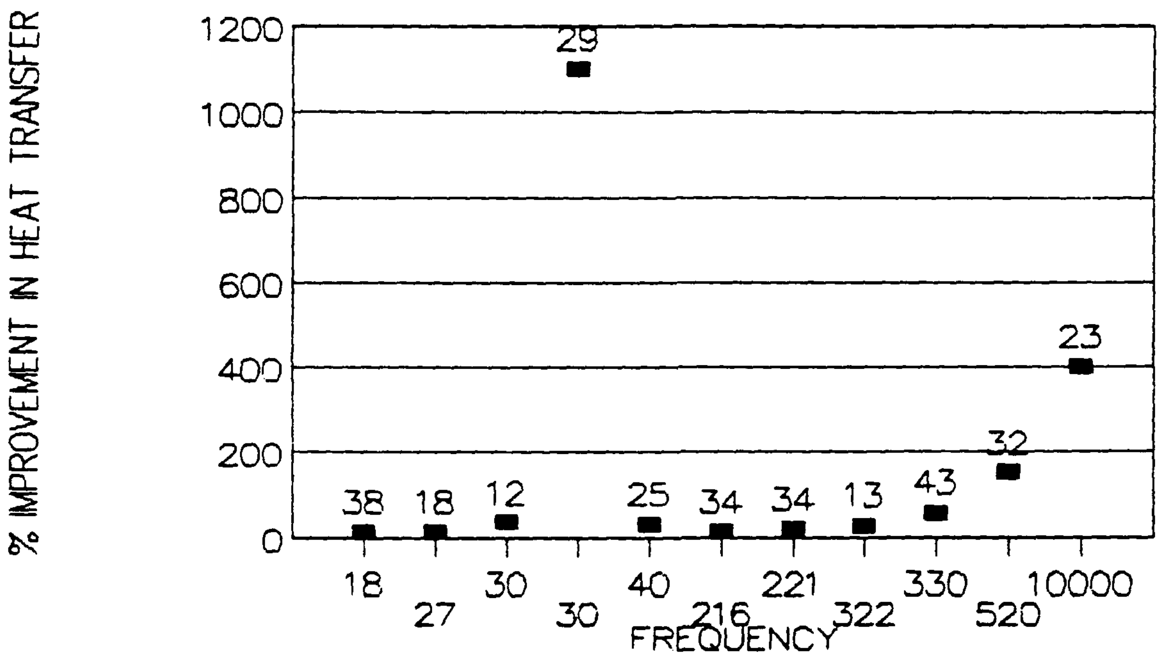

Figure 3-2, Prior Research Forced Convection
References Labeled

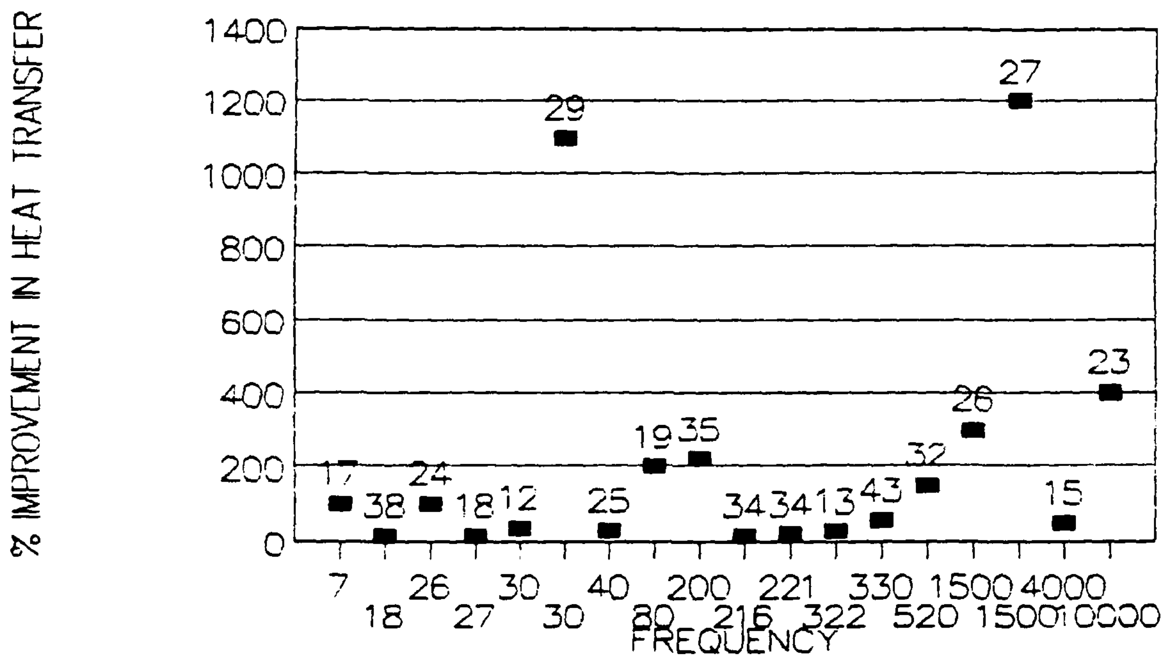

Figure 3-3, Overview of Prior Research
References Labeled

Figure 3-2, that research dealing with forced convection. Figure 3-3 combines free and forced convection. In summary, the prior research is very helpful in establishing the basic phenomenon that heat transfer can be enhanced with a variety of methods which reduce or disrupt the boundary layer. Methods used in the past include acoustic drivers, mechanical scrapers, varying cross sections causing flow velocity to increase and decrease, and varying bypass flow. The frequencies investigated bracket the present experiment, from 4 Hz to 10000 Hz. The amplitude or strength of the disruption varies from a modest sound wave to the mechanical scraping of the boundary layer, the equivalent of a very strong pulse. Free convection, forced convection in laminar flow and forced convection in turbulent flow have been investigated.

The following general statements can be made from the prior research.
- The stronger the pulse, the greater the influence on the boundary layer.
- There is a minimum strength below which no effect is observed.
- The more turbulent the baseline flow, the less potential for improvement. The free convection baseline has the most potential for improvement.
- Although not always observed, frequency has an influence on the boundary layer.

4.0 EXPERIMENTAL APPARATUS

The design objective of the test apparatus is to simulate the gas turbine blade in a manner to permit control over the environment, provide for extensive and accurate data taking, yet maintain the near true model. The experimental apparatus is configured as shown in the sketch at Figure 4-1. The general arrangement is shown in the photograph at Figure 4-2.

The blade and the environment were designed to simulate the high pressure blade of the AGT1500 gas turbine. A six-inch, .305-inch diameter stainless steel tube with .035-inch wall thickness was used as the test section. The length was sized to the length of the cooling passage of the AGT1500 high-pressure turbine blade (Figure 1-1). The diameter of the round test section was sized to best represent the cross section of the same cooling passage.

The tube was welded into a fixture (Figure 4-3) which allows passage of hot air over the tube in the direction normal to the centerline of the tube, simulating main-engine gas flow through the turbine. The inlet to the test section (point T7, Figure 4-1) exits from the chopper or flow interrupter shown at Figure 4-4. The cooling air exits the test section at point T6, Figure 4-1.

The chopper was designed and built at TACOM to permit complete interruption of the airflow, without leakage from 0 to 720 Hz. The seals are graphite-filled chemlon-face seals with Hastelloy C loading springs (Figure 4-5) built specially for this experiment by Crane Packing. The Crane part number is Type 8B2, .563 diameter. The chopper with the seal removed is shown in Figure 4-3. Speed of the chopper and hole pass frequency were measured by the controller and independently by a Hewlett Packard model 5512A Counter (Figure 4-7) driven by a photo transistor receiving light interrupted by the chopper. (Figure 4-8)

The Toshiba polyphase, 3-hp, 230-volt induction motor (Model B0034FG2A4) (Figure 4-9) and matching speed controller (Series ESP-130, Model 8) (Figure 4-10) provide accurate, steady and repeatable frequency control. The motor was coupled to the chopper by a Lovejoy flexible coupling (Figure 4-11).

Two 440-volt three-phase electrical heaters were used with independent closed-loop temperature control (Figures 4-12, 4-13). These provided air for the hot side and cooling-air side of the blade simulation.

Air flow was measured by ASME smooth-approach nozzles (Figure 4-14).

Pressures were measured by pressure transducers except for the pressure differential across the flow nozzles where inclined manometers were used (Figure 4-15).

Data was accumulated and recorded on a Fluke 2240 Datalogger. (Figure 4-7)

Air was taken from the TACOM central shop air supply, routed through a dryer and filter (Figure 4-16), in addition to the facility dryer and filter, through a two-stage pressure regulator (Figure 4-17) and to the two electic heaters. On the cooling side, the air goes from the heater to a bypass and adjusting valve (Figure 4-18), to the chopper, through the test specimen, through a cooling system to bring the air to a temperature compatible with the flow nozzle (T8, Figure 4-1), and then through the flow-measuring nozzle. The bypass ratio was about 100:1. This kept pressure at that point independent of flow through the chopper.

On the hot side, the air leaves the filter (T2, Figure 4-1), goes through a flow control valve, through the flow-measuring nozzle (T5, Figure 4-1), through the electric heater, across the test section (T4 to T3, Figure 4-1) and exits into the room.

The iron - constantan thermocouples and their placement are shown in Figures 4-19, 4-20.

Heat transfer is determined by measuring the mass flow and temperature rise in the test section.

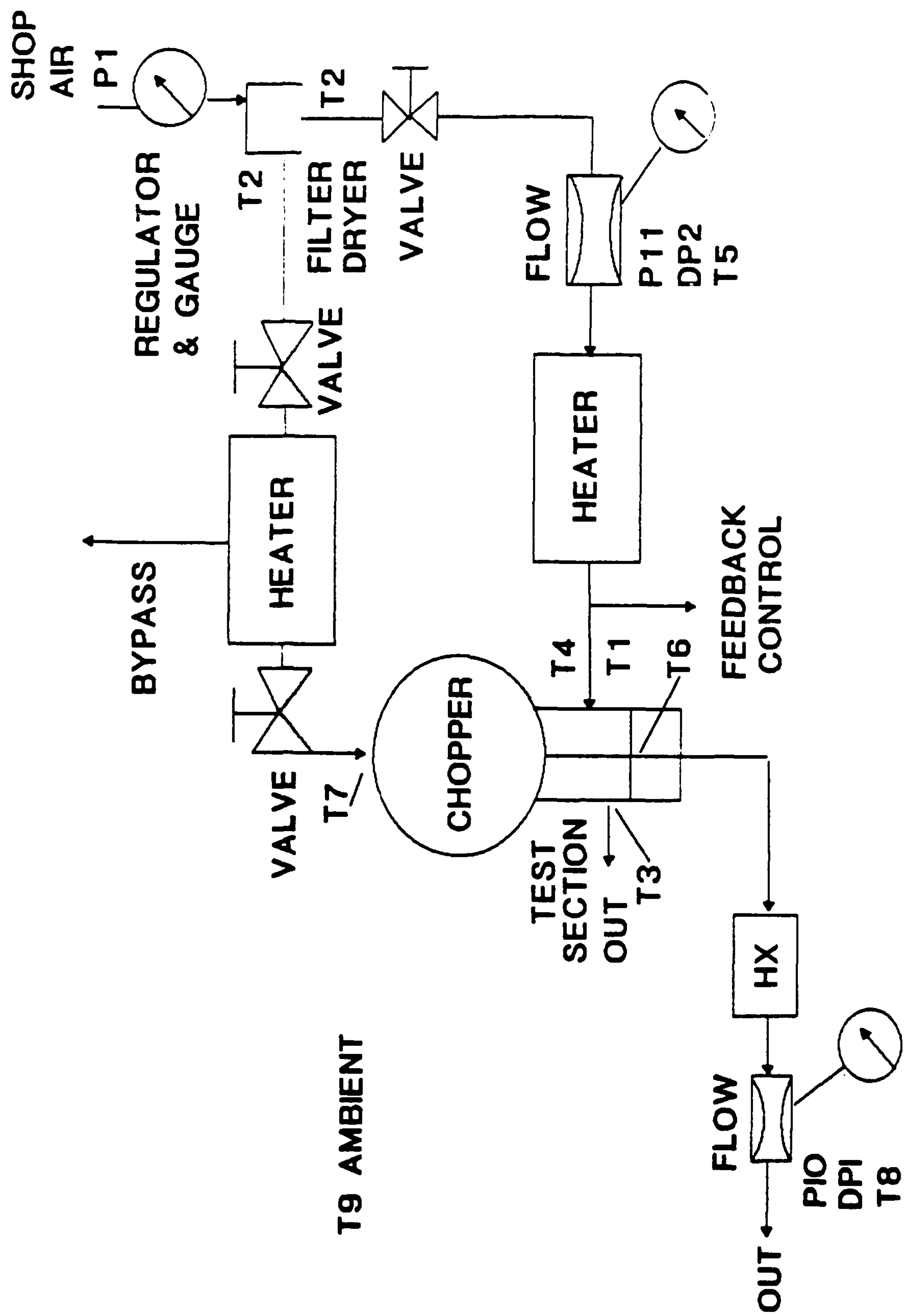

Figure 4-1, Experimental Apparatus

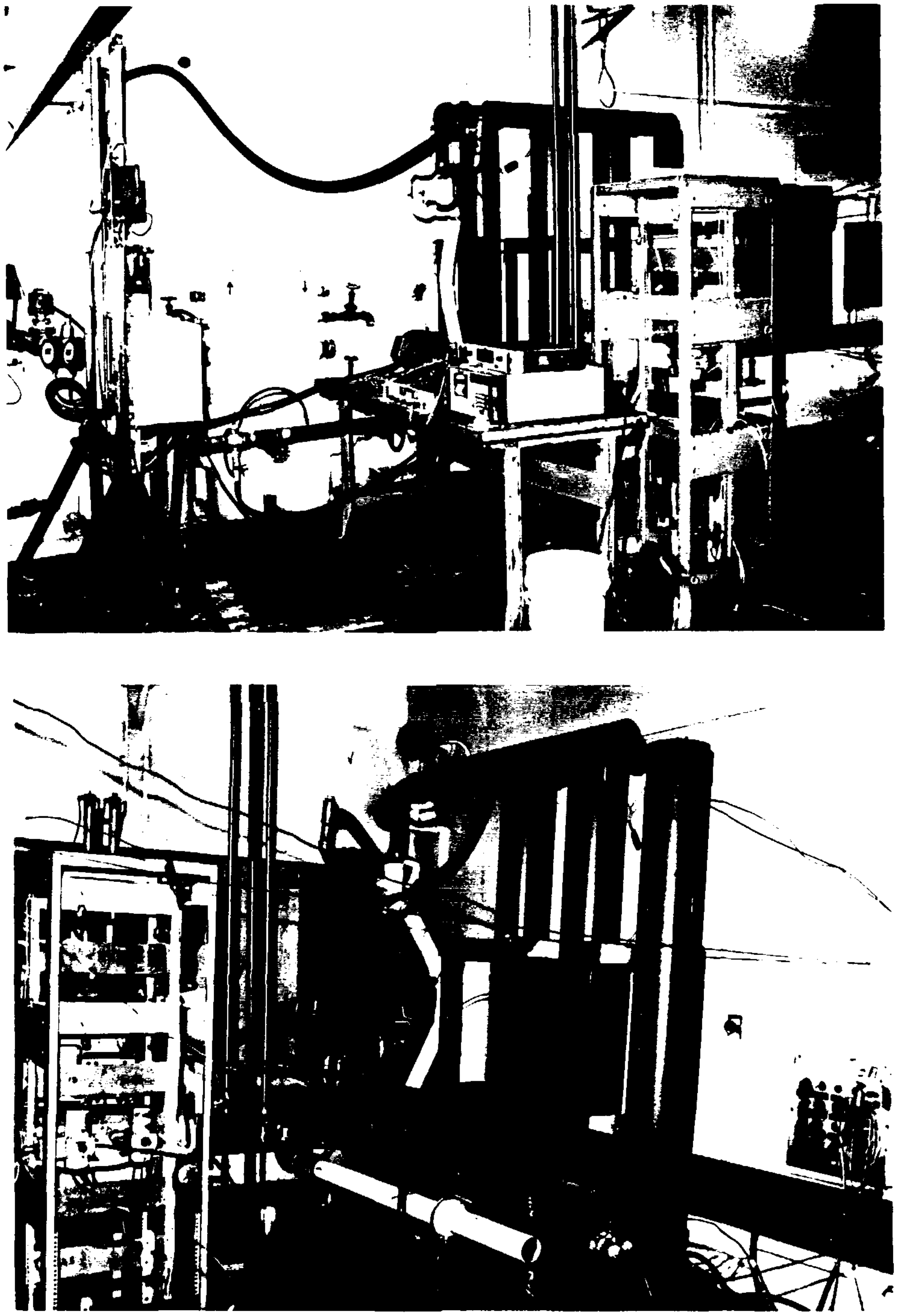

Figure 4-2, The General Arrangement of the Test Setup

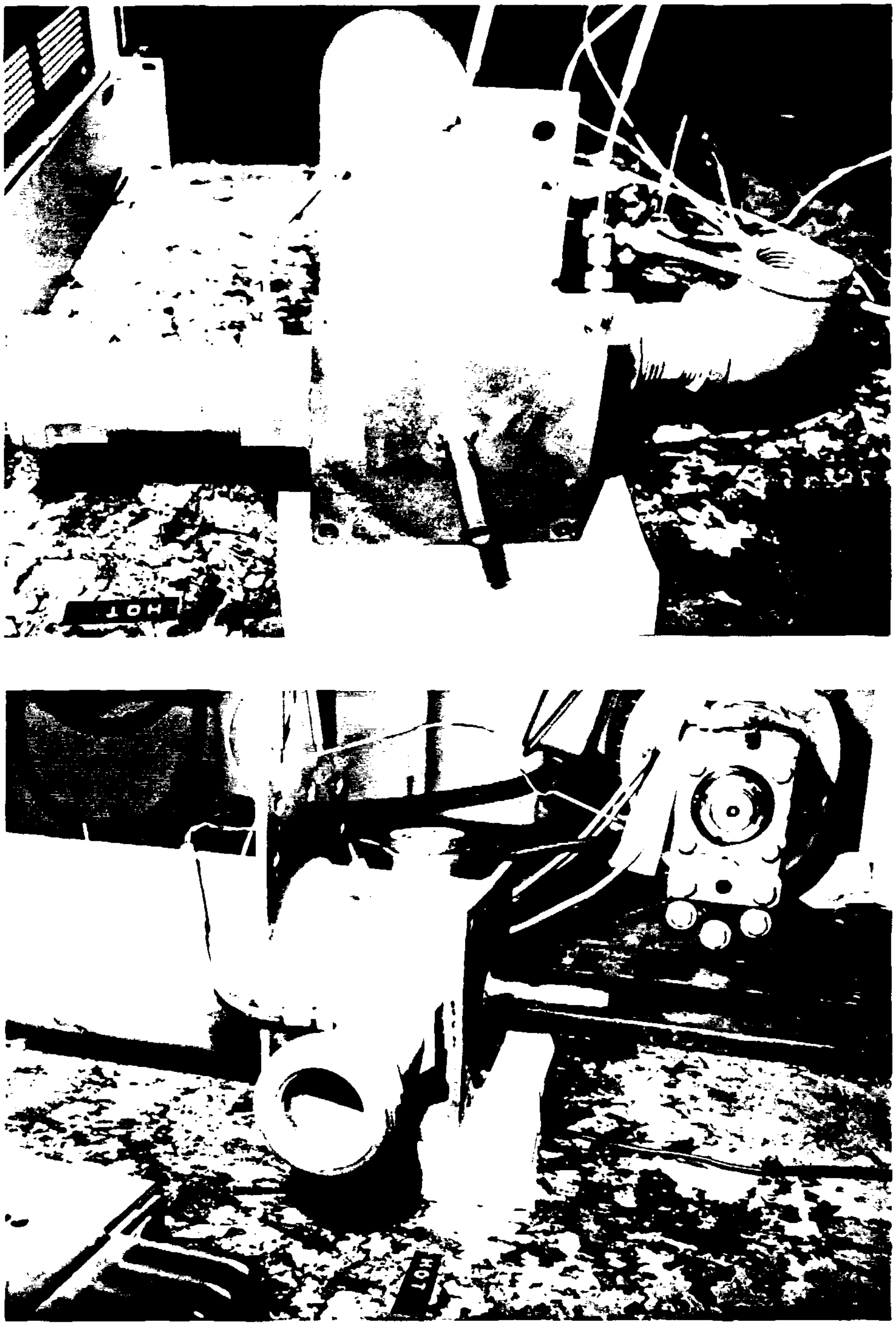

Figure 4-3, The Test Section Removed from the Chopper

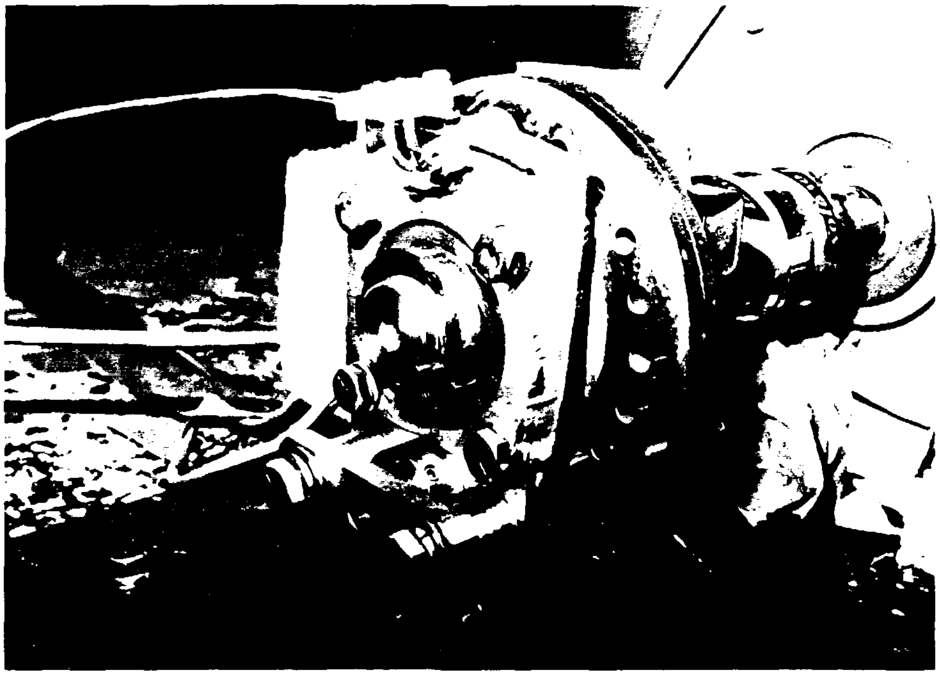

Figure 4-4, The Chopper Bears Resemblance to a Siren

(The seals prevent leakage and frequency is controlled and stable.)

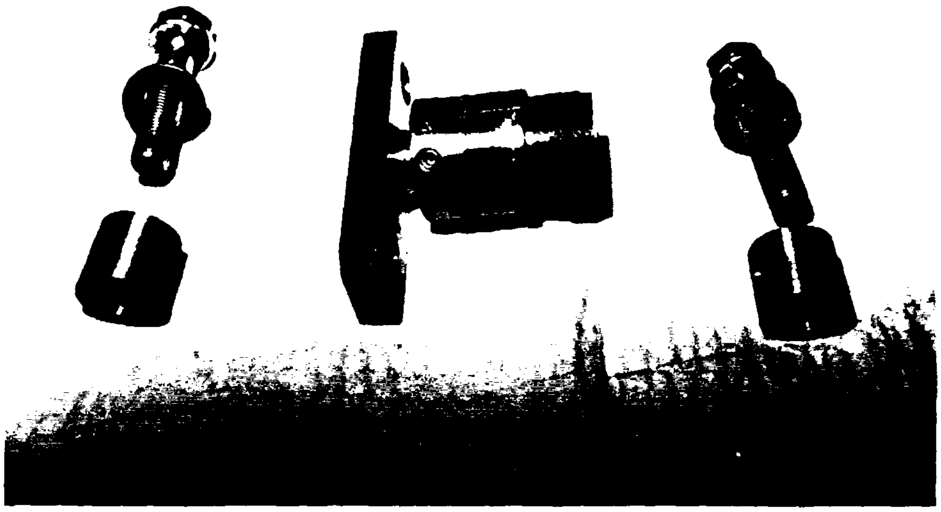

Figure 4-5, The Graphite Face Seal

Figure 4-6, The Chopper with Seal Removed

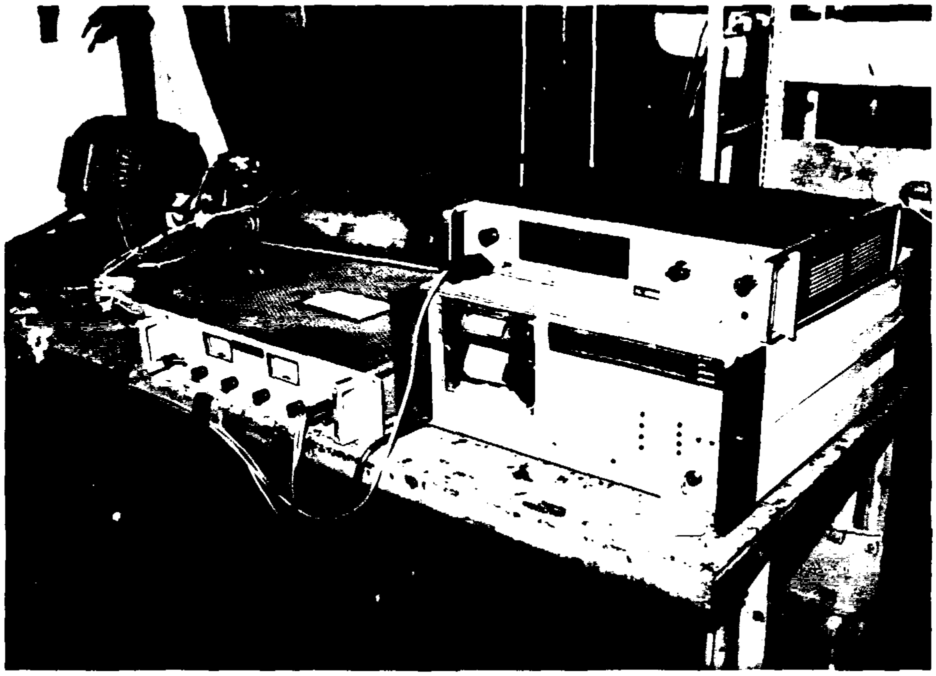

Figure 4-7, Power Supply, Counter, Datalogger

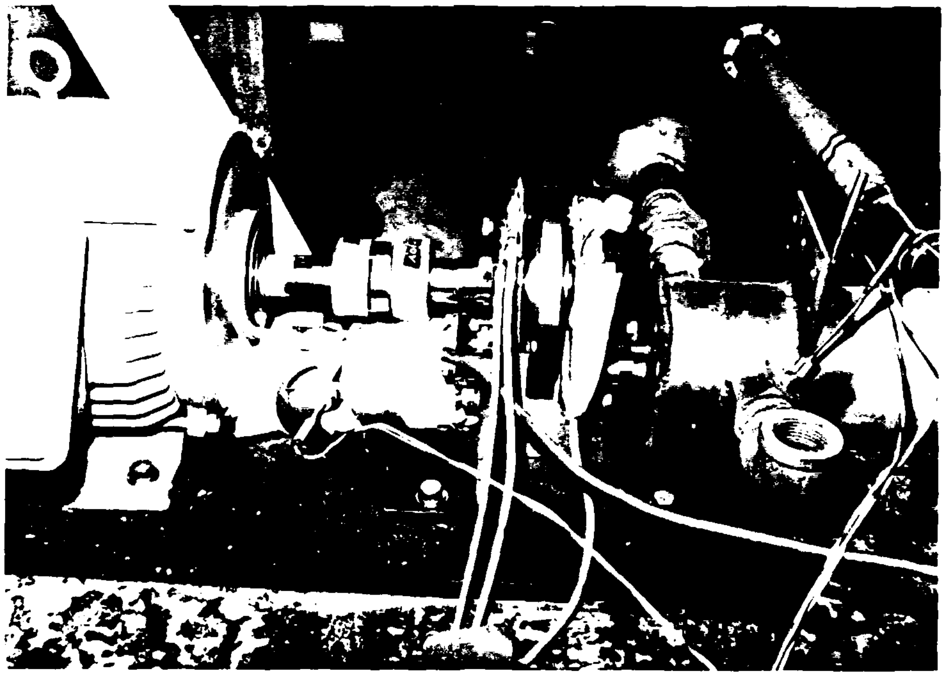

Figure 4-8, Light and Photo Transistor Used to Drive the Counter

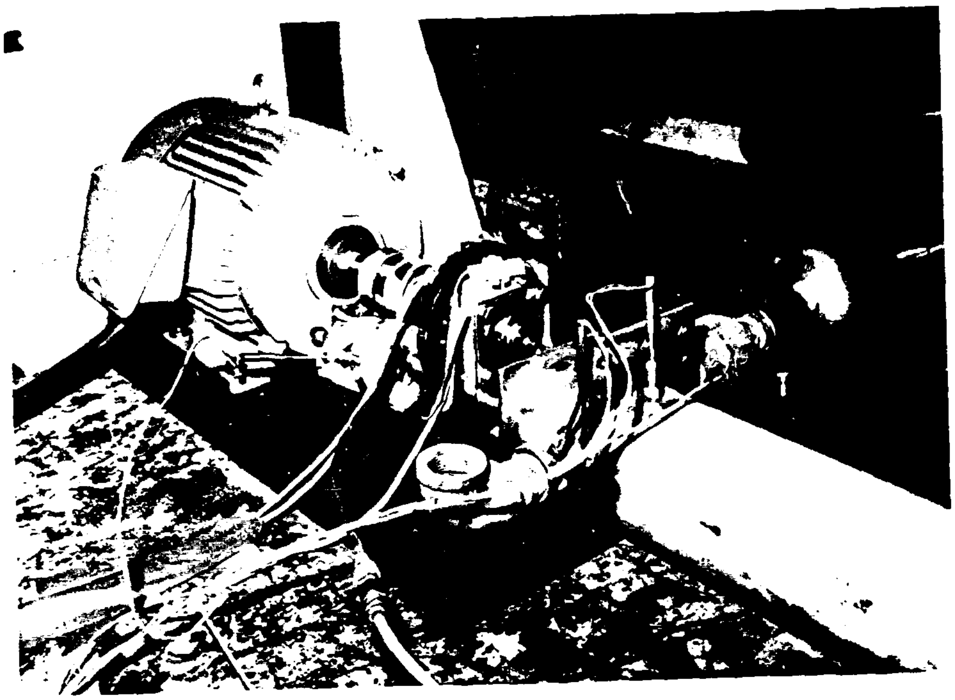

Figure 4-9, Chopper and Test Section

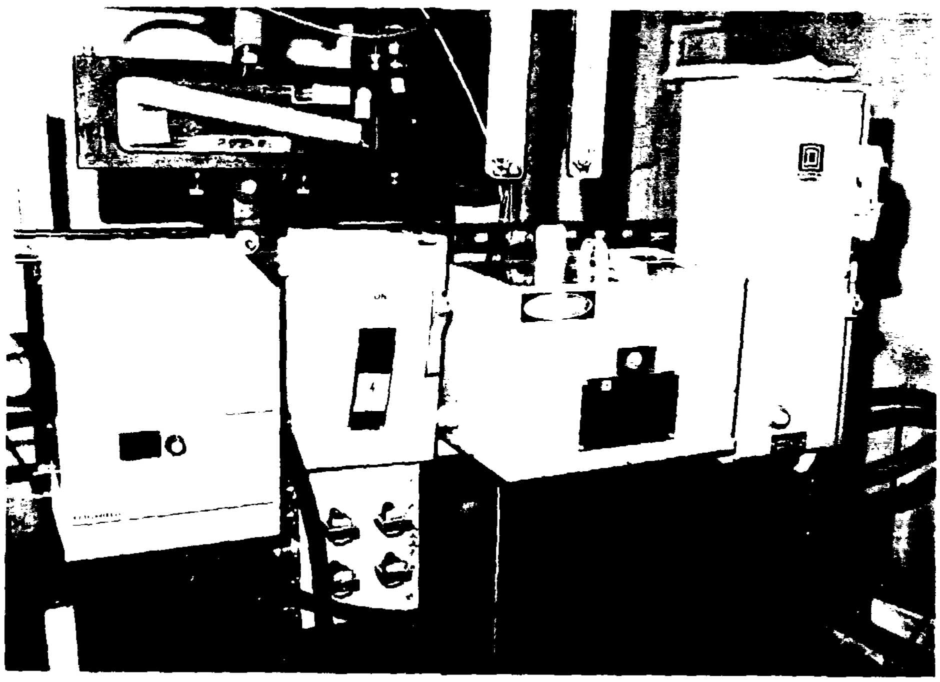

Figure 4-10, Power Supply and Toshiba Motor Speed Controller

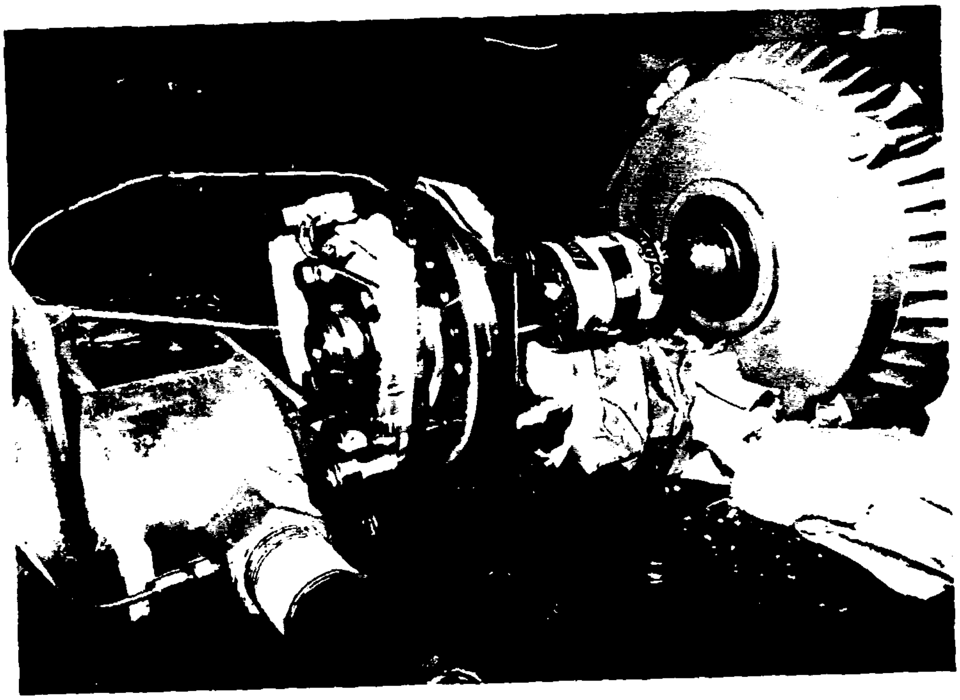

Figure 4-11, The Lovejoy Coupling

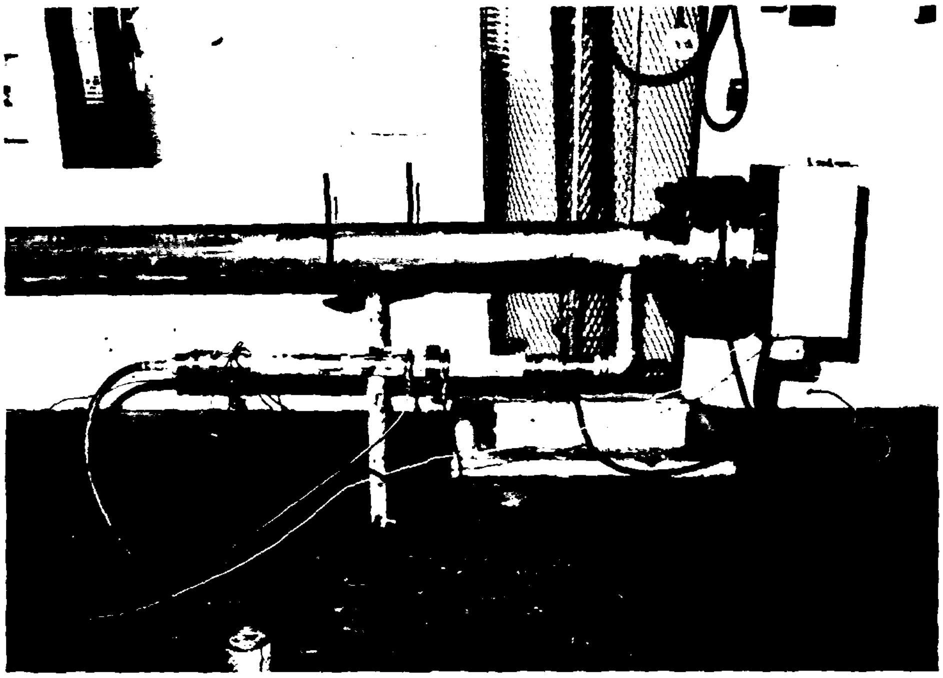

(a) 35KW Three-Pass Concentric Heater

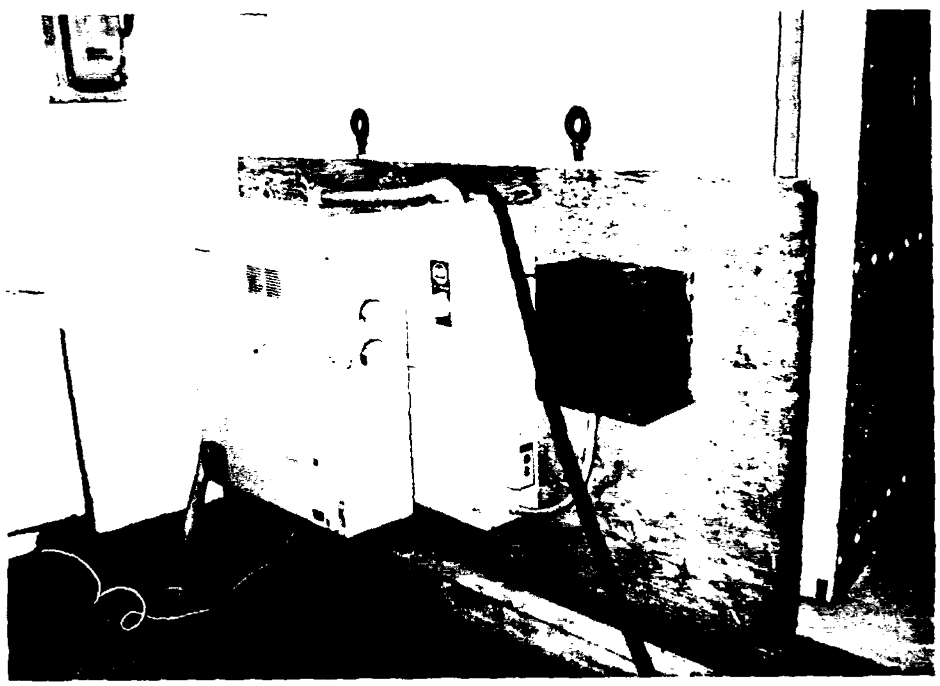

(b)

Figure 4-12, Power Supply and Controller

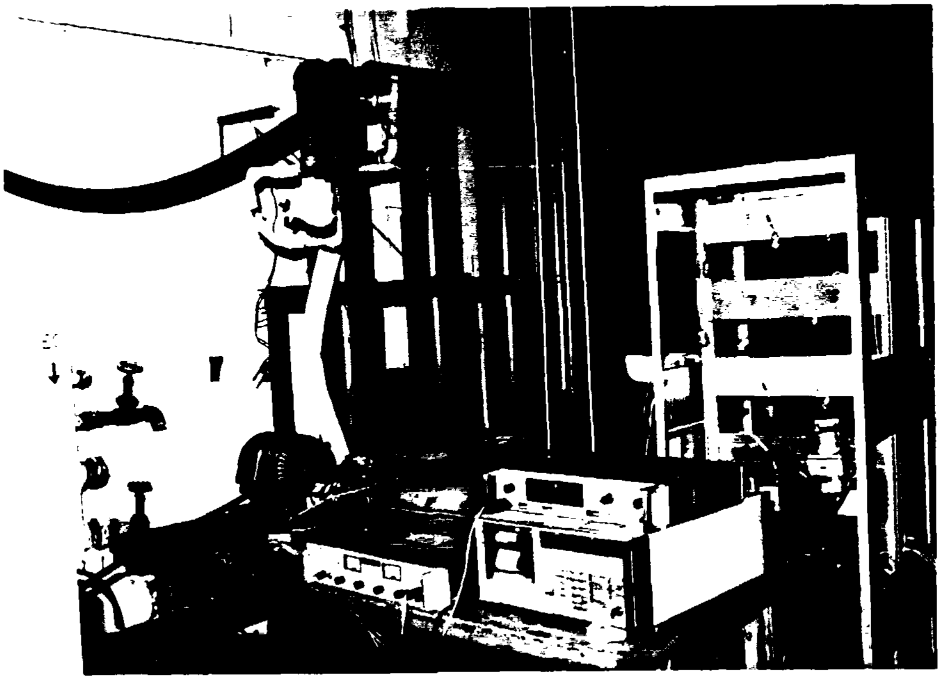

(a) The Three Vertical Heaters

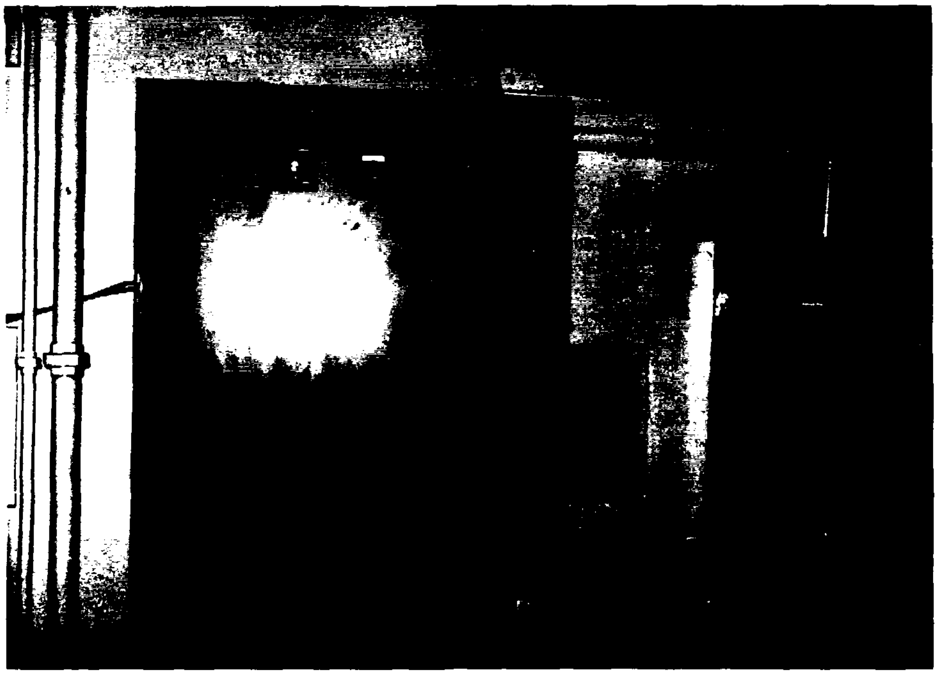

(b)

Figure 4-13, Coolant Temperature Control, Power Supply and Controller

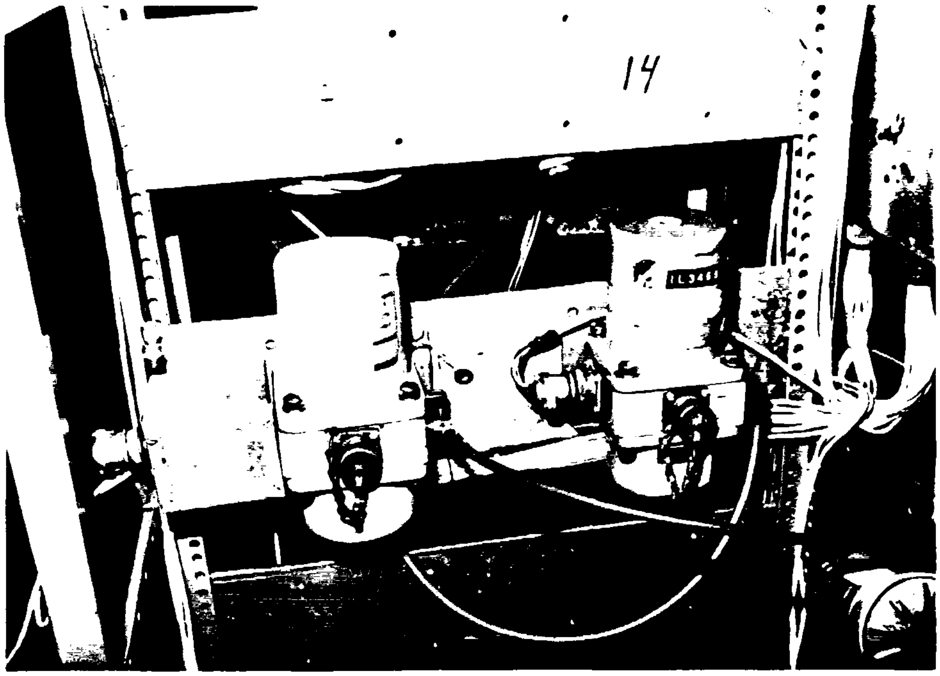

(a) Pressure Transducers

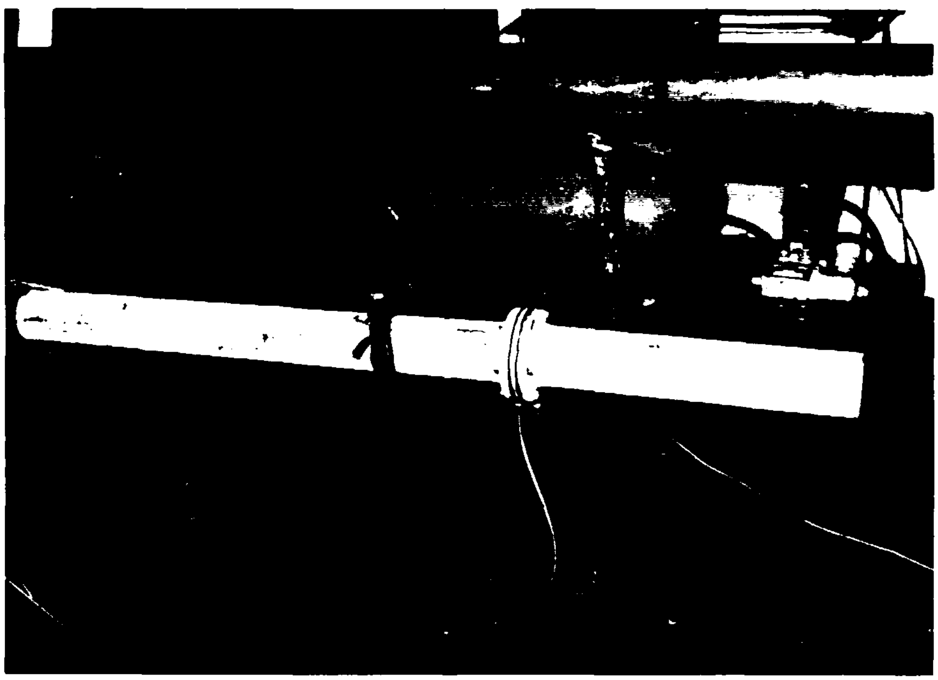

(b)

Figure 4-14, The ASME Smooth-Approach Flow Nozzles

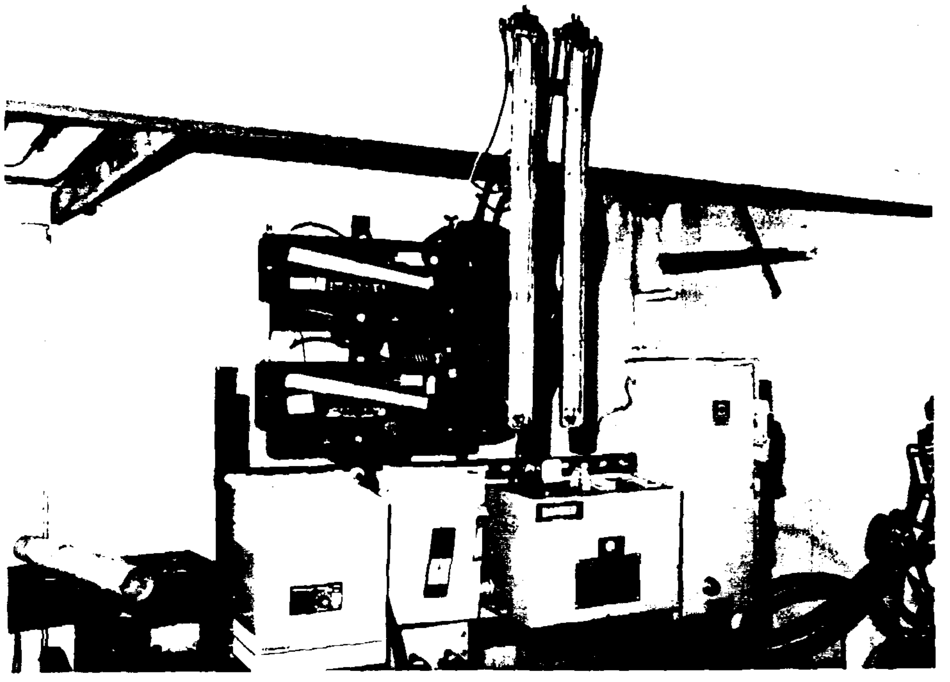

Figure 4-15, The Manometers for the ASME Flow Nozzles

(The inclinometers and vertical manometers are redundant.)

Figure 4-16, The Dryer / Filter

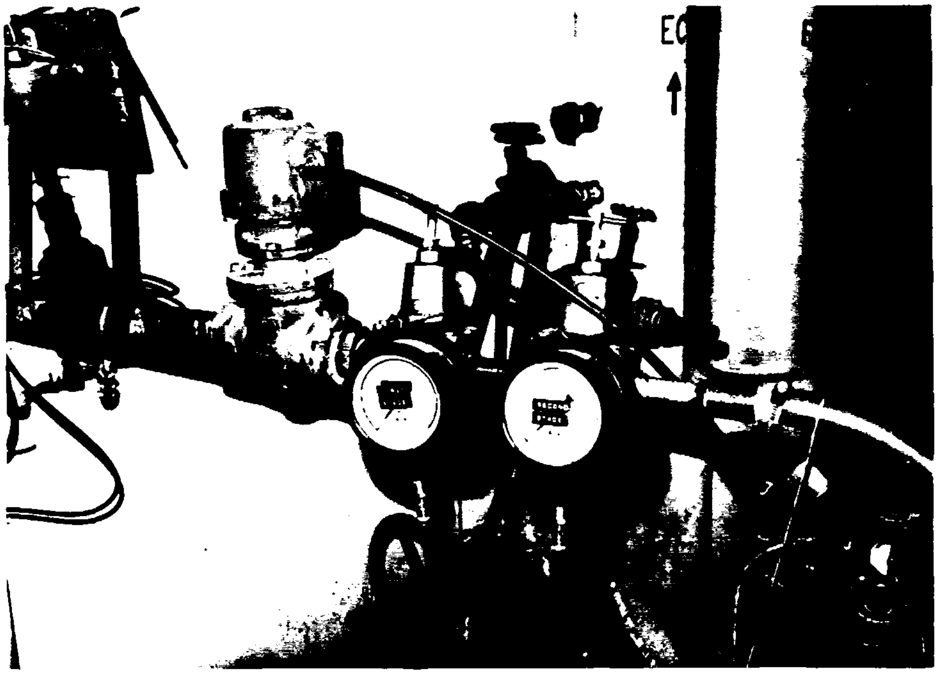

Figure 4-17, Dual In-line Pressure Regulators

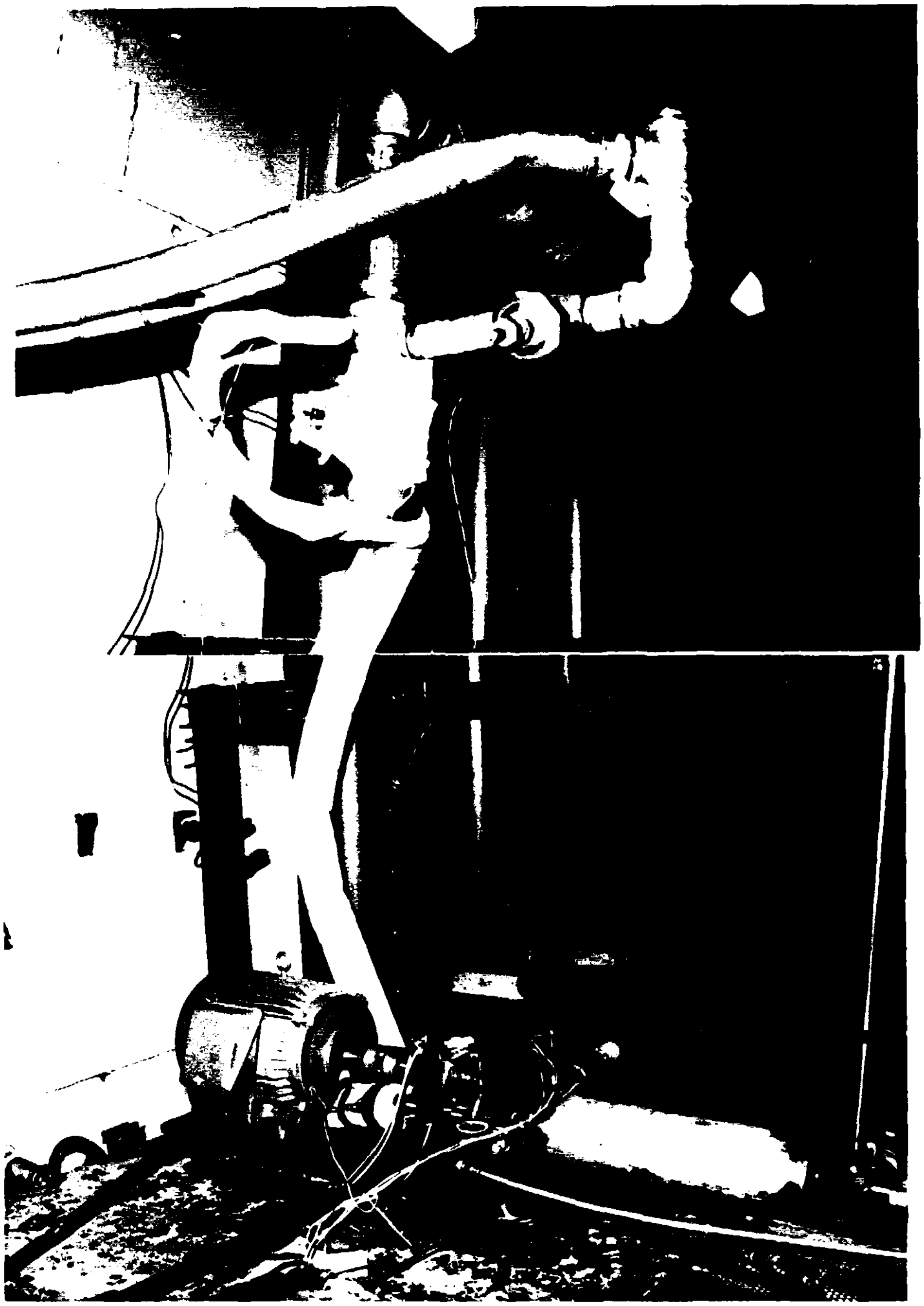

Figure 4-18, A Bypass was Used on the Heater for the "Coolant" Flow (This allowed more flow through the heaters, giving more stable control and also eliminated changes in upstream pressure due to changes in flow, except, of course, for friction drop from the bypass to the chopper. A small bypass valve was used for fine adjustment.)

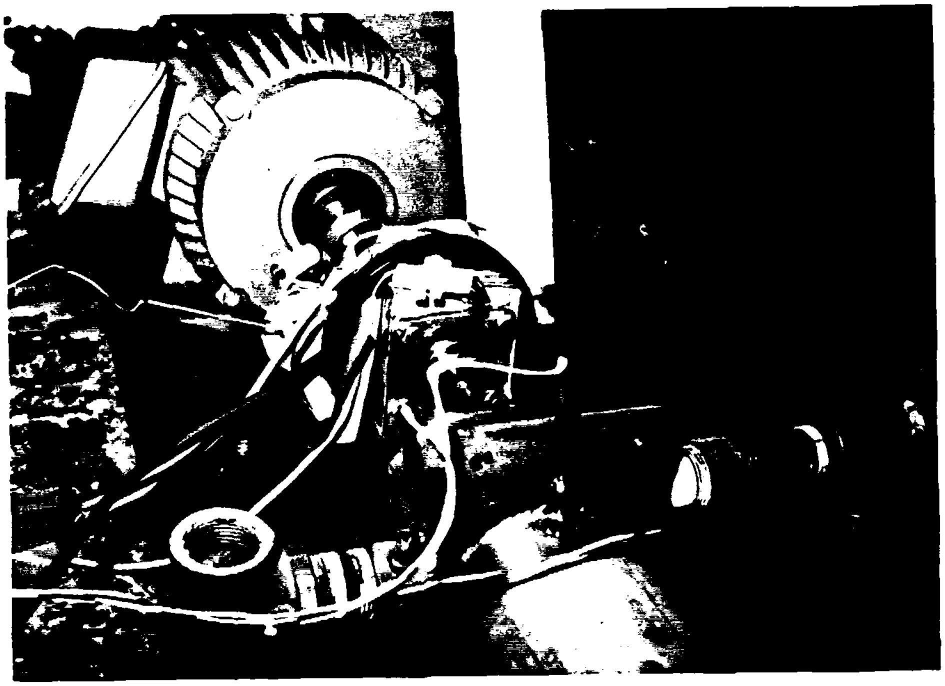

Figure 4-19, The Four Thermocouples Measuring Air Temperature In and Out for Hot and Cold Side are Shown

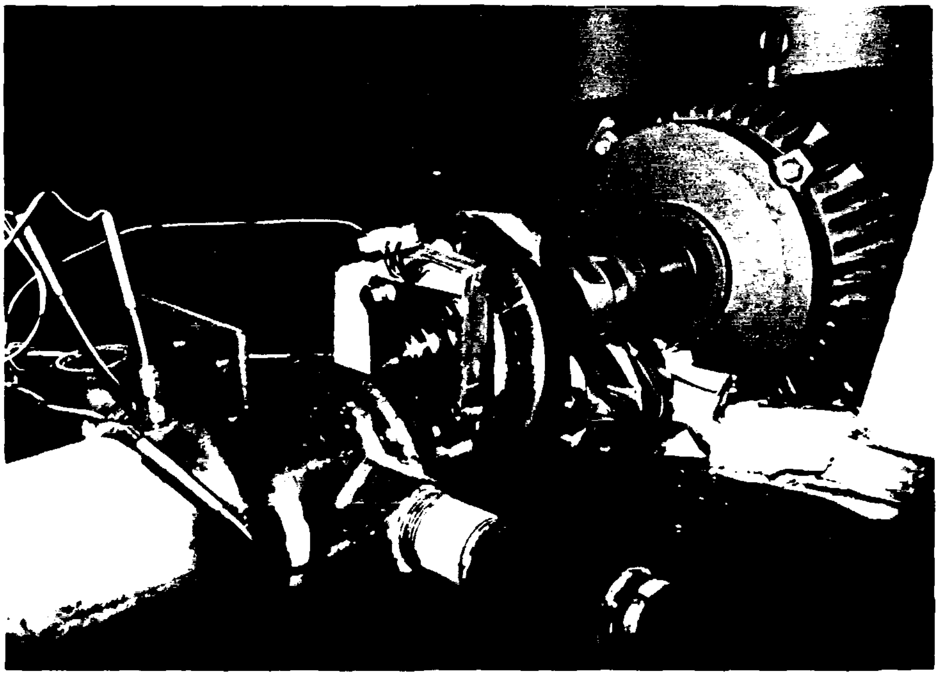

Figure 4-20, The "Hot - In" Location is Shown

5.0 EXPERIMENTAL RESULTS

The test apparatus was operated over a range of disturbance frequencies from 0 to 720 Hz. Sensitivity analyses were conducted on flow, temperature, and pressure. Several hundred runs were made and all data that is presented was repeated on different days for reproducibility.

The rated speed of the high-pressure shaft of the AGT1500 engine is 720 Hz. Normal operation is from 60% to 100% speed. This gives the area of prime interest. To complete the data base and to provide correlation with other researchers, data to 0 Hz was taken and is presented. The baseline to which all data is compared is 0 Hz.

To ensure that the baseline has not wandered and considering that it takes several hours to take a modest set of data, the 0-Hz baseline data was rerun before and after every data point at frequency. It can be seen from the data that the baseline does wander slightly and comparisons are only made with zero baseline data taken before and after the data point at frequency.

The data is presented in two ways:

- Heat Transfer to the cooling air as a function of frequency (Table 5-1, Figure 5-1).
- Change in heat transfer to the cooling air, represented by the heat transfer at frequency divided by the 0-Hz baseline data (Figure 5-2). This gives a number between 1.0 and 2.0. The 0 Hz data always appears as 1.0.

Where significant harmonics are evident, additional data is presented to verify that the phenomena is not data scatter and to give finer resolution to the data.
Figures 5-1 and 5-2 clearly show the following:

- Heat transfer is enhanced in all cases by the presence of pulsed flow as compared to steady flow at the same flow rate and temperatures.
- There is a general trend of increasing heat transfer with frequency.
- The data has many peaks and valleys that must be explained.

The most dramatic change in the heat transfer characteristics is in the range 340 Hz to 400 Hz. Additional data was taken in this range to confirm this trend and provide greater resolution. (Figures 5-3, 5-4)

It is interesting to see the data just as it was taken. Figure 5-5 shows the baseline data along with the data at frequency. If the data were perfect, the 0-Hz points would lie on a constant value line. The change of each peak from its surrounding 0-Hz baseline points is the enhancement in heat transfer when the flow is pulsed at that frequency.

The data in Table 5-2 and Figure 5-6 shows the pressure at the inlet to the chopper as a function of frequency. No change is made to the upstream conditions. Also shown is the 0 Hz flowing condition and the pressure when the flow is completely stopped.

The data in Table 5-3 and Figure 5-7 shows the pressure at the inlet to the chopper as a function of flow for the steady-flow condition (0 Hz) and for 400 Hz. As in the previous chart, at no flow the pressure is 11.6 psi. This is the pressure of the bypass flow at the point that the flow for the cooling air is bled off. When the cooling flow is zero, as Pascal would have it, the pressure at the chopper is that same pressure.

The pressure at the inlet to the chopper for the intermittent flow, varies from a peak pressure at no flow to a lower pressure equal to the pressure at steady flow with the pulse generator holes aligned. The peak pressure varies, however, with frequency. As frequency increases, the time between peaks decreases. There is a set length that the pressure wave must travel (56 inches) to the bypass (Figure 4-18) which remains at essentially constant pressure. As long as the time between peaks is greater than the time required for the finite wave to negotiate the 56 inches, the peak will be the pressure at the bypass. When the period of the pulse is shorter than the time required for the finite wave to travel 56 inches, the pressure will be less. The pressure will be equal to the pressure at the limit of travel of the wave in the line leading from the bypass to the chopper.

Using the computed velocity of the pressure wave in chapter V, below 350 Hz the pressure pulse is as high as the no-flow condition. The amplitude is a function of the velocity through the chopper and the lines going to the chopper. It was not possible to achieve large amplitudes at low flow rates.

All of the data shown thus far was taken by reading the temperatures stabilized at 0 Hz, starting the motor, adjusting the frequency, then adjusting the upstream air valve so that the mass flow through the test section was identical to the 0 Hz baseline case.

In Figure 5-8, the flow was not adjusted. The baseline case was read, the motor was started and adjusted to speed. No change was made to the flow valves. The flows are lower, but total heat transfer is still enhanced. 400 Hz was selected because it is the most prominent resonance condition.

Tables 5-4 and 5-5 and Figures 5-9 and 5-10 show data at 0 Hz and 100 Hz at varying flows from the normal test condition, .104 lb/min, down toward zero. The validity of the experiment breaks down at very low flows. This is perhaps because the temperature of the surrounding metal influences the thermocouple at the very low flows.

Earlier published works have reported a phenomenon whereby no effect was made on heat transfer until the strength of the flow or pressure variation was increased to some critical value, after which changes in heat transfer were recorded. This test setup has the characteristic of giving strong pulses as flow is completely stopped and started as compared to earlier apparata which either superimposed a sound wave on the flow or modulated a bypass line. None the less, the flow was decreased gradually toward zero from the normal test condition by instituting upstream pressure drops, and heat transfer was again compared between 0 Hz and 100 Hz.

The data at Table 5-6 and Figure 5-11 shows that such a condition occurs, if at all, at around .057 lb/min, although, again, data scatter at the very low flows makes it difficult to be precise. It is possible that this phenomenon does not occur when a chopper completely interrupts the flow.

Of significance to this experiment, however, is that with the complete flow interruption, the critical point referenced by earlier researchers is always exceeded at even low flows and certainly at flows pertinent to gas turbine blade cooling.

5.1 Error Analysis

The uncertainties associated with the calculation of the heat transfer are estimated following the procedure used by Kline (46). The uncertainty WR in R is given by

$$\omega_R = \left[\left(\frac{\partial R}{\partial v_1}\Delta v_1\right)^2 + \left(\frac{\partial R}{\partial v_2}\Delta v_2\right)^2 + \ldots \left(\frac{\partial R}{\partial v_n}\Delta v_n\right)^2\right]^{1/2} \qquad (27)$$

where R is a function of V1,V2,...,Vn, and _V1, _V2, etc are the uncertainties in V1, V2...Vn,respectively. This can also be represented as:

$$\frac{\omega_R}{R} = \left[\left(\frac{\Delta v_1}{v_1}\right)^2 + \left(\frac{\Delta v_1}{v_2}\right)^2 + \ldots \left(\frac{\Delta v_n}{v_n}\right)^2\right]^{1/2} \qquad (28)$$

In the present experiment, four measurements are made that distinguish the comparators: hot-side flow, cold-side flow, temperature change across the cold side, temperature difference between hot side and average cold side.

Estimate of the system accuracy of the thermocouples and the data acquisition system is provided by the manufacturer. For type J thermocouples in the range of this experiment, the estimated error is .7 F. This includes the thermocouple, scanner, a-d converter and the electronic reference junction.

Accuracy of the flow measurement is a combination of the ability to measure the pressure differential across the nozzle, air temperature and pressure and barometer for density calculation.

The accuracy of the pressure differential measurement is taken as the resolution of the inclined manometer, .01 inch. The accuracy of the temperature is .7 F, and the barometer is .01 in Hg.

The significance of the cold-side temperature difference is much greater than the hot side. This is taken into account by using the temperature difference in and out for the cold side and the difference between the hot-side initial temperature and the cold-side initial temperature for the hot side. The accuracy of the cold side flow is much more significant than the hot side. This is taken into consideration by comparing to the magnitude of the flows, since the level of significance is a result of the relative magnitude of the flows.

Table 5-7 shows the representative values used in the error analysis and the calculations of the composite uncertainty.

The uncertainty associated with the cold side temperature difference is represented by:

$$\omega_{TC} = \frac{\Delta T}{T_6 - T_7} = \frac{0.01}{77} = 0.00013 \qquad (29)$$

The uncertainty associated with the hot side temperature difference is represented by:

$$\omega_{TH} = \frac{\Delta T}{T_3 - T_4} = \frac{0.01}{43} = 0.000233 \qquad (30)$$

The uncertainty associated with the cold side mass flow is:

$$\omega_{in\ c} = \left[\left(\frac{\Delta P}{\text{manometer}}\right)^2 + \left(\frac{\Delta T}{T_8}\right)^2 + \left(\frac{\Delta P}{P_{10}}\right)^2 + \left(\frac{\Delta B}{\text{barometer}}\right)^2\right]^{1/2} \quad (31)$$

$$= \left[\left(\frac{0.01}{2.0}\right)^2 + \left(\frac{0.1}{80}\right)^2 + \left(\frac{0.001}{0.2}\right)^2 + \left(\frac{0.01}{30}\right)^2\right]^{1/2}$$

$$= 0.0072$$

The uncertainty associated with the hot-side mass flow is:

$$\omega_{in\ h} = \left[\left(\frac{\Delta P}{\text{manometer}}\right)^2 + \left(\frac{\Delta T}{T_5}\right)^2 + \left(\frac{\Delta P}{P_{11}}\right)^2 + \left(\frac{\Delta B}{\text{Barometer}}\right)^2\right]^{1/2} \quad (32)$$

$$= \left[\left(\frac{0.01}{1.0}\right)^2 + \left(\frac{0.1}{80}\right)^2 + \left(\frac{0.001}{6.5}\right)^2 + \left(\frac{0.01}{30}\right)^2\right]^{1/2}$$

$$= 0.00037$$

The composite uncertainty is represented by:

$$\left[\omega_{TH}^2 + \omega_{TC}^2 + \omega_{in\ h}^2 + \omega_{in\ c}^2\right]^{1/2} \quad (33)$$

$$= 0.0072$$

Hz	BTU/min	Change
0	2.08	
20	2.30	1.08
0	2.19	
40	2.53	1.18
0	2.09	
60	2.69	1.25
0	2.20	
80	2.44	1.13
0	2.11	
100	2.48	1.15
0	2.21	
110	2.62	1.19
0	2.21	
120	2.63	1.18
0	2.24	
140	2.58	1.17
0	2.18	
160	2.48	1.12
0	2.24	
180	2.54	1.15
0	2.17	
200	2.61	1.18
0	2.24	
210	2.62	1.20
0	2.14	
220	2.54	1.16
0	2.23	
240	2.74	1.23
0	2.23	
260	2.64	1.18
0	2.25	
280	2.59	1.17
0	2.18	
300	2.60	1.19
0	2.18	
320	2.59	1.19
0	2.19	
340	2.34	1.08
0	2.14	
360	2.56	1.20
0	2.14	
380	2.76	1.26
0	2.23	
400	2.92	1.34
0	2.14	
420	2.82	1.32
0	2.12	
440	2.66	1.23
0	2.19	
460	2.70	1.22
0	2.24	
480	2.80	1.26
0	2.20	
500	2.82	1.30
0	2.14	
520	2.71	1.27
0	2.13	
540	2.63	1.22
0	2.17	
560	2.71	1.25
0	2.18	
580	2.65	1.22
0	2.17	
600	2.78	1.31
0	2.06	
620	2.91	1.36
0	2.23	
640	2.96	1.35
0	2.15	
660	2.89	1.35
0	2.12	
680	2.81	1.31
0	2.16	
700	2.77	1.23
0	2.33	
720	2.67	1.21
0	2.09	

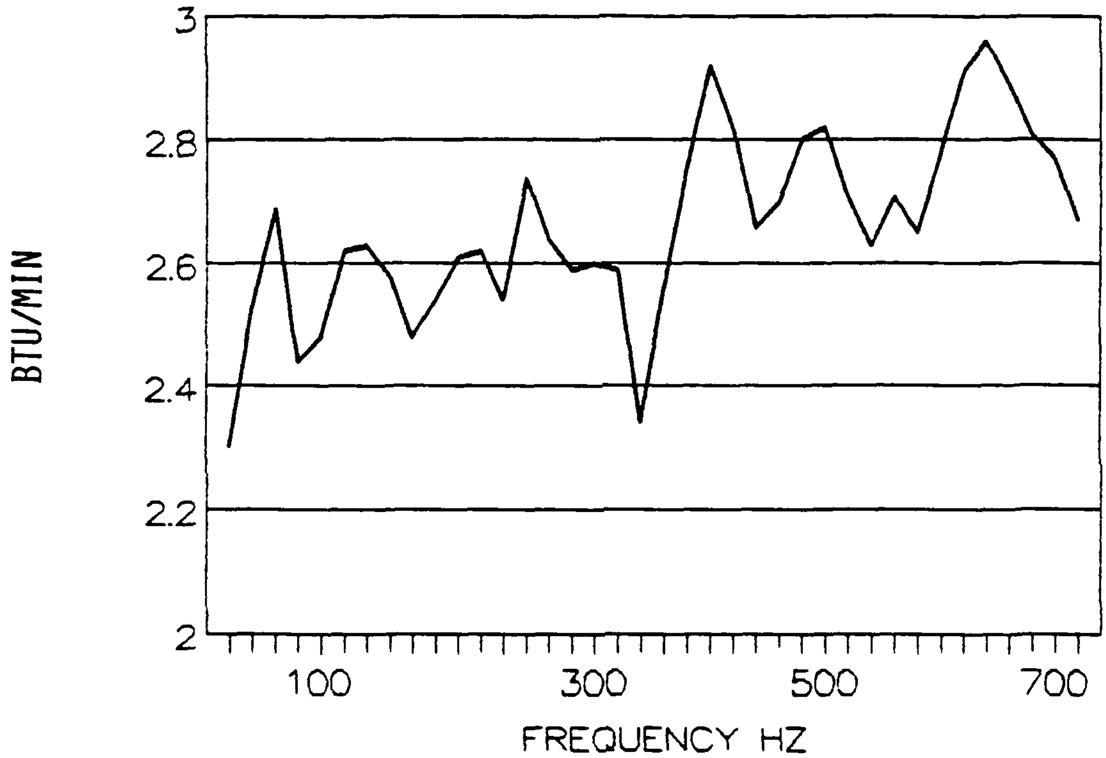

Figure 5-1, Heat Transfer VS Frequency

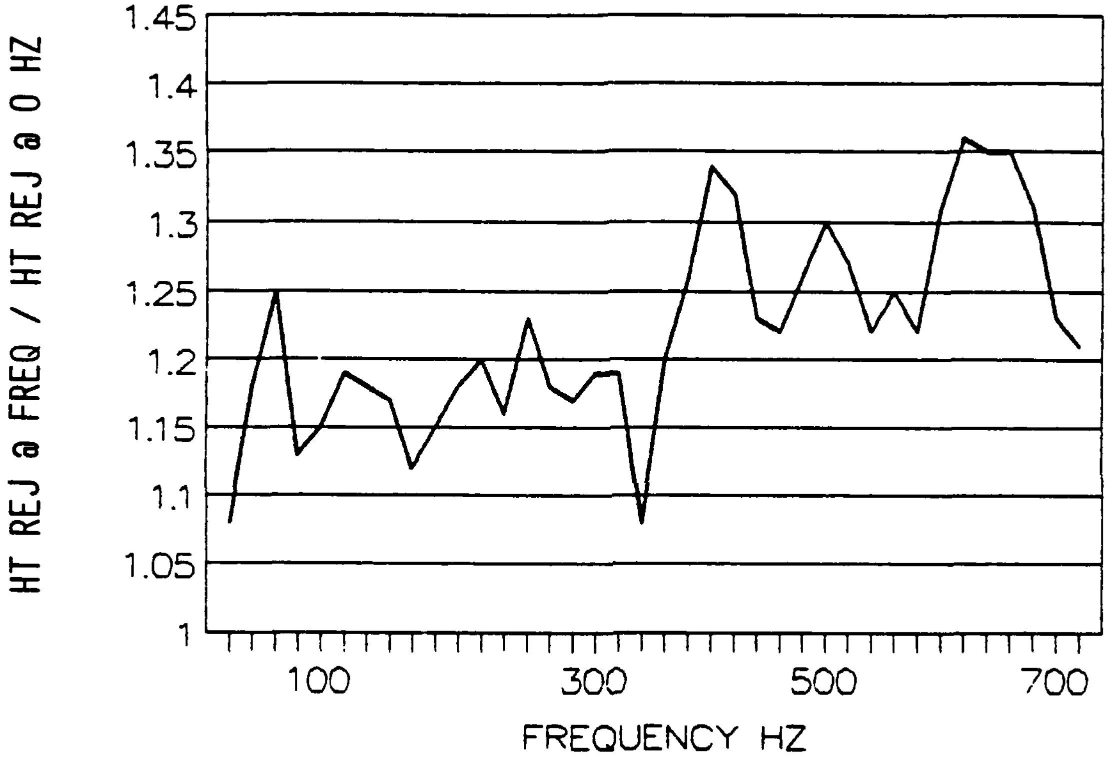

Figure 5-2, Increase in Heat Transfer

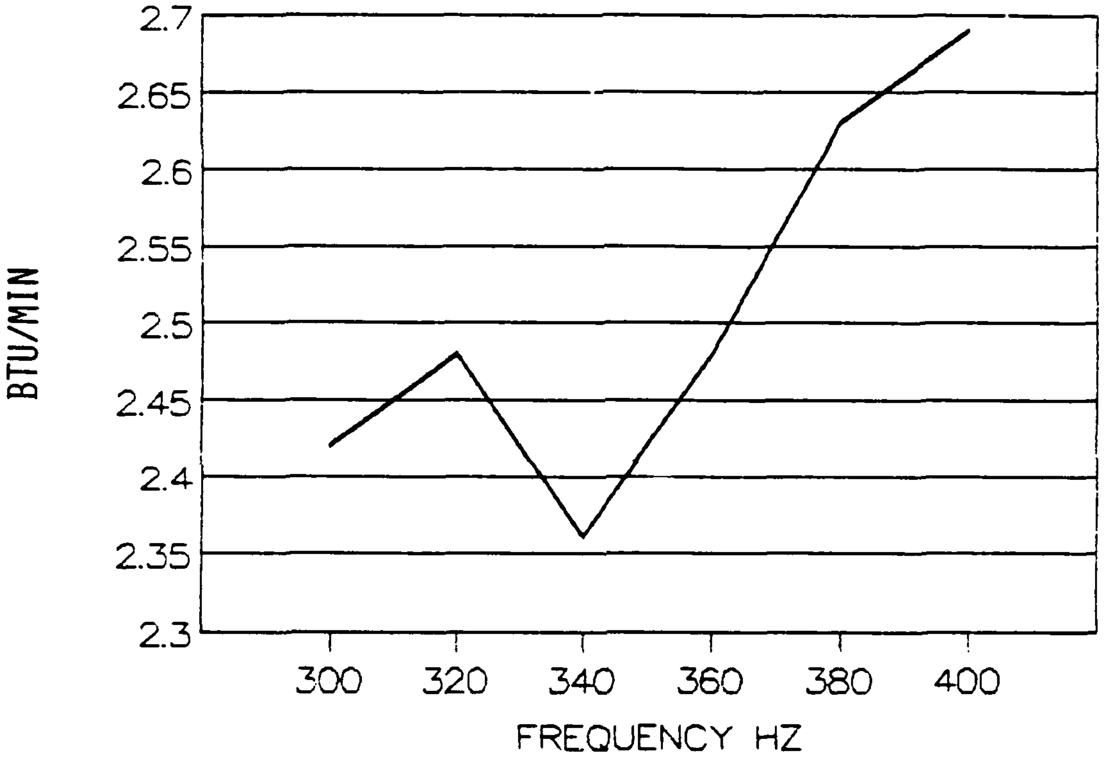

Figure 5-3, Heat Transfer VS Frequency

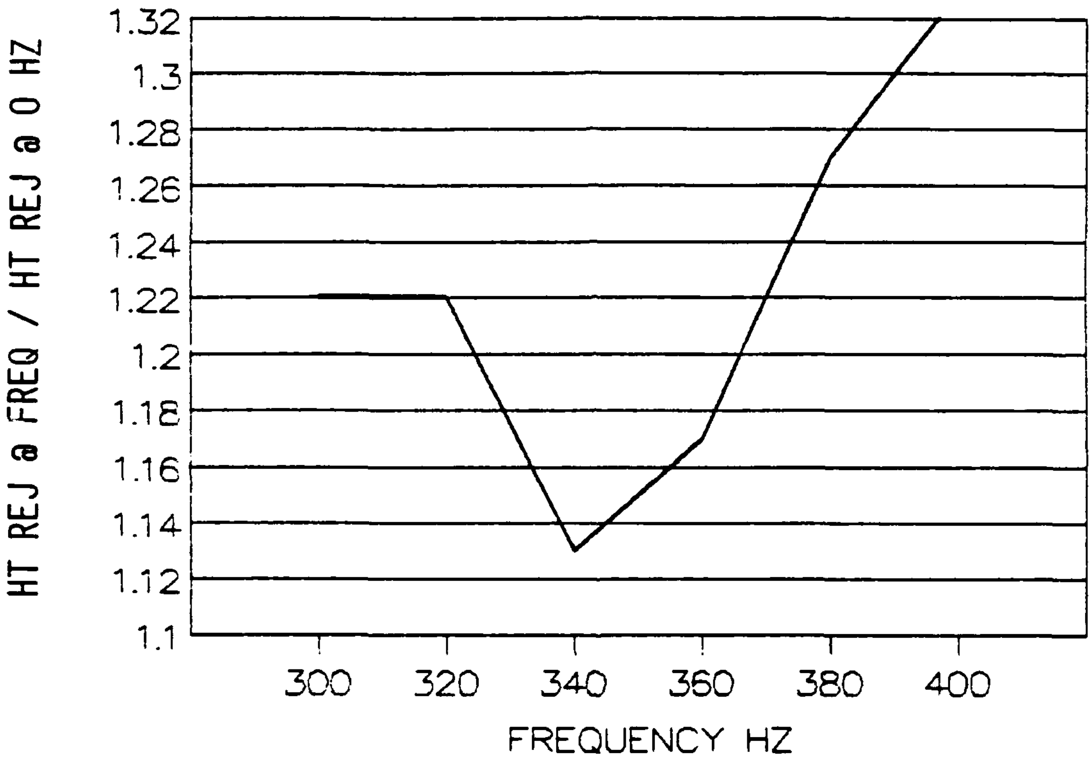

Figure 5-4, Increase in Heat Transfer

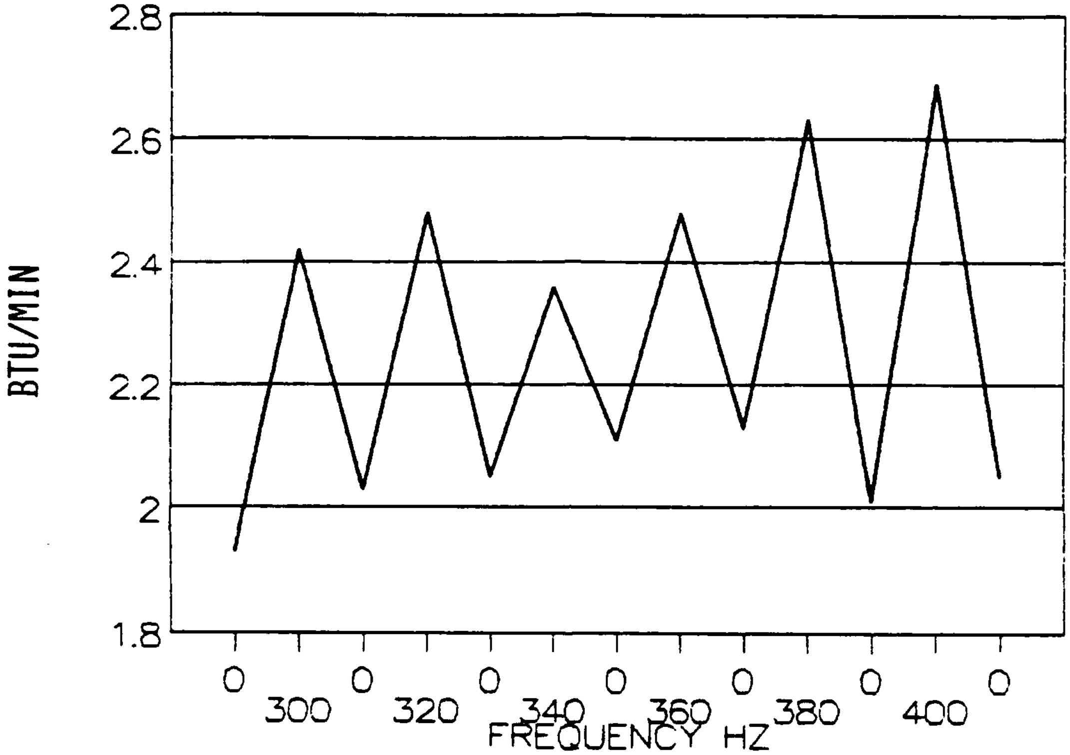

Figure 5-5, Heat Transfer VS Frequency

Table 5-2, Pressure into chopper as a function of frequency

Hz	psi	
Ø	11.6	no flow
Ø	Ø.38	flowing
2Ø	1.4	
1ØØ	1.5	
14Ø	1.1	
18Ø	1.24	
2ØØ	1.53	
24Ø	1.44	
28Ø	1.16	
3ØØ	1.4	
34Ø	1.82	
38Ø	1.74	
4ØØ	1.81	
44Ø	2.4	
48Ø	2.83	
5ØØ	2.85	
54Ø	2.45	
58Ø	2.55	
6ØØ	2.42	
64Ø	2.65	
68Ø	2.1	
7ØØ	1.79	
72Ø	1.66	

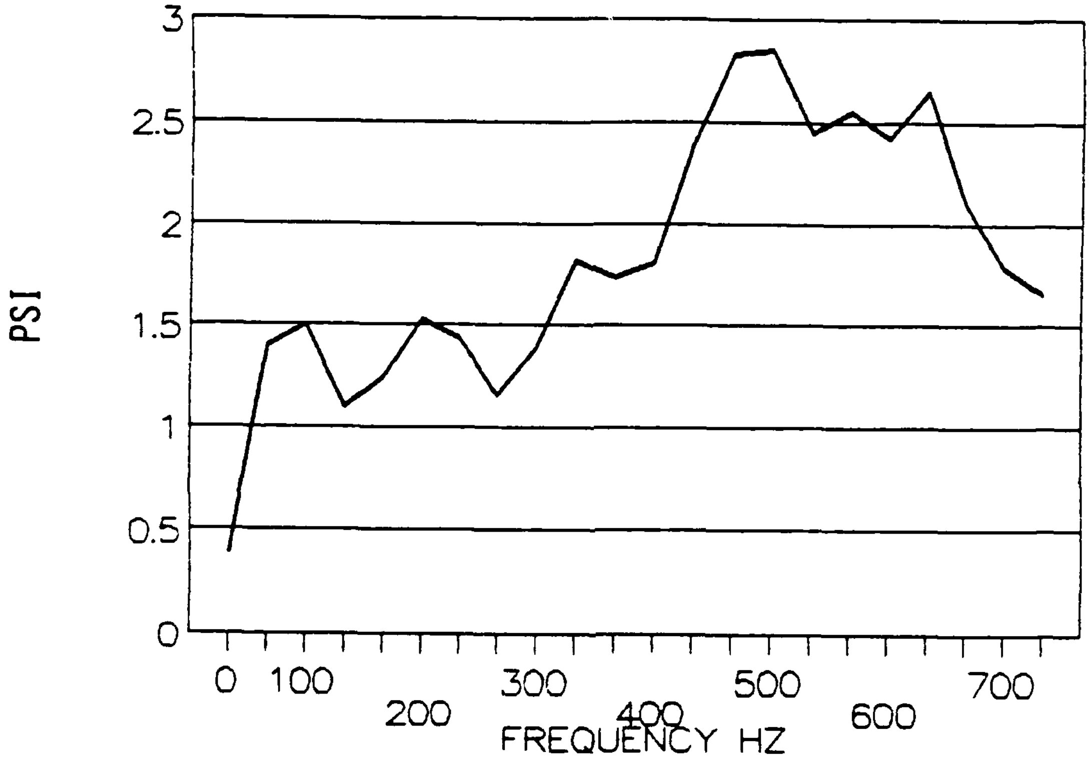

Figure 5-6, Pressure Into Chopper VS Frequency

Table 5-3, Flow Rate vs Pressure

Flow lb/min	Ø Hz psi	4ØØ Hz psi
Ø.1Ø4	Ø.645	2.23
Ø.1Ø1	Ø.612	2.Ø4
Ø.Ø99	Ø.6	1.91
Ø.Ø98	Ø.55	1.72
Ø.Ø96	Ø.5	1.92
Ø.Ø93	Ø.45	1.73
Ø.Ø9	Ø.43	1.55
Ø.Ø87	Ø.42	1.38
Ø.Ø8	Ø.4	1.12
Ø.Ø77	Ø.348	1.12
Ø.Ø68	Ø.312	Ø.9Ø6
Ø.Ø59	Ø.2	Ø.651
Ø.Ø51	Ø.138	Ø.459

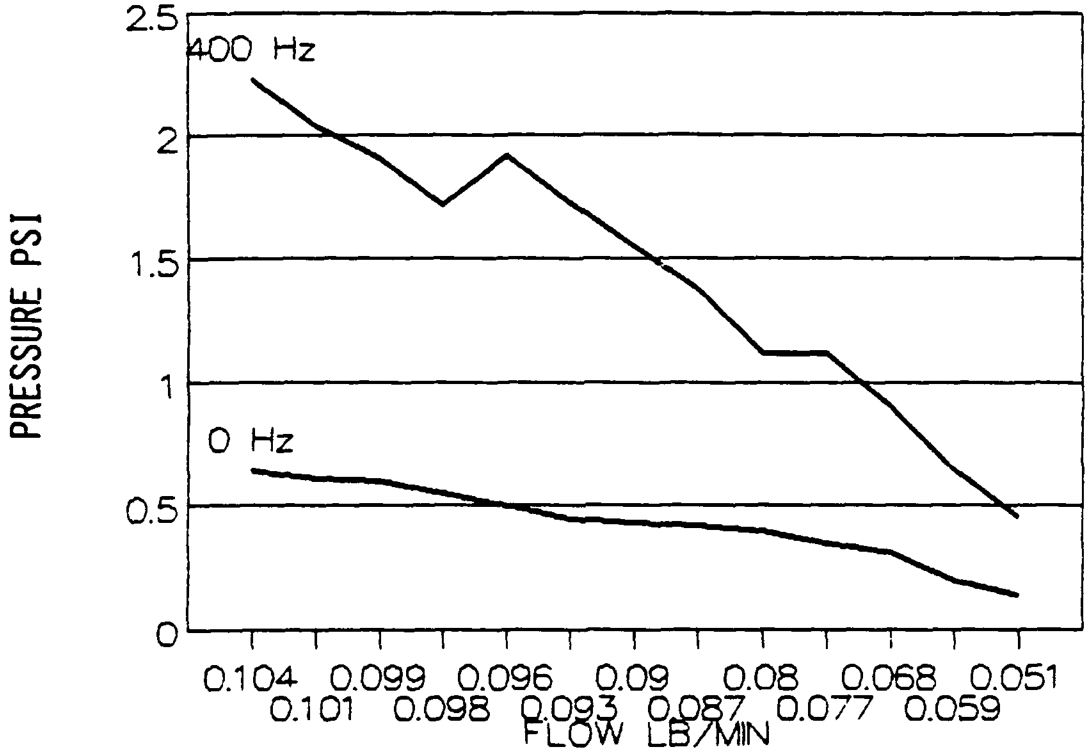

Figure 5-7, Pressure Into Chopper VS Flow

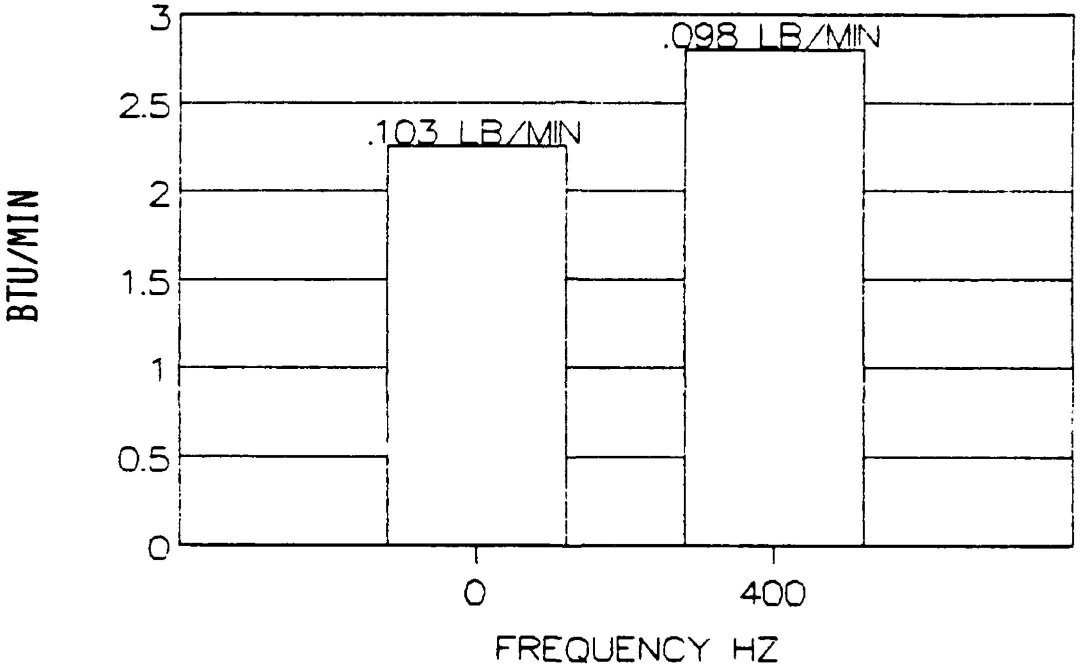

Figure 5-8, Change in Heat Rejection

No Change in Flow Setting

Table 5-4, Heat Rejection at Diminishing Flows

Hz	BTU/min	Pressure	Flow
0	1.71	0.09	0.052
100	1.83	0.43	0.052
0	1.82	0.24	0.073
100	2.13	0.94	0.073
0	2.10	0.31	0.090
100	2.47	1.18	0.090
0	2.23	0.42	0.104
100	2.58	1.40	0.104

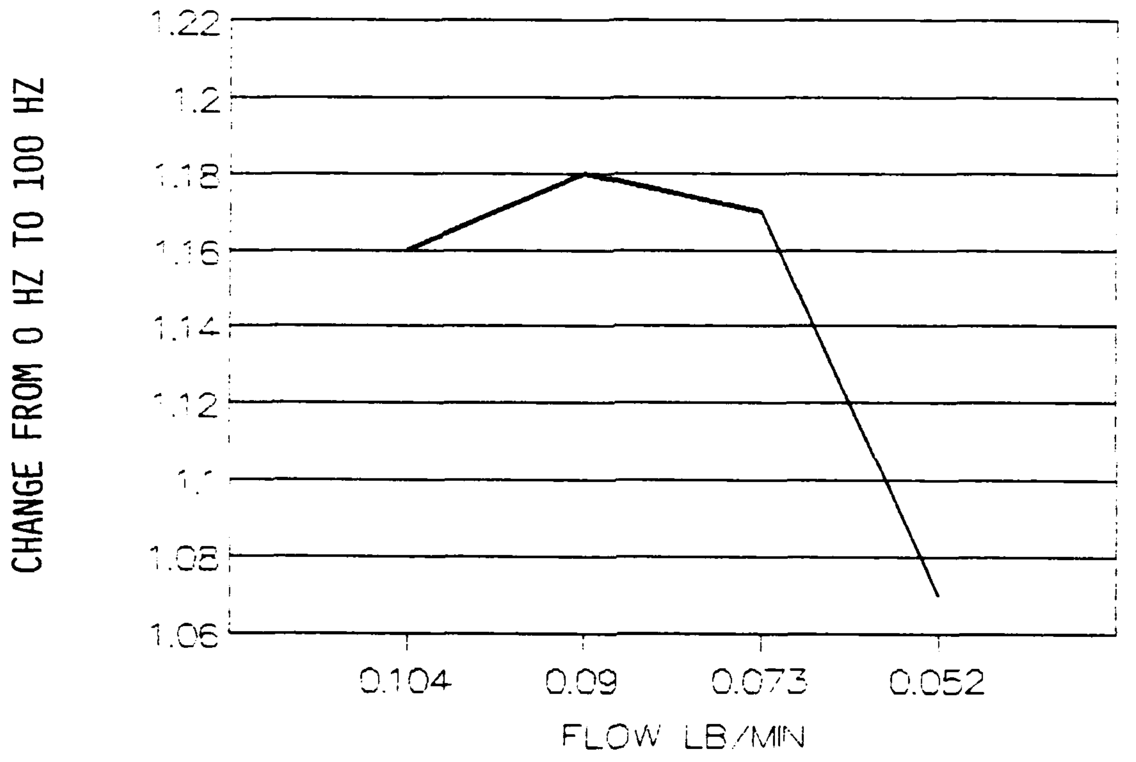

Figure 5-9, Change in Heat Transfer

0 HZ VS 100 HZ

Table 5-5

Hz	Setting	Flow	BTU/Min	
0	2.00	0.103	2.07	
400	1.82	0.098	2.69	Same valve setting as 0 Hz, .103 lb/
400	1.52	0.090	2.54	
400	1.43	0.087	2.46	
400	1.20	0.080	2.36	
400	1.13	0.077	2.46	
400	0.87	0.068	2.16	
400	0.67	0.059	2.29	
400	0.50	0.051	2.48	
0	0.50	0.051	1.90	
0	2.00	0.103	2.22	
400	1.83	0.099	2.80	Same valve setting as 0 Hz, .103 lb/
400	2.00	0.103	2.64	

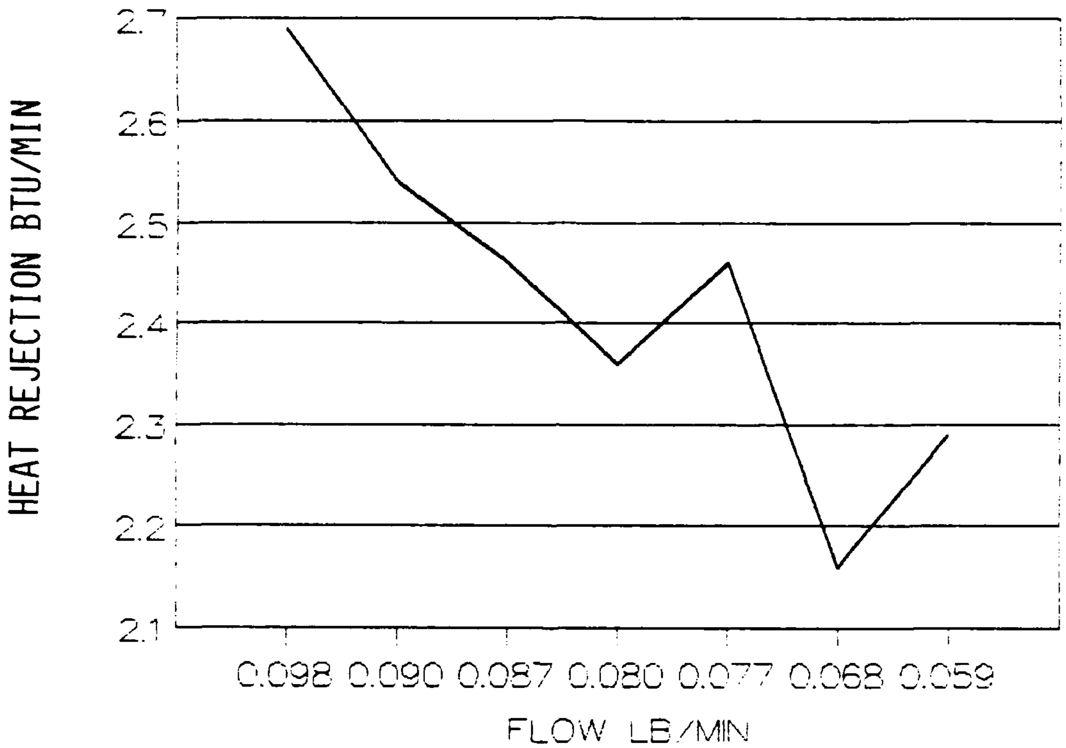

Figure 5-10, Heat Rejection VS Flow

Table 5-6, A test to find a break point of pulse strength below which the pulse has no effect on the boundary layer

Hz	Flow	Pressure	BTU/Min	Change
0	0.073	0.555	1.68	
100	0.073	1.18	1.82	1.08
0	0.066	0.516	1.66	
100	0.066	0.981	1.9	1.14
0	0.057	0.399	1.98	
100	0.057	0.657	1.99	1.01
0	0.048	0.369	2.34	
100	0.048	0.447	2.43	1.04

Table 5-7 Uncertainty

Measurement	uncertainty	Representative value
Temperature,cold	.7	77
Temperature,hot	.7	43
delP,flow,hot	.01	1.0
Temp,nozzle	.7	80
Pressure,nozzle	.01	6.5
delP,flow,cold	.01	2.0
Temp,nozzle	.7	80
Pressure,nozzle	.01	.2
Barometer	.01	30

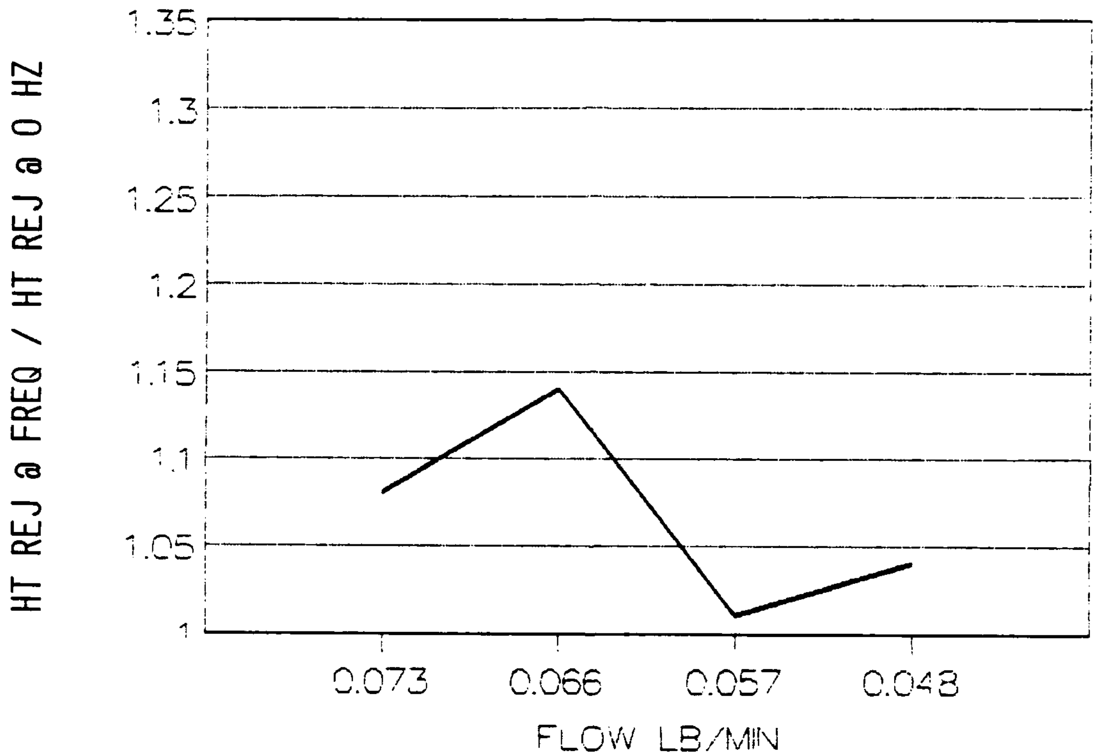

Figure 5-11, Heat Transfer Change VS Flow

6.Ø ANALYSIS AND CORRELATION

The effect being noted in the test data is similar to that of turbulence generators placed in heat transfer fins and passages in many applications. The boundary layer on the inside of the cooling passage wall acts as an insulator, a hindrance to heat transfer from the wall of the passage to the cooling fluid. This limits the effectiveness of the cooling process. The intermittent interruption of the cooling flow disrupts the boundary layer, scrubbing it from the wall, enhancing the heat transfer process. As seen from the data and the publications of earlier work, this phenomenon is a function of both the strength of the pulse and frequency.

The test data shows a general increase in the effectiveness of the heat transfer process with resonance effects superimposed. Although there are some very significant variations with frequency, at no time does the heat transfer become worse than the steady flow case, nor does it reach a level as low as the steady flow case. This differs from several of the earlier researchers mentioned.

The analysis of the phenomena will be be based on three separate, though not discrete, differences between the steady flow and the pulsed flow.

- The peaks in the change in heat transfer which occur at harmonics of the physical system.
- Increased turbulence due to an increased effective Reynolds number.
- An increase in heat transfer as a function of frequency due to the decreased time available to form the boundary layer after the flow is restarted.

Each of the effects will be described separately and compared to the steady flow case.

Harmonics occur when the pressure wave travels the length of the tube, reflects back and arrives at the fore end simultaneous with the generation of the next pressure wave, reinforcing that wave. Harmonics in the passages before and after the tube can affect heat transfer by altering the pressure at the inlet and exit of the test specimen.

Additional harmonics occur with the combined effects of these primary harmonics. The frequency of these harmonics is a function of geometry and the velocity of wave propagation.

The velocity of propagation of the wave is the sum of the media velocity and the velocity of the finite disturbance.

The compression wave of the finite disturbance caused by the flow interruption is propagated at some velocity, w, which is greater than the fluid particle velocity. The derivation of the velocity of propagation is at Appendix D. The finite wave always travels faster than the sonic velocity and velocity of the finite wave is dependent on both fluid conditions and wave strength (P2/P1).

Using this equation the test apparatus was evaluated for resonance conditions. The small tube that represents the cooling passage has a primary resonance at 1633 Hz, well above the test range of this research. The tube prior to the chopper has a primary resonance at 186 Hz. The chamber after the test section has a primary resonance at 570 Hz. The cavities both before and after the test section appear capable of generating significant harmonics in the test data.

The most pronounced resonances appearing in the heat transfer data are 340 Hz (a minimum), 400 Hz (a maximum), 620 Hz (a maximum). The resolution on this data is 20 Hz. Because these are characteristic only of the test rig, there is no good reason to generalize on this data except to say that the cavities external to the blade itself can provide very significant influence on the heat transfer inside the blade and are an area for careful design and test.

While the predicted resonance frequencies differ from the data by 10% and more, the characteristics are demonstrated. The test section resonance would be much easier to predict accurately than the rather complex arrangements of tubes before and after the test section. There are, without a doubt, peaks in the data that are the result of combinations of resonance effects in the apparatus. An exhaustive search for these resonances would be of no particular value.

The second influencing factor is the effectively higher Reynolds number. In the present experiment, the mass flow was kept constant by adjusting the restriction between the supply bypass (see Figure 4-1) and the chopper. With the geometry of the chopper, the flow is reduced whenever the holes are not exactly aligned. During the phase of the cycle that the valve is completely open, the velocity, and thus Reynolds number, is higher than the steady flow case. The pressure at the inlet to the chopper during that phase of the cycle that the passage is reduced and closed, rises above the pressure at 0 Hz steady flow (.38 psig), and will reach the pressure at the bypass (11.6 psig) at frequencies below about 350 Hz.

Assuming that the effective valve area, when rotating, is 50 percent of the area of the valve when the pulse frequency is zero, the average Reynolds number, during flow, is twice the steady flow value. In accordance with equation 3, the heat transfer at any frequency other than zero should be increased by the ratio of the Reynolds numbers to the .8 power, a factor of 1.74. This should be independent of driving frequency. In Figure 6-5, this appears as the top line.

The flow can be interrupted at any frequency that the chopper will operate. This will cause a rarefaction as the fluid downstream of the chopper attempts to continue motion due to inertia. The fluid will backflow, if time permits, to even the pressure. Flow reversals such as this have been reported in the references of chapter 1 as a major cause of increased heat transfer. Re-establishment of the boundary layer is not so sudden an event. If the open time of the chopper cycle is shorter than the time required to reestablish a boundary layer equal to the steady flow case, then resistance to heat transfer equal to the steady flow case cannot occur in the portion of the cycle that fluid is flowing. If the entire mass of fluid were brought abruptly to a halt when the chopper closes, one would envision a period of heat transfer by conduction only, with sharply reduced heat transfer during this phase of the cycle. This does not occur and, in fact, the movement by inertia and rarefaction during the closed down phase of the cycle may well result in heat transfer equal to or greater than the steady flow rate.

The remaining effect is the the time available to re-establish the boundary layer. This is the frequency dependent model.

The increasing trend of heat transfer versus frequency can be generalized independent of the test apparatus. Figure 6-1 and Figure 6-2 show the increasing trend of the heat transfer coefficient as calculated from the heat transfer data. Figure 6-3 shows the same data with frequency represented by the Strouhal number. Using a least squares technique, an approximation of the data is shown in Figure 6-4.

The test data was limited to 720 Hz. This is partly because it represents the maximum speed of the engine, but also the design limit of the apparatus. The heat transfer data was going down from the maximum at 640 Hz. It is not known whether this is a local decline or whether the general trend upward is at an end and a general decline had begun. A general decline is inevitable. It is predicted that at very high frequencies the effect of the flow interruption will be simply to reduce flow.

The increase in heat transfer with frequency is a result of a reduction in boundary layer thickness as the higher pulse frequency makes creation of a substantial boundary layer increasingly more difficult. The cause is the time available to re-establish the boundary layer. This is the frequency dependent model. The time available to re-establish a boundary layer is inversely proportional to the driving frequency. If the time required to effectively re-establish a boundary layer equivalent to the steady flow case could be calculated, an important inflection in the rate of heat transfer versus frequency should have been identified.

A first order analysis can be made. The rate of momentum diffusion from the wall to the moving fluid is, in fact, the kinematic viscosity. The rate of thermal diffusion can be related to the momentum diffusion by use of the Prandtl Number. At Pr=1.0, these would be identical. Air, at roughly Pr=.7, will see a lag of the thermal diffusion relative to momentum diffusion. As the frequency of the pulse is increased, the time available to re-establish the boundary layer is decreased. For a given velocity, if the kinematic viscosity is constant and represents the primary factor in determining the rate at which the boundary layer is re-established, then the boundary layer thickness is inversely a function of the frequency.

Schlichting (47), in an approximate solution of the Navier-Stokes equations for flow across the "suddenly accelerated wall", determined the thickness of the boundary layer, during formation, to be proportional to the square root of the product of kinematic viscosity and time.

$$\delta \approx 4\sqrt{\upsilon t} \tag{22}$$

This suggests that the heat transfer coefficient for flow, in which the boundary layer is forming, should be a function of the square root of frequency. The influence of the thickness of the boundary layer on heat transfer must be estimated. The generally accepted, empirically derived relationship of Prandtl number and Reynolds number to Nusselt number for turbulent flow inside a tube (equation 3), will apply. The conductance heat transfer equation, Q = kA T/, says that as the boundary layer thickness increases, or as the conductivity decreases in the same proportion, there is the same negative effect on heat transfer. From this it may be said that the effect on heat transfer due to boundary layer thickness will be the same as a proportional but opposite change in conductance and will be represented by the Prandtl number to the .4 power. Combining with the influence of frequency on boundary layer thickness, we obtain an influence coefficient of frequency, represented by the Strouhal number to the (.5 x.4=) .2 power. Figure 6-5 shows the previously presented test data with the modeled curve overlay. The straight lines are the value of the Nusselt number at steady state from the test data (below), and the Nusselt number at the higher effective Reynolds number calculated from equation 3 . This does not take into account any of the effects of harmonics in the system which appear in the data.

On the other hand, if we assume that the effect of the Reynolds number is simply to reduce the thickness of the boundary layer, then the reduced boundary layer thickness will have an effect on heat transfer as represented by the Reynolds number to the .8 power. This gives Strouhal number to the (.5 x .8 =) .4 power. This curve is also plotted on Figure 6-5. These compare poorly with the curve fit of Figure 6-4.

Another model will be attempted. The data provides a way to calculate an average thermal boundary layer thickness as a function of frequency that can then be used to estimate the time required to re-establish the boundary layer. Treating the boundary layer as if it were a solid material and using the electrical analogy for heat transfer through a tube, the thickness of the boundary layer can be calculated from the heat transfer data. This assumes that the boundary layer is a constant. This, of course, is not true, as the boundary layer is disrupted and re-established to some extent with every cycle of the chopper. But an effective thickness could be interesting.

The heat transfer equation for the cylinder is:

$$Q = \frac{T_\omega - T_a}{R_{TH}} \qquad (23)$$

where

$$R_{TH} = \frac{\ln\left({r_0}/{r_0 - \delta} \right)}{2\pi k L} \qquad (24)$$

is the thermal resistance. is the boundary layer thickness. The calculation of boundary layer thickness vs. frequency is at Table 6-3. This boundary layer thickness is then used with equation 22 to calculate the time required to establish a boundary layer of that thickness.

The data is plotted two ways in Figure 6-6. First the boundary layer thickness, Schlichting model (equation 22) and the boundary layer calculated from the data using the conduction model. The conduction model uses average heat transfer data. If peak data were used, the curve would move up, making the cross-over point with time available at a lower frequency. This supports the data better and would approach more closely the real case.

Below this is the plot of the required time along with the period/2, 1/2f, of the driving frequency. The calculated time, using the steady state heat rejection values is also shown. This gives an indication of a time to establish a stable boundary layer. Again, the "calculated time" is from average data and would move up on the graph if peak values were plotted. These charts show that, neglecting other effects which influence the heat transfer data, the time available, for most or all of the data taken, is not sufficient to re-establish a boundary layer equivalent to the steady flow case.

One last model will be attempted. If the pulsed velocity, a function of time, is modeled by a periodic function such as,

$$v(t) = A\cos(\omega t) \qquad (25)$$

the time averaged velocity

$$\frac{1}{T}\int_0^T v(t)dT \qquad (26)$$

will equal the velocity of the steady state flow at the same total mass flow. Equation 3 will predict equivalent Nusselt number. This assumes an incompressible fluid, a good assumption since the Mach number is less than .1. Since the Reynolds number influences Nusselt Number to the .8 power, any intervention of velocity, albeit made up by increased peak velocity during part of the cycle, should lower heat transfer. This theory considers turbulence only and not the reduced time to establish boundary layers at higher frequency. Thinking of the very low frequency, 5 minutes on, 5 minutes off, the time to establish a boundary layer is insignificant. Heat transfer will be reduced even though the velocity when flowing is twice the velocity during the steady flow case.

One last thought describing the physical case. Since the pulsations tend to attenuate as they travel down the tube, the flow at the exit of the tube may be more like the steady flow case than the cleanly pulsed flow entering the tube. This is a simple explanation for the Nusselt number being lower than that predicted by the higher Reynolds number alone. A model of this decay would be an exponential term that makes the model approach the steady state value at high time.

Due to the effects of harmonics, any model that does not deal with the harmonics is not sufficient to describe the heat transfer at any given frequency. Such a model is appropriate, however, to predict the effect of a range of frequencies.

Table 6-1, Calculation of h and Nu
Characteristic length is tube diameter = .0254 ft

Hz	Q BTU/min	A ft2	Th F	Tc F	h BTU/hrft2F	k	Nu hD/k
0	2.08	0.0399	800.0	190.4	5.131	0.0177	7.366
20	2.30	0.0399	800.0	188.3	5.654	0.0176	8.140
0	2.19	0.0399	800.0	187.0	5.372	0.0176	7.747
40	2.53	0.0399	800.0	187.2	6.208	0.0176	8.951
0	2.09	0.0399	800.0	187.9	5.135	0.0176	7.396
60	2.69	0.0399	800.0	188.5	6.615	0.0176	9.520
0	2.20	0.0399	800.0	189.9	5.423	0.0177	7.790
80	2.44	0.0399	800.0	189.3	6.008	0.0177	8.638
0	2.11	0.0399	800.0	192.3	5.221	0.0177	7.476
100	2.48	0.0399	800.0	190.6	6.120	0.0177	8.783
0	2.21	0.0399	800.0	193.3	5.478	0.0178	7.833
110	2.62	0.0399	800.0	190.6	6.465	0.0177	9.279
0	2.21	0.0399	800.0	192.1	5.467	0.0177	7.830
120	2.63	0.0399	800.0	190.4	6.488	0.0177	9.313
0	2.24	0.0399	800.0	191.8	5.538	0.0177	7.936
140	2.58	0.0399	800.0	188.5	6.345	0.0176	9.131
0	2.18	0.0399	800.0	191.0	5.383	0.0177	7.721
160	2.48	0.0399	800.0	188.1	6.095	0.0176	8.776
0	2.24	0.0399	800.0	191.6	5.537	0.0177	7.935
180	2.54	0.0399	800.0	188.9	6.250	0.0177	8.991
0	2.17	0.0399	800.0	191.8	5.365	0.0177	7.688
200	2.61	0.0399	800.0	188.5	6.418	0.0176	9.237
0	2.24	0.0399	800.0	190.1	5.523	0.0177	7.932
210	2.62	0.0399	800.0	187.2	6.429	0.0176	9.269
0	2.14	0.0399	800.0	190.6	5.281	0.0177	7.579
220	2.54	0.0399	800.0	187.5	6.236	0.0176	8.987
0	2.23	0.0399	800.0	190.1	5.498	0.0177	7.896
240	2.74	0.0399	800.0	187.9	6.731	0.0176	9.696
0	2.23	0.0399	800.0	190.8	5.505	0.0177	7.898
260	2.64	0.0399	800.0	188.7	6.494	0.0177	9.344
0	2.25	0.0399	800.0	190.6	5.552	0.0177	7.968
280	2.59	0.0399	800.0	187.9	6.363	0.0176	9.165
0	2.18	0.0399	800.0	190.6	5.379	0.0177	7.720
300	2.60	0.0399	800.0	187.2	6.380	0.0176	9.198
0	2.18	0.0399	800.0	191.3	5.386	0.0177	7.722
320	2.59	0.0399	800.0	189.2	6.376	0.0177	9.168
0	2.19	0.0399	800.0	191.7	5.414	0.0177	7.758
340	2.34	0.0399	800.0	190.1	5.769	0.0177	8.286
0	2.14	0.0399	800.0	193.3	5.304	0.0178	7.585
360	2.56	0.0399	800.0	191.1	6.322	0.0177	9.068
0	2.14	0.0399	800.0	193.3	5.304	0.0178	7.585
380	2.76	0.0399	800.0	189.5	6.798	0.0177	9.771
0	2.23	0.0399	800.0	192.1	5.516	0.0177	7.901
400	2.92	0.0399	800.0	188.1	7.176	0.0176	10.333
0	2.14	0.0399	800.0	190.2	5.277	0.0177	7.578
420	2.82	0.0399	800.0	184.6	6.891	0.0176	9.969
0	2.12	0.0399	800.0	187.8	5.207	0.0176	7.502
440	2.66	0.0399	800.0	184.5	6.499	0.0176	9.403
0	2.19	0.0399	800.0	187.7	5.378	0.0176	7.749
460	2.70	0.0399	800.0	186.3	6.616	0.0176	9.550

0	2.24	0.0399	800.0	190.0	5.522	0.0177	7.931
480	2.80	0.0399	800.0	187.7	6.877	0.0176	9.907
0	2.20	0.0399	800.0	189.8	5.422	0.0177	7.789
500	2.82	0.0399	800.0	187.0	6.918	0.0176	9.976
0	2.14	0.0399	800.0	189.8	5.274	0.0177	7.577
520	2.71	0.0399	800.0	187.0	6.648	0.0176	9.587
0	2.13	0.0399	800.0	190.2	5.253	0.0177	7.542
540	2.63	0.0399	800.0	189.1	6.474	0.0177	9.310
0	2.17	0.0399	800.0	191.6	5.364	0.0177	7.687
560	2.71	0.0399	800.0	189.1	6.671	0.0177	9.593
0	2.18	0.0399	800.0	190.2	5.376	0.0177	7.719
580	2.65	0.0399	800.0	187.5	6.506	0.0176	9.376
0	2.17	0.0399	800.0	189.8	5.348	0.0177	7.683
600	2.78	0.0399	800.0	186.7	6.816	0.0176	9.834
0	2.06	0.0399	800.0	191.2	5.088	0.0177	7.297
620	2.91	0.0399	800.0	189.0	7.162	0.0177	10.301
0	2.23	0.0399	800.0	193.0	5.525	0.0178	7.903
640	2.96	0.0399	800.0	190.2	7.299	0.0177	10.481
0	2.15	0.0399	800.0	191.7	5.315	0.0177	7.617
660	2.89	0.0399	800.0	189.4	7.117	0.0177	10.231
0	2.12	0.0399	800.0	191.7	5.241	0.0177	7.510
680	2.81	0.0399	800.0	190.4	6.932	0.0177	9.951
0	2.16	0.0399	800.0	192.8	5.349	0.0178	7.655
700	2.77	0.0399	800.0	189.3	6.821	0.0177	9.806
0	2.33	0.0399	800.0	181.6	5.666	0.0175	8.230
720	2.67	0.0399	800.0	186.4	6.543	0.0176	9.444
0	2.09	0.0399	800.0	188.8	5.142	0.0177	7.398

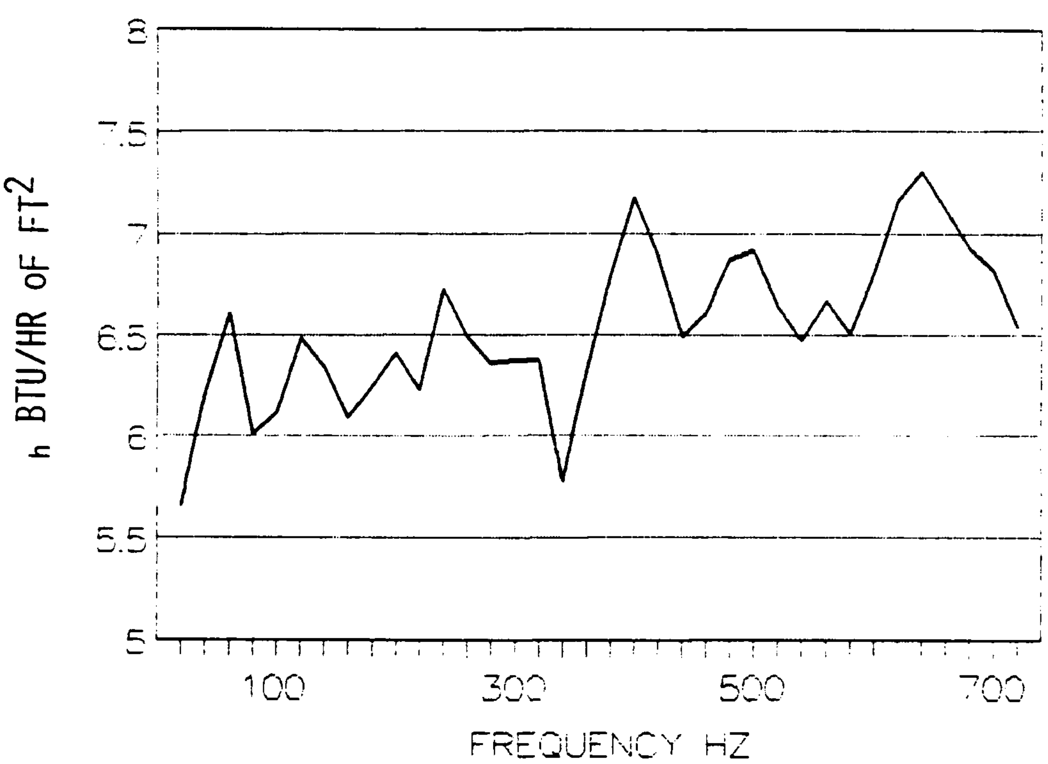

Figure 6-1, h vs Frequency

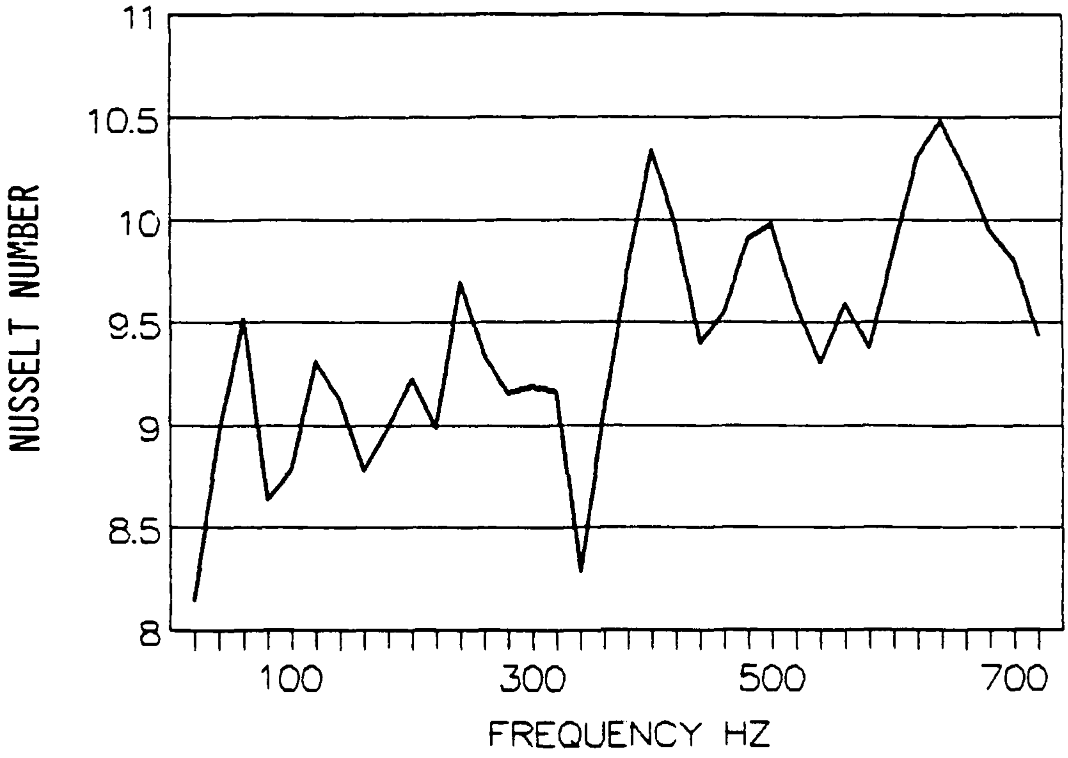

Figure 6-2, Nusselt Number vs Frequency

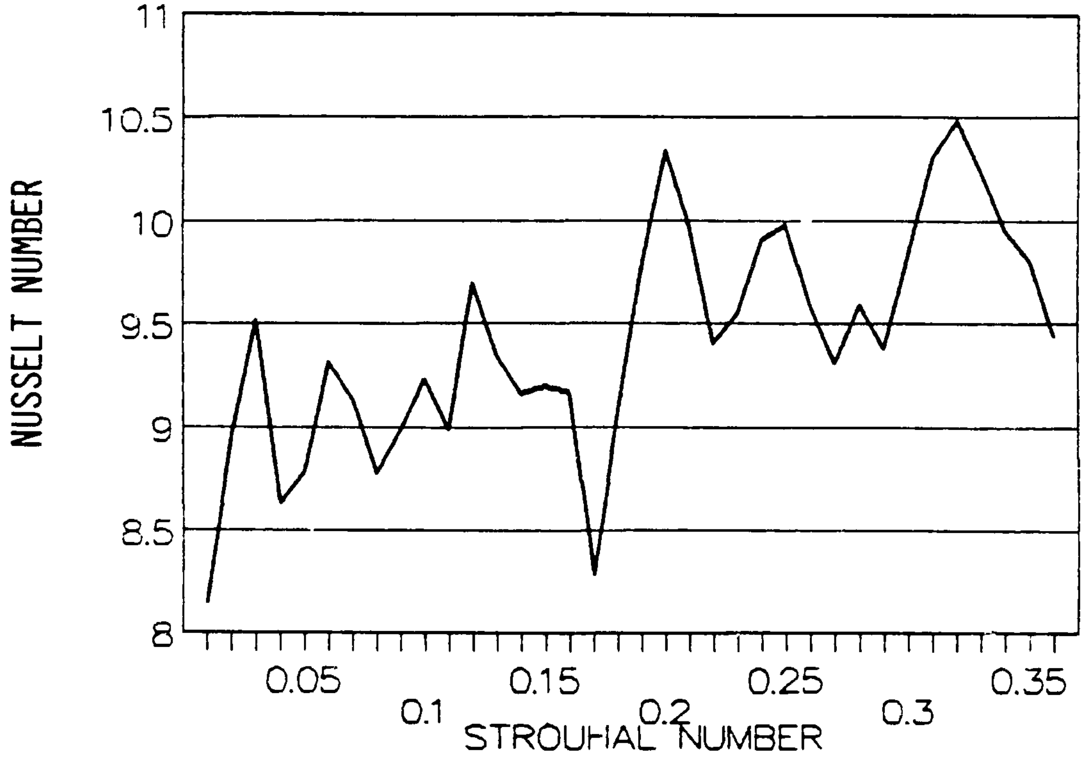

Figure 6-3, Nusselt Number vs Strouhal Number

Table 6-2, Least Squares Fit of Nu vs Str

Hz	Str fD/v	x logStr	x2	Nu hD/k	Nufit	yo logNu	xyo
20	0.010	-2.003	4.010	8.140	8.318	0.911	-1.824
40	0.020	-1.702	2.895	8.951	8.589	0.952	-1.620
60	0.030	-1.525	2.327	9.520	8.752	0.979	-1.493
80	0.040	-1.400	1.961	8.638	8.869	0.936	-1.311
100	0.050	-1.304	1.699	8.783	8.961	0.944	-1.230
120	0.060	-1.224	1.499	9.313	9.037	0.969	-1.187
140	0.070	-1.157	1.340	9.131	9.102	0.961	-1.112
160	0.080	-1.099	1.209	8.776	9.158	0.943	-1.037
180	0.089	-1.048	1.099	8.991	9.208	0.954	-1.000
200	0.099	-1.003	1.005	9.237	9.253	0.966	-0.968
220	0.109	-0.961	0.924	8.987	9.294	0.954	-0.917
240	0.119	-0.923	0.853	9.696	9.332	0.987	-0.911
260	0.129	-0.889	0.790	9.344	9.366	0.971	-0.862
280	0.139	-0.856	0.733	9.165	9.398	0.962	-0.824
300	0.149	-0.826	0.683	9.198	9.428	0.964	-0.796
320	0.159	-0.798	0.638	9.168	9.457	0.962	-0.768
340	0.169	-0.772	0.596	8.286	9.483	0.918	-0.709
360	0.179	-0.747	0.558	9.068	9.508	0.957	-0.716
380	0.189	-0.724	0.524	9.771	9.532	0.990	-0.717
400	0.199	-0.702	0.492	10.333	9.555	1.014	-0.712
420	0.209	-0.680	0.463	9.969	9.576	0.999	-0.679
440	0.219	-0.660	0.436	9.403	9.597	0.973	-0.642
460	0.229	-0.641	0.411	9.550	9.617	0.980	-0.628
480	0.239	-0.622	0.387	9.907	9.636	0.996	-0.620
500	0.249	-0.605	0.366	9.976	9.654	0.999	-0.604
520	0.258	-0.588	0.345	9.587	9.671	0.982	-0.577
540	0.268	-0.571	0.326	9.310	9.688	0.969	-0.553
560	0.278	-0.555	0.308	9.593	9.705	0.982	-0.545
580	0.288	-0.540	0.292	9.376	9.720	0.972	-0.525
600	0.298	-0.525	0.276	9.834	9.736	0.993	-0.522
620	0.308	-0.511	0.261	10.301	9.750	1.013	-0.518
640	0.318	-0.497	0.247	10.481	9.765	1.020	-0.508
660	0.328	-0.484	0.234	10.231	9.779	1.010	-0.489
680	0.338	-0.471	0.222	9.951	9.792	0.998	-0.470
700	0.348	-0.458	0.210	9.806	9.805	0.991	-0.455
720	0.358	-0.446	0.199	9.444	9.818	0.975	-0.435
		-30.522	30.820			35.04417	-29.4824
SUM		x	x2			yo	xyo

1.012682 = loga
0.046275 = b
10.29633 = a

Nu = a(STR)**b

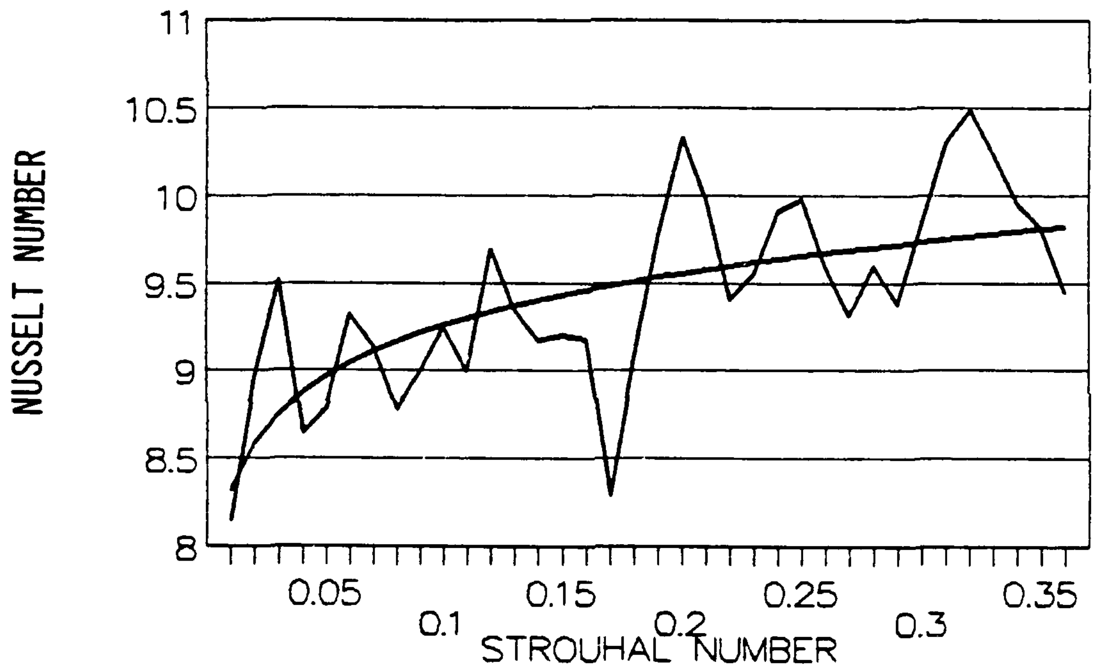

Figure 6-4, Nusselt Number vs Strouhal Number

Curve Fit

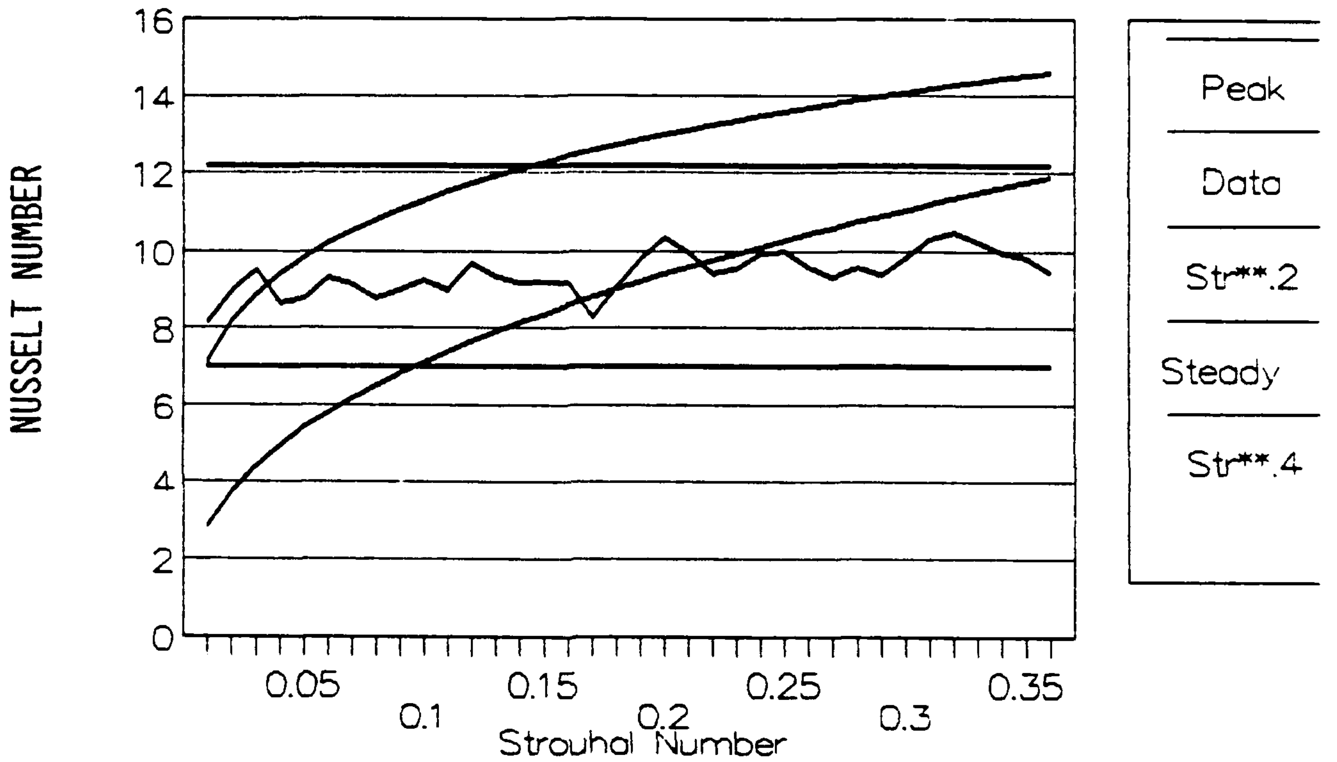

Figure 6-5, Model, Nu vs Str

Table 6-3, A Calculation of Boundary Layer Thickness and Time Required to Form

Hz	Nu hD/k	BL Thick	Time Calc	1/2f	SSeq time
20	8.140	0.00277	0.00239	0.02500	0.0026
40	8.951	0.00254	0.00202	0.01250	0.0026
60	9.520	0.00241	0.00181	0.00833	0.0026
80	8.638	0.00262	0.00215	0.00625	0.0026
100	8.783	0.00259	0.00209	0.00500	0.0026
120	9.313	0.00245	0.00188	0.00417	0.0026
140	9.131	0.00250	0.00195	0.00357	0.0026
160	8.776	0.00259	0.00209	0.00313	0.0026
180	8.991	0.00253	0.00200	0.00278	0.0026
200	9.237	0.00247	0.00191	0.00250	0.0026
220	8.987	0.00253	0.00201	0.00227	0.0026
240	9.696	0.00237	0.00175	0.00208	0.0026
260	9.344	0.00245	0.00187	0.00192	0.0026
280	9.165	0.00249	0.00194	0.00179	0.0026
300	9.198	0.00248	0.00192	0.00167	0.0026
320	9.168	0.00249	0.00194	0.00156	0.0026
340	8.286	0.00272	0.00232	0.00147	0.0026
360	9.068	0.00251	0.00197	0.00139	0.0026
380	9.771	0.00235	0.00173	0.00132	0.0026
400	10.333	0.00223	0.00156	0.00125	0.0026
420	9.969	0.00231	0.00167	0.00119	0.0026
440	9.403	0.00243	0.00185	0.00114	0.0026
460	9.550	0.00240	0.00180	0.00109	0.0026
480	9.907	0.00232	0.00168	0.00104	0.0026
500	9.976	0.00231	0.00166	0.00100	0.0026
520	9.587	0.00239	0.00179	0.00096	0.0026
540	9.310	0.00246	0.00188	0.00093	0.0026
560	9.593	0.00239	0.00178	0.00089	0.0026
580	9.376	0.00244	0.00186	0.00085	0.0026
600	9.834	0.00234	0.00171	0.00083	0.0026
620	10.301	0.00224	0.00157	0.00081	0.0026
640	10.481	0.00221	0.00152	0.00078	0.0026
660	10.231	0.00225	0.00159	0.00076	0.0026
680	9.951	0.00231	0.00167	0.00074	0.0026
700	9.806	0.00234	0.00172	0.00071	0.0026
720	9.444	0.00242	0.00184	0.00069	0.0026

COMPARISON OF BOUNDARY LAYER THICKNESS

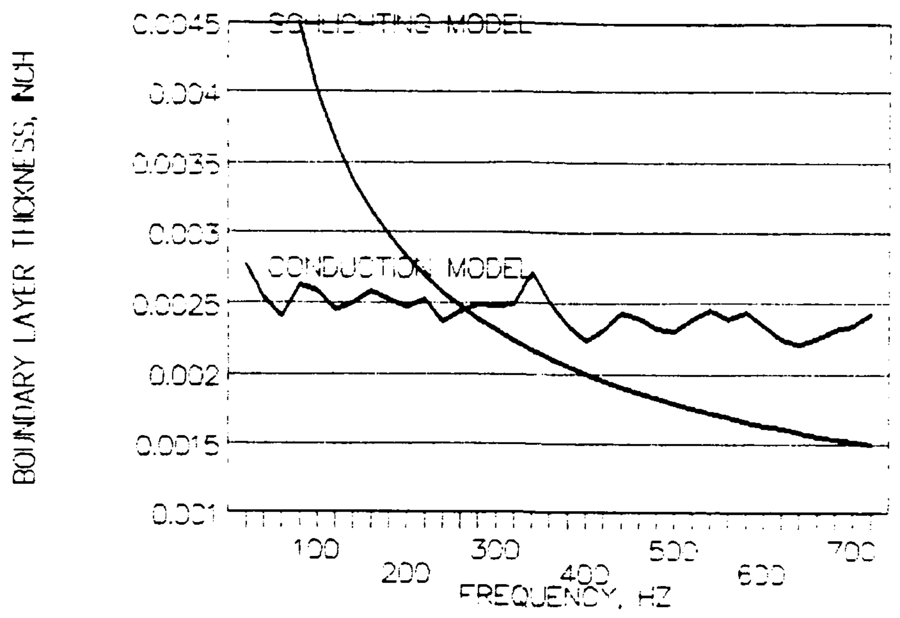

TIME TO ESTABLISH BOUNDARY LAYER

COMPARED TO PERIOD/2

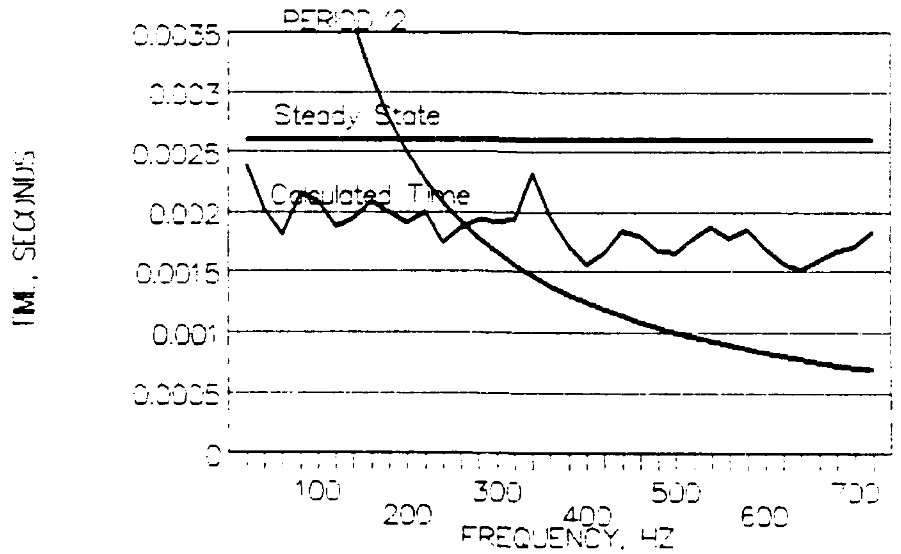

Figure 6-6

7.0 CONCLUSIONS

The experimental data successfully demonstrates that the convective heat transfer coefficient can be markedly increased by interrupting the air flow, producing a pulsed flow.

The increase in heat transfer is a function of frequency, increasing generally with frequency. This was demonstrated to the limit of the present apparatus, however, it is obvious that the effect will diminish and at very high frequency will be indistinguishable from steady flow.

Harmonics in the flow stream will influence the increase in heat transfer both positively and negatively.

The data demonstrated an increase in heat transfer as high as 30 percent, when compared to a steady flow at Reynolds number equal to 5900.

This is a potential decrease in required cooling flow of 30 percent.

8.0 RECOMMENDATIONS FOR FURTHER RESEARCH

There are several areas from which to recommend further work following this present research. The results of the experimental work were dramatic. The papers reviewed in Chapter II describe the expectations at the outset of the experimentation. It was believed at the outset of this research that a pulsed flow had the potential to create the necessary turbulence to enhance heat transfer. It was believed that the magnitude of change would depend, in part, on the degree of turbulence in the baseline flow. It was believed that there would be a dependence upon frequency although it was expected to be a negative trend at frequencies as high as 720 Hz. The frequency trend was found to be decidedly positive in the range of frequencies investigated. It would not have been a surprise to see that at the frequencies of interest (720 Hz), the inertia of the air was such that it could not differentiate between the high-frequency interruption and a static upstream pressure drop. This was not the case. So many had reported the minimum "critical" amplitude of disturbance that that was expected to be obvious. The curves in the previous chapter show little sign of a critical amplitude. This has to be related to the difference between this method of generating pulses and others earlier reported.

All of the results presented in this paper indicate that the original goal of presenting a practical method of increasing the heat transfer coefficient inside the cooling passages of a turbine blade can be achieved. But several unanswered questions remain:

- Do the low pressure test results presented here apply to cooling air at 200 PSI? Follow-on work should approach and even exceed the projected pressure of the engine. Reynolds number at the steady-flow baseline should equal or exceed the Reynolds number in the current engine.

- Does the generally positive trend in heat transfer versus frequency continue beyond 720 Hz? Extend the frequency range until a general downward trend is evident.
- Will critical areas of the blade, such as the thin trailing edge, require air flow in excess of the interior passages because the pulses have no effect there?
- Will pulses be a source of objectionable vibration excitation?
- If the cooling of the pulse cooled blade equals the film, impingement, or intricate convection-cooled blade, does pulse cooling offer an economic advantage?
- In the present research the pulses were evenly distributed between flow time and no-flow time. Is this the most effective distribution? Investigate distributions with more off time than on and vice versa.
- A hot turbine stage test rig demonstration is recommended. The present chopper could be used, but a blade from the engine would be mounted and the experiment run at engine temperatures using a propane burner on the hot side and the present electrical heater on the cold side. The blade would be enclosed in an outer chamber representing the engine flowpath, allowing the use of high pressure air.
- An investigation of the response time of the boundary layer would give insight not only the effect that the pulse has on the boundary layer but also the most effective timing and duration of the pulse

List of References

1. Lorimer, R., "Design and Development of a 1500 HP Regenerative Turbine for use in Army Ground Vehicle", TACOM Technical Report Number 10813, 1970.

2. Moffitt, T. P., Stepka,Francis S., Rohlik, Harold E., "Summary of NASA Aerodynamic and Heat Transfer Studies in Turbine Vanes and Blades", Society of Automotive Engineers, Report Number 760917, December 1976.

3. Esgan, J.B., Colloday, R.S., Kaufman,A.,"An Analysis of the Capabilities and Limitations of Turbine Air Cooling Methods" NASA Technical Note D-5992, 1970.

4. McAdams, W.H., 1Heat0 1Transmission0, McGraw Hill Book Company, 1954.

5. Ishigaki, H., "The Effect of Oscillation on Flat Plate Heat Transfer", Journal of Fluid Mechanics, Volume 47, 1971, pages 537-549.

6. Dittus, F.W., Boelter, L.M.K., University of California, "Heat Transfer in Automobile Radiators of the Tubular Type", Publications in Engineering, Volume 2, 1930, page 443.

7. Colburn, A.P., "A Method of Correlating Forced Convection in Heat Transfer Data and a Comparison with Fluid Friction", Transactions of the American Institute of Chemical Engineers, Volume 29, 1933, pages 174-210.

8. Sieder, E.N., Tate, G.E., "Heat Transfer and Pressure Drop of Liquids in Tubes" Industrial Engineering Chemistry, Volume 28, 1936, pages 1429-1436.

9. Martinelli, R.C., "Heat Transfer to Molten Metals" ASME Transactions, Volume 69, 1947, pages 947-959.

10. Lyon, R.N., "Liquid Metal Heat Transfer Coefficients" Chemical Engineering Progress, Volume 47, 1951, pages 75-79.

11. Seban, R.A., "The Influence of Free Stream Turbulence on the Local Heat Transfer from Cylinders", Journal of Heat Transfer, Volume 82, Series C, Number 2, May 1960, pages 101-107.

12. Bayley,F.J., Edwards,P.A., Singh,P.P., "The Effect of Flow Pulsations on Heat Transfer by Forced Convection from a Flat Plate", International Developments in Heat Transfer, Volume, 1961, pages 499-509.

13. Hwu, C., "The Effect of Vibration on Forced Convective Heat

Transfer", Ph.D. Thesis, University of Cincinnati, 1959.

14. Wang, P., "An Experimental Study of Unsteady Turbulent Flows", Ph.D. Thesis, University of Utah, 1976.

15. Forbes, R.E., Carley, C.T., Bell, C.J., "Vibration Effects on Convective Heat Transfer in Enclosures", Journal of Heat Transfer, Volume 92, Series C, Number 3, August 1970, pages 429-438.

16. Wendland, D. W., "The Effect of Periodic Pressure and Temperature Fluctuations on Unsteady Heat Transfer in a Closed System", Ph.D. Thesis, The University of Wisconsin, 1968.

17. Cheng,I.M.,Chang,P.C.,"Non-stationary turbulence in periodic Turbulent Boundary Layers", Technical Report UTEC CE 71-042, Fluid Mechanics and Hydraulics Laboratory, University of Utah, 1971.

18. Baxi,C.B.,Ramachandran,A.,"Effect of Vibration on Heat Transfer from Spheres", Journal of Heat Transfer, Volume 91, Series C, Number 3, August 1969, pages 337-344.

19. Bergles,A.E., "The Influence of Heated-Surface Vibration on Pool Boiling", Journal of Heat Transfer, Volume 90, Series C, Number 1, February 1969, pages 152-154.

20. Bergles,A.E., "The Influence of Flow Vibrations on Forced-Convection Heat Transfer", Journal of Heat Transfer, Volume 86, Series C, Number 4, November 1964, pages 559-560.

21. Blair, M.F., "Influence of Free Stream Turbulence on Turbulent Boundary Layer Heat Transfer and Mean Profile Development, Part I - Experimental Data", Volume 105, Series C, Number 1, February 1983, pages 33-40.

22. Blair, M.F., "Influence of Free Stream Turbulence on Turbulent Boundary Layer Heat Transfer and Mean Profile Development, Part II - Analysis of Results", Volume 105, Series C, Number 1, February 1983, pages 41-47.

23. Bayle, F.J., Priddy, W.J., "Effects of Free Stream Turbulence Intensity and Frequency on Heat Transfer to Turbine Blading", ASME Journal of Engineering for Power, Volume 104, 1981, pages 60-64.

24. DiCicco, D.A., Schoenhals, R.J., "Heat Transfer in Film Boiling with Pulsation Pressures", Journal of Heat Transfer, Volume 86, Series C, No.3, August 1964, pages 457-461.

25. Faircloth, J.M.Jr., Schaetzle, W.J., "Effect of Vibration on Heat Transfer for Flow Normal to a Cylinder", Journal of Heat Transfer, Volume 90, Series C, Number 1, February 1969, pages 140-144.

26. Fand, R. M., Kaye, J., "The Influence of Sound on Free Convection from a Horizontal Cylinder", Journal of Heat Transfer, Volume 83, Series C, Number 2, May 1961, pages 133-148.

27. Fand, R.M., Roos,J., Cheng, P., Kaye, J., "The Local Heat-Transfer Coefficient Around a Heated Cylinder in an Intense Sound Field.", Journal of Heat Transfer, Volume 84, Series C, Number 3, August 1962, pages 245-250.

28. Fand, R.M., "Evaluation of Richardson's Correlation of the Influence of Sound on Heat Transfer as Measured by Fand and Kaye", Journal of Heat Transfer, Volume 88, Series C, Number 2, May 1966, pages 247-248.

29. Hagge, J.K., Junkhan, G.H., "Mechanical Augmentation of Convective Heat Transfer in Air", Journal of Heat Transfer, Volume 97 , Series C, Number 4, November 1975, pages 516-520.

30. Junkhan, G.H., "Some Effects of Mechanically- Produced Unsteady Boundary Layer Flows on Convective Heat Transfer Augmentation", Journal of Heat Transfer, Volume 100, Series C, Number 1, February 1978, pages 25-29.

31. Holman, J.P., "The Mechanism of Sound Field Effects on Heat Transfer", Journal of Heat Transfer, Volume 82, Series C, Number 4, November 1960, pages 393-396.

32. Jackson, T.W., Harrison, W.B., Boteler, W.C., "Free Convection, Forced Convection, and Acoustic Vibrations in a Constant Temperature Vertical Tube", Journal of Heat Transfer, Volume 81, Series C, Number 1, February 1959, pages 68-74.

33. Jackson, T.W., Purdy, K.R., "Resonant Pulsating Flow and Convective Heat Transfer", Journal of Heat Transfer, Volume 87, Series C, Number 4, November 1965, pages 507-512.

34. Jackson, T.W., Purdy, K.R., Oliver, C.C., "The Effects of Resonant Acoustic Vibrations on the Nusselt Numbers for a Constant Temperature Horizontal Tube", International Developments in Heat Transfer, ASME, 1961, pages 483-489.

35. June, R.R., Baker, M.J., "The Effect of Sound on Free Convection Heat Transfer From a Vertical Flat Plate.", Journal of Heat Transfer, Volume 85, Series C, Number 3, August 1963, pages 279-280.

36. Mendes, P. Souza, Sparrow, E.M., "Periodically Converging-Diverging Tubes and their Turbulent Heat Transfer, Pressure Drop, Fluid Flow, and Enhancement Characteristics", Journal of Heat Transfer, Volume 106, Series C, Number 1, February 1984, pages 55-63.

37. Sparrow, E.M., Tao, W.Q., "Enhanced Heat Transfer in a Flat Rectangular Duct with Streamwise-Periodic Disturbances at One Principal Wall", Journal of Heat Transfer, Volume 105, Series C, Number 4, November 1983, pages 852-861.

38. Nevins, R.G., Ball, H.D., "Heat Transfer Between a Flat Plate and a Pulsating Impinging Jet", International Developments in Heat Transfer, 1961, pages 510-525.

39. Siegal, R., Perlmutter, M., "Heat Transfer for Pulsating Laminar Duct Flow", Journal of Heat Transfer, Volume 84, Series C, Number 2, May 1962, pages 111-123.

40. Siegal, R., Perlmutter, M., "Laminar Heat Transfer in a Channel with Unsteady Flow and Wall Heating Varying with Position and Time", Journal of Heat Transfer, Volume 85, Series C, Number 4, November 1963, pages 358-365.

41. Seban, R.A., Shimazaki, T.T., "Heat Transfer to a Fluid Flowing Turbulently in a Smooth Pipe with Walls at Constant Temperature" ASME Transactions, Volume 73, 1951, pages 803-809.

42. Simonich, J.C., Bradshaw, P., "Effect of Free-Stream Turbulence on Heat Transfer through a Turbulent Boundary Layer", Journal of Heat Transfer, Volume 100, Series C, Number 4, November 1978, pages 671-677.

43. Mathewson, W.F., Jr., "Effects of Sonic Pulsations on Forced Convective Heat Transfer to Air, on Film Condensation on Isopropyl Alcohol in the Presence of Air", Ph.D. Thesis, Cornell University, 1962.

44. Hanratty, T.J., "Turbulent Exchange of Mass and Momentum with Boundary" American Institute of Chemical Engineers, Volume 2, 1956, page 359.

45. Chapman, A.J., Walker, W.F., 1Introductory0 1Gas0 1Dynamics0, Holt, Rinehart and Winston, Inc., 1971.

46. Kline, S.J., McClintock, F.A., "The Descriptions of Uncertainties in Single Sample Experiments", Mechanical Engineering, 75, 1953.

47. Schlicting, H., 1Boundary0 1Layer0 1Theory0, McGraw-Hill Book Company, Inc., 1960.

Selected Bibliography

Ahmed, M.H.S., "The Effect of Surface Vibration on Forced Convective Heat Transfer", PhD Thesis, Durham University, 1953.

Chao, B.T., "End-Wall Heat Transfer in a Rarefraction Wave Tube", Journal of Heat Transfer, Volume 87, Series C, Number 3, August 1965, pages 349-352.

Colladay, R.S., "Turbine Cooling", 1Turbine0 1Design0 land0 1Application0, 1975.

Eckert, E.R.G., "Pioneering Contributions to our Knowledge of Convective Heat Transfer", Journal of Heat Transfer, Volume 103, Series C, No.3, August 1981, pages 409-414.

Ede, A.J., "The Effect of a Right-Angled Bend on Heat Transfer in a Pipe", International Developments in Heat Transfer, 1961, pages 634-642.

Edgerton, R.H., "Heat Convection in Periodic Flow and the Application of Radiation Pyrometers to Unsteady Heat Transfer Investigations", Ph.D. Thesis, Cornell University, 1961.

Forbes, R.E., "The Effect of Vibration on Natural Convective Heat Transfer in a Rectangular Enclosure", Ph.D. Thesis, Mississippi State University, 1968.

Goluba, R.W., "The Effect of Periodic Shock-Fronted Pressure Waves on the Instantaneous Heat Flux at the End Wall of a Tube", PhD Thesis, University of Wisconsin, 1968.

Goria,R.S.R., "Effects of Unsteady Free Stream Vevocity and Free Stream Turbulence on Stagnation Point Heat Transfer", NASA Contractor Report 3804, Cleveland State University , 1984.

Haremann, H.A., Rao, N.N., "Heat Transfer in Pulsating Flow", NATURE, Volume 174, Number 4418, 1954, page 41.

Kaufman, A., "Analytical Study of Cooled Turbine Blades Considering Combined Steady-State and Transient Conditions", NASA TM X-1951, Lewis Research Center, January 1970.

Kays, W.M., 1Convective0 1Heat0 land0 1Mass0 1Transfer0, McGraw- Hill Book Company, 1966.

Kopelev, S.Z., Gurov, S.V., Avilova-Shulgina, M.V., "Heat Transfer in Cooled Flow Passages of Turbines", Heat Transfer - Soviet Research, Volume 4, Number 6, November-December 1972, pages 105-111 .

Lewalle, J., "Contribution to the Theory and Modelling of Interface-Related Phenomena in Intermittant Turbulent Flows", Ph.D.

Thesis, Cornell University, 1981.

Lighthill, M.J., "The Response of Laminar Skin Friction and Heat Transfer to Fluctuations in Stream Velocity", Proceedures of the Royal Society on Aeronautics, Volume 224, 1954.

Mumma, S.A., "Heat Transfer Via the Wall and Longitudinal Dispersion between Alternate Pulses of Warm and Cool Air Flowing in a Pipe", Ph.D. Thesis, University of Illinois at Urbana-Champaign, 1974.

Nash, J.F., "Further Studies on Unsteady Boundary Layers with Flow Reversal", NASA Contractor Report 2767, 1976.

Nickerson, R.J., "The Effect of Free Stream Oscillations on the Laminar Boundary Layer of a Flat Plate", WADC Technical Report Number 57-481, 1958.

Patel, D.R., "Computation of Unsteady Turbulent Boundary Layers with Flow Reversal and Evaluation of Two Separate Turbulence Models", Master of Science Thesis, California State University, 1980.

Retelle, J.P.,Jr., "Unsteady Boundary Layer Flow Reversal in a Longitudinally Oscillating Flow", Ph.D. Thesis, University of Colorado at Boulder, 1978.

Romie, F.E., "Heat Transfer to Fluids Flowing with Velocity Pulsations in a Pipe", PhD Thesis, University of California at Los Angeles, 1956.

Scanlan, J.A., "Effects of Normal Surface Vibration on Laminar Forced Convective Heat Transfer", Industrial and Engineering Chemistry, Volume 50, Number 10, October 1958, pages 1565-1568.

Shai, I., Rotem, Z. "Heat Transfer to Water in Turbulent Flow in Internally Heated Annuli Part II, Pulsating Flow", ASME Paper 60-HT-21, Journal of Mechanical Engineers, November 1960.

Siegal, R., "Influence of Oscillation-Induced Diffusion on Heat Transfer in a Uniformly Heated Channel", Transactions of the ASME, Volume 109, February 1987, pages 244-246.

Siegal, R., "Effect of Flow Oscillations on Axial Energy Transport in a Porous Material", Transactions of the ASME, Volume 109, February 1987, pages 242-244.

Siegal, R., Perlmutter, M., "Two-Dimensional Pulsating Laminar Flow in a Duct with a Constant Wall Temperature", International Developments in Heat Transfer, 1961, pages 517-525.

Simon, H.A., Chang, M.H., Chow, J.C.F., "Heat Transfer in Curved Tubes with Pulsitile, Fully Developed, Laminar Flows", Journal of Heat

Transfer, Volume 99, Series C, Number 4, November 1977, pages 590-595.

Sparrow, E.M., Siegal, R., "Unsteady Turbulent Heat Transfer in Tubes", Journal of Heat Transfer, Volume 82, Series C, Number 3, August 1960, pages 170-180.

Spurlock, J.M., Jackson,T.W., Purdy,C.C., Johnson,H.L., "The Effects of Resonant Acoustic Vibrations on Heat Transfer to Air in Horizontal Tubes", WADC Technical Note 59-330, 1959.

Thomas, L.C., "Adaptation of the Surface Renewal Approach to Momentum and Heat Transfer for Turbulent Pulsitile Flow", Journal of Heat Transfer, Volume 96, Series C, Number 3, August 1974, pages 348-353.

Weber, H., "The Effect of Impinging Periodic Shock Waves on Heat Transfer to a Cooled Wall", Ph.D. Thesis, The University of Wisconsin, 1973.

West, F.B., Taylor, A.T., "The Effects of Pulsations on Heat Transfer", Chemical Engineering Progress, Volume 48, Number 1, January 1952, pages 39-43.

Yea, F., Meitner, P., Russell, L., "Turbine Vane Coolant Flow Variations and Calculated Effects on Metal Temperatures", NASA TMX-3249.

APPENDIX A

TEST SPECIFICATION

Within the limitations of the test equipment, the experiment was designed to simulate the blade or vane of the gas producer turbine of a small gas turbine engine. Flows, geometry, temperatures and pressures were taken from the cycle of the AGT1500 gas turbine engine which powers the Army's Abrams family of main battle tank.

Engine Characteristics:

Three percent mass flow used for cooling the first turbine stage x 12 lb/sec total mass flow = .36 lb/sec

.36 lb/sec / 28 blades x 60 sec/min = .771 lb/min cooling

Table A-1 is a comparison of the engine and the test rig.

The primary data runs were to produce heat transfer rates or convective heat transfer coefficients in a range of frequencies with corresponding steady flow baseline data so that a comparison with the steady flow case can be made with all relevant parameters identical.

The procedure for the data runs was as follows.

- Initiate flow through both heaters, apply power to the heaters and begin warm-up.
- Set the temperature controls and the flow rates to the test condition and allow the apparatus to stabilize. This takes about one hour.
- Set water flow through the cooling tower to give an air temperature through the flow nozzle equal to that at which the orifice was calibrated.
- Check pressure at the regulators, adjust valves to give correct flow rates through the chopper (cooling flow) and the hot side. The chopper is adjusted by hand to align the holes for the steady-flow case. The disc was marked for this purpose.
- Take a data reading every five minutes until all temperatures are stabilized.
- Record the steady flow (0 Hz) data. This data will be rerecorded before and after every data point at frequency to ensure that the baseline has not wandered.
- Turn on the power supply to the motor controller and set the controller to the first required frequency. Adjust the flow valve upstream of the chopper until the flow is identical to the steady flow case. Observe the data until the [illegible] has stabilized. When the data has stabilized, record three sets of data.
- Return to the zero Hz baseline ca[illegible]
- Set the motor for the next data point.

Table A-1

APPENDIX B

SAMPLE DATA

Following is one sample data sheet (Table B-1), describing the calculations that are made. Following that is a representative sample of the data generated for this paper. The data selected is the region from 300 Hz to 400 Hz. This region is selected for the pronounced harmonics and most interesting data.

Table B-1

Test Data	Date	Time	Run No.
Barometer		as read	in Hg
Ambient Temperature		as read	oF
Relative Pressure into Flowmeter (Cooling Air)		as read	PSI
Absolute Pressure into Flowmeter (Cooling Air)		Bar + Rel	PSI
Delta Pressure across Flowmeter (Cooling Air)		as read	in H2O
Temperature into Flowmeter (Cooling Air)		as read	oF
Air Flow from Calibration Curve (Cooling Air)		as read	CFM
Air Density (Cooling Air)	.075 x 530/T x P/14.7		Lbm/ft3
Air Mass Flow (Cooling Air)	Density x CFM		Lb/min
Relative Pressure into Flowmeter (Gas Flow)		as read	PSI
Absolute Pressure into Flowmeter (Gas Flow)		Bar + Rel	PSI
Delta Pressure Across Flowmeter (Gas Flow)		as read	in H2O
Temperature into Flowmeter (Gas Flow)		as read	oF
Air Flow from Calibration Curve (Gas Flow)		as read	CFM
Air Density (Gas Flow)	.075 x 530/T x P/14.7		Lbm/ft3
Air Mass Flow (Gas Flow)	Density x CFM		Lbm/min
Pulse Frequency		as read	Hz
Temperature into Blade		as read	oF
Temperature out of Blade		as read	oF
Specific Heat	0.236 + .0000255 x T		BTU/LboF
Cooling Heat Transfer	Mass Flow x Cp x Delta T		BTU/min
Temperature Gas In		as read	oF
Temperature, Gas Out		as read	oF
Specific Heat	0.236 + .0000255 x T		BTU/LboF
Gas Heat Loss	Mass Flow x Cp x Delta T		BTU/min
Pressure Before Chopper	as read		PSI
Thermal Effectiveness	(Tco - Tcin)/(Tgin - Tcin)		%

Run Number

Data Point			Description
12	as read	PSI	Pressure, Before Chopper
11	as read	PSI	Pressure,Orifice, Hot Side
10	as read	PSI	Pressure,Orifice,Cooling
9	as read	oF	Temperature,Ambient
8	as read	oF	Temperature,Orifice,Cooling
7	as read	oF	Temperature,Cooling,In
6	as read	oF	Temperature,Cooling,Out
5	as read	oF	Temperature,Orifice,Gas
4	as read	oF	Temperature,Gas,In
3	as read	oF	Temperature,Gas,Out
2	as read	oF	Temperature,Air Supply
1	as read	oF	Temperature,Cooling,Control
Time	as read		
Date	as read		
Pulse Rate	as read	Hz	
Barometer	as read	in Hg	
Orifice,Cool	as read	in H2O	
Orifice, Gas	as read	in H2O	

Test Data	Date 61	Time 1619	Run No. 1
Barometer		29.58	in Hg
Ambient Temperature		85.5	oF
Relative Pressure into Flowmeter (Cooling Air)		0.19	PSI
Absolute Pressure into Flowmeter (Cooling Air)		14.71	PSI
Delta Pressure across Flowmeter (Cooling Air)		4.8	in H2O
Temperature into Flowmeter (Cooling Air)		77.0	oF
Air Flow from Calibration Curve (Cooling Air)		1.4	CFM
Air Density (Cooling Air)		0.074	Lbm/ft3
Air Mass Flow (Cooling Air)		0.104	Lb/min
Relative Pressure into Flowmeter (Gas Flow)		6.8	PSI
Absolute Pressure into Flowmeter (Gas Flow)		21.3	PSI
Delta Pressure Across Flowmeter (Gas Flow)		2.4	in H2O
Temperature into Flowmeter (Gas Flow)		82.0	oF
Air Flow from Calibration Curve (Gas Flow)		43.7	CFM
Air Density (Gas Flow)		0.106	Lbm/ft3
Air Mass Flow (Gas Flow)		4.65	Lbm/min
Pulse Frequency		0.00	Hz
Temperature into Blade		188.3	oF
Temperature out of Blade		265.4	oF
Specific Heat		0.242	BTU/LboF
Cooling Heat Transfer		1.93	BTU/min
Temperature Gas In		820.2	oF
Temperature, Gas Out		777.2	oF
Specific Heat		0.256	BTU/LboF
Gas Heat Loss		51.24	BTU/min
Thermal Effectiveness		12.2	%

Run Number 1

Data Point			Description
11	6.8	PSI	Pressure,Orifice, Hot Side
10	0.19	PSI	Pressure,Orifice,Cooling
9	85.5	oF	Temperature,Ambient
8	77	oF	Temperature,Orifice,Cooling
7	188.3	oF	Temperature,Cooling,In
6	265.4	oF	Temperature,Cooling,Out
5	82	oF	Temperature,Orifice,Gas
4	820.2	oF	Temperature,Gas,In
3	777.2	oF	Temperature,Gas,Out
2	82.2	oF	Temperature,Air Supply
1	305.8	oF	Temperature,Cooling,Control
Time	1619		
Date	61		
Pulse Rate	0	Hz	
Barometer	29.58	in Hg	
Orifice,Cool	2.00	in H2O	
Orifice, Gas	1.00	in H2O	

Test Data	Date	61	Time	1623	Run No.	2

Barometer	29.58	in Hg
Ambient Temperature	86.0	oF
Relative Pressure into Flowmeter (Cooling Air)	0.18	PSI
Absolute Pressure into Flowmeter (Cooling Air)	14.70	PSI
Delta Pressure across Flowmeter (Cooling Air)	4.8	in H2O
Temperature into Flowmeter (Cooling Air)	75.5	oF
Air Flow from Calibration Curve (Cooling Air)	1.4	CFM
Air Density (Cooling Air)	0.074	Lbm/ft3
Air Mass Flow (Cooling Air)	0.104	Lb/min
Relative Pressure into Flowmeter (Gas Flow)	6.6	PSI
Absolute Pressure into Flowmeter (Gas Flow)	21.1	PSI
Delta Pressure Across Flowmeter (Gas Flow)	2.4	in H2O
Temperature into Flowmeter (Gas Flow)	81.5	oF
Air Flow from Calibration Curve (Gas Flow)	43.9	CFM
Air Density (Gas Flow)	0.106	Lbm/ft3
Air Mass Flow (Gas Flow)	4.63	Lbm/min
Pulse Frequency	300.00	Hz
Temperature into Blade	189.6	oF
Temperature out of Blade	286.0	oF
Specific Heat	0.242	BTU/LboF
Cooling Heat Transfer	2.42	BTU/min
Temperature Gas In	820.0	oF
Temperature, Gas Out	769.4	oF
Specific Heat	0.256	BTU/LboF
Gas Heat Loss	60.05	BTU/min
Thermal Effectiveness	15.3	%

Run Number 2

Data Point			Description
11	6.62	PSI	Pressure,Orifice, Hot Side
10	0.18	PSI	Pressure,Orifice,Cooling
9	86	oF	Temperature,Ambient
8	75.5	oF	Temperature,Orifice,Cooling
7	189.6	oF	Temperature,Cooling,In
6	286	oF	Temperature,Cooling,Out
5	81.5	oF	Temperature,Orifice,Gas
4	820	oF	Temperature,Gas,In
3	769.4	oF	Temperature,Gas,Out
2	82.2	oF	Temperature,Air Supply
1	304	oF	Temperature,Cooling,Control
Time	1623		
Date	61		
Pulse Rate	300	Hz	
Barometer	29.58	in Hg	
Orifice,Cool	2.00	in H2O	
Orifice, Gas	1.00	in H2O	

Test Data	Date 61	Time 1625	Run No.	3
Barometer			29.58	in Hg
Ambient Temperature			88.0	oF
Relative Pressure into Flowmeter (Cooling Air)			0.19	PSI
Absolute Pressure into Flowmeter (Cooling Air)			14.71	PSI
Delta Pressure across Flowmeter (Cooling Air)			4.8	in H2O
Temperature into Flowmeter (Cooling Air)			75.3	oF
Air Flow from Calibration Curve (Cooling Air)			1.4	CFM
Air Density (Cooling Air)			0.074	Lbm/ft3
Air Mass Flow (Cooling Air)			0.104	Lb/min
Relative Pressure into Flowmeter (Gas Flow)			6.7	PSI
Absolute Pressure into Flowmeter (Gas Flow)			21.2	PSI
Delta Pressure Across Flowmeter (Gas Flow)			2.4	in H2O
Temperature into Flowmeter (Gas Flow)			82.6	oF
Air Flow from Calibration Curve (Gas Flow)			43.9	CFM
Air Density (Gas Flow)			0.106	Lbm/ft3
Air Mass Flow (Gas Flow)			4.63	Lbm/min
Pulse Frequency			0.00	Hz
Temperature into Blade			193.7	oF
Temperature out of Blade			274.4	oF
Specific Heat			0.242	BTU/LboF
Cooling Heat Transfer			2.03	BTU/min
Temperature Gas In			822.0	oF
Temperature, Gas Out			773.4	oF
Specific Heat			0.256	BTU/LboF
Gas Heat Loss			57.67	BTU/min
Thermal Effectiveness			12.8	%

Run Number 3

Data Point			Description
11	6.65	PSI	Pressure,Orifice, Hot Side
10	0.19	PSI	Pressure,Orifice,Cooling
9	88	oF	Temperature,Ambient
8	75.3	oF	Temperature,Orifice,Cooling
7	193.7	oF	Temperature,Cooling,In
6	274.4	oF	Temperature,Cooling,Out
5	82.6	oF	Temperature,Orifice,Gas
4	822	oF	Temperature,Gas,In
3	773.4	oF	Temperature,Gas,Out
2	82	oF	Temperature,Air Supply
1	305	oF	Temperature,Cooling,Control
Time	1625		
Date	61		
Pulse Rate	0	Hz	
Barometer	29.58	in Hg	
Orifice,Cool	2.00	in H2O	
Orifice, Gas	1.00	in H2O	

Test Data	Date	61	Time	1631	Run No.	4

Barometer	29.58	in Hg
Ambient Temperature	87.3	oF
Relative Pressure into Flowmeter (Cooling Air)	0.19	PSI
Absolute Pressure into Flowmeter (Cooling Air)	14.71	PSI
Delta Pressure across Flowmeter (Cooling Air)	4.8	in H2O
Temperature into Flowmeter (Cooling Air)	73.6	oF
Air Flow from Calibration Curve (Cooling Air)	1.4	CFM
Air Density (Cooling Air)	0.075	Lbm/ft3
Air Mass Flow (Cooling Air)	0.104	Lb/min
Relative Pressure into Flowmeter (Gas Flow)	6.4	PSI
Absolute Pressure into Flowmeter (Gas Flow)	20.9	PSI
Delta Pressure Across Flowmeter (Gas Flow)	2.4	in H2O
Temperature into Flowmeter (Gas Flow)	81.8	oF
Air Flow from Calibration Curve (Gas Flow)	44.1	CFM
Air Density (Gas Flow)	0.104	Lbm/ft3
Air Mass Flow (Gas Flow)	4.61	Lbm/min
Pulse Frequency	320.00	Hz
Temperature into Blade	196.4	oF
Temperature out of Blade	295.0	oF
Specific Heat	0.242	BTU/LboF
Cooling Heat Transfer	2.48	BTU/min
Temperature Gas In	823.6	oF
Temperature, Gas Out	767.1	oF
Specific Heat	0.256	BTU/LboF
Gas Heat Loss	66.70	BTU/min
Thermal Effectiveness	15.7	%

Run Number 4

Data Point			Description
11	6.41	PSI	Pressure,Orifice, Hot Side
10	0.19	PSI	Pressure,Orifice,Cooling
9	87.3	oF	Temperature,Ambient
8	73.6	oF	Temperature,Orifice,Cooling
7	196.4	oF	Temperature,Cooling,In
6	295	oF	Temperature,Cooling,Out
5	81.8	oF	Temperature,Orifice,Gas
4	823.6	oF	Temperature,Gas,In
3	767.1	oF	Temperature,Gas,Out
2	82.4	oF	Temperature,Air Supply
1	303.6	oF	Temperature,Cooling,Control
Time	1631		
Date	61		
Pulse Rate	320	Hz	
Barometer	29.58	in Hg	
Orifice,Cool	2.00	in H2O	
Orifice, Gas	1.00	in H2O	

Test Data	Date	61	Time	1634	Run No.	5

Barometer	29.58	in Hg
Ambient Temperature	88.0	oF
Relative Pressure into Flowmeter (Cooling Air)	0.18	PSI
Absolute Pressure into Flowmeter (Cooling Air)	14.70	PSI
Delta Pressure across Flowmeter (Cooling Air)	4.8	in H2O
Temperature into Flowmeter (Cooling Air)	74.0	oF
Air Flow from Calibration Curve (Cooling Air)	1.4	CFM
Air Density (Cooling Air)	0.074	Lbm/ft3
Air Mass Flow (Cooling Air)	0.104	Lb/min
Relative Pressure into Flowmeter (Gas Flow)	6.5	PSI
Absolute Pressure into Flowmeter (Gas Flow)	21.0	PSI
Delta Pressure Across Flowmeter (Gas Flow)	2.4	in H2O
Temperature into Flowmeter (Gas Flow)	82.5	oF
Air Flow from Calibration Curve (Gas Flow)	44.0	CFM
Air Density (Gas Flow)	0.105	Lbm/ft3
Air Mass Flow (Gas Flow)	4.61	Lbm/min
Pulse Frequency	0.00	Hz
Temperature into Blade	199.4	oF
Temperature out of Blade	280.8	oF
Specific Heat	0.242	BTU/LboF
Cooling Heat Transfer	2.05	BTU/min
Temperature Gas In	826.6	oF
Temperature, Gas Out	773.6	oF
Specific Heat	0.256	BTU/LboF
Gas Heat Loss	62.66	BTU/min
Thermal Effectiveness	13.0	%

Run Number 5

Data Point			Description
11	6.48	PSI	Pressure,Orifice, Hot Side
10	0.18	PSI	Pressure,Orifice,Cooling
9	88	oF	Temperature,Ambient
8	74	oF	Temperature,Orifice,Cooling
7	199.4	oF	Temperature,Cooling,In
6	280.8	oF	Temperature,Cooling,Out
5	82.5	oF	Temperature,Orifice,Gas
4	826.6	oF	Temperature,Gas,In
3	773.6	oF	Temperature,Gas,Out
2	81.8	oF	Temperature,Air Supply
1	305.4	oF	Temperature,Cooling,Control
Time	1634		
Date	61		
Pulse Rate	0	Hz	
Barometer	29.58	in Hg	
Orifice,Cool	2.00	in H2O	
Orifice, Gas	1.00	in H2O	

Test Data	Date	61	Time	1636	Run No.	6

Barometer	29.58	in Hg
Ambient Temperature	87.6	oF
Relative Pressure into Flowmeter (Cooling Air)	0.19	PSI
Absolute Pressure into Flowmeter (Cooling Air)	14.71	PSI
Delta Pressure across Flowmeter (Cooling Air)	4.8	in H2O
Temperature into Flowmeter (Cooling Air)	73.4	oF
Air Flow from Calibration Curve (Cooling Air)	1.4	CFM
Air Density (Cooling Air)	0.075	Lbm/ft3
Air Mass Flow (Cooling Air)	0.104	Lb/min
Relative Pressure into Flowmeter (Gas Flow)	6.5	PSI
Absolute Pressure into Flowmeter (Gas Flow)	21.0	PSI
Delta Pressure Across Flowmeter (Gas Flow)	2.4	in H2O
Temperature into Flowmeter (Gas Flow)	81.8	oF
Air Flow from Calibration Curve (Gas Flow)	44.0	CFM
Air Density (Gas Flow)	0.105	Lbm/ft3
Air Mass Flow (Gas Flow)	4.62	Lbm/min
Pulse Frequency	340.00	Hz
Temperature into Blade	199.7	oF
Temperature out of Blade	293.3	oF
Specific Heat	0.242	BTU/LboF
Cooling Heat Transfer	2.36	BTU/min
Temperature Gas In	824.2	oF
Temperature, Gas Out	769.9	oF
Specific Heat	0.256	BTU/LboF
Gas Heat Loss	64.24	BTU/min
Thermal Effectiveness	15.0	%

Run Number 6

Data Point			Description
11	6.49	PSI	Pressure,Orifice, Hot Side
1Ø	Ø.19	PSI	Pressure,Orifice,Cooling
9	87.6	oF	Temperature,Ambient
8	73.4	oF	Temperature,Orifice,Cooling
7	199.7	oF	Temperature,Cooling,In
6	293.3	oF	Temperature,Cooling,Out
5	81.8	oF	Temperature,Orifice,Gas
4	824.2	oF	Temperature,Gas,In
3	769.9	oF	Temperature,Gas,Out
2	82.2	oF	Temperature,Air Supply
1	3Ø4.1	oF	Temperature,Cooling,Control
Time	1636		
Date	61		
Pulse Rate	34Ø	Hz	
Barometer	29.58	in Hg	
Orifice,Cool	2.ØØ	in H2O	
Orifice, Gas	1.ØØ	in H2O	

Test Data	Date	61	Time	1639	Run No.	7

Barometer	29.58	in Hg
Ambient Temperature	86.8	oF
Relative Pressure into Flowmeter (Cooling Air)	0.18	PSI
Absolute Pressure into Flowmeter (Cooling Air)	14.70	PSI
Delta Pressure across Flowmeter (Cooling Air)	4.8	in H2O
Temperature into Flowmeter (Cooling Air)	73.5	oF
Air Flow from Calibration Curve (Cooling Air)	1.4	CFM
Air Density (Cooling Air)	0.075	Lbm/ft3
Air Mass Flow (Cooling Air)	0.104	Lb/min
Relative Pressure into Flowmeter (Gas Flow)	6.4	PSI
Absolute Pressure into Flowmeter (Gas Flow)	20.9	PSI
Delta Pressure Across Flowmeter (Gas Flow)	2.4	in H2O
Temperature into Flowmeter (Gas Flow)	81.7	oF
Air Flow from Calibration Curve (Gas Flow)	44.1	CFM
Air Density (Gas Flow)	0.104	Lbm/ft3
Air Mass Flow (Gas Flow)	4.61	Lbm/min
Pulse Frequency	0.00	Hz
Temperature into Blade	203.7	oF
Temperature out of Blade	287.4	oF
Specific Heat	0.242	BTU/LboF
Cooling Heat Transfer	2.11	BTU/min
Temperature Gas In	826.7	oF
Temperature, Gas Out	775.8	oF
Specific Heat	0.256	BTU/LboF
Gas Heat Loss	60.13	BTU/min
Thermal Effectiveness	13.4	%

Run Number 7

Data Point			Description
11	6.41	PSI	Pressure,Orifice, Hot Side
10	0.18	PSI	Pressure,Orifice,Cooling
9	86.8	oF	Temperature,Ambient
8	73.5	oF	Temperature,Orifice,Cooling
7	203.7	oF	Temperature,Cooling,In
6	287.4	oF	Temperature,Cooling,Out
5	81.7	oF	Temperature,Orifice,Gas
4	826.7	oF	Temperature,Gas,In
3	775.8	oF	Temperature,Gas,Out
2	82.2	oF	Temperature,Air Supply
1	304.2	oF	Temperature,Cooling,Control
Time	1639		
Date	61		
Pulse Rate	0	Hz	
Barometer	29.58	in Hg	
Orifice,Cool	2.00	in H2O	
Orifice, Gas	1.00	in H2O	

Test Data	Date	61	Time	1642	Run No.	8

Barometer	29.58	in Hg
Ambient Temperature	87.0	oF
Relative Pressure into Flowmeter (Cooling Air)	0.17	PSI
Absolute Pressure into Flowmeter (Cooling Air)	14.69	PSI
Delta Pressure across Flowmeter (Cooling Air)	4.8	in H2O
Temperature into Flowmeter (Cooling Air)	74.0	oF
Air Flow from Calibration Curve (Cooling Air)	1.4	CFM
Air Density (Cooling Air)	0.074	Lbm/ft3
Air Mass Flow (Cooling Air)	0.104	Lb/min
Relative Pressure into Flowmeter (Gas Flow)	6.4	PSI
Absolute Pressure into Flowmeter (Gas Flow)	20.9	PSI
Delta Pressure Across Flowmeter (Gas Flow)	2.4	in H2O
Temperature into Flowmeter (Gas Flow)	82.2	oF
Air Flow from Calibration Curve (Gas Flow)	44.1	CFM
Air Density (Gas Flow)	0.104	Lbm/ft3
Air Mass Flow (Gas Flow)	4.60	Lbm/min
Pulse Frequency	360.00	Hz
Temperature into Blade	201.3	oF
Temperature out of Blade	299.8	oF
Specific Heat	0.242	BTU/LboF
Cooling Heat Transfer	2.48	BTU/min
Temperature Gas In	828.0	oF
Temperature, Gas Out	771.4	oF
Specific Heat	0.256	BTU/LboF
Gas Heat Loss	66.82	BTU/min
Thermal Effectiveness	15.7	%

Run Number 8

Data Point			Description
11	6.41	PSI	Pressure,Orifice, Hot Side
10	0.17	PSI	Pressure,Orifice,Cooling
9	87	oF	Temperature,Ambient
8	74	oF	Temperature,Orifice,Cooling
7	201.3	oF	Temperature,Cooling,In
6	299.8	oF	Temperature,Cooling,Out
5	82.2	oF	Temperature,Orifice,Gas
4	828	oF	Temperature,Gas,In
3	771.4	oF	Temperature,Gas,Out
2	81.7	oF	Temperature,Air Supply
1	303.6	oF	Temperature,Cooling,Control
Time	1642		
Date	61		
Pulse Rate	360	Hz	
Barometer	29.58	in Hg	
Orifice,Cool	2.00	in H2O	
Orifice, Gas	1.00	in H2O	

Test Data	Date 61	Time 1645	Run No.	9
Barometer			29.58	in Hg
Ambient Temperature			86.8	oF
Relative Pressure into Flowmeter (Cooling Air)			0.17	PSI
Absolute Pressure into Flowmeter (Cooling Air)			14.69	PSI
Delta Pressure across Flowmeter (Cooling Air)			4.8	in H2O
Temperature into Flowmeter (Cooling Air)			73.6	oF
Air Flow from Calibration Curve (Cooling Air)			1.4	CFM
Air Density (Cooling Air)			0.074	Lbm/ft3
Air Mass Flow (Cooling Air)			0.104	Lb/min
Relative Pressure into Flowmeter (Gas Flow)			6.4	PSI
Absolute Pressure into Flowmeter (Gas Flow)			21.0	PSI
Delta Pressure Across Flowmeter (Gas Flow)			2.4	in H2O
Temperature into Flowmeter (Gas Flow)			82.3	oF
Air Flow from Calibration Curve (Gas Flow)			44.1	CFM
Air Density (Gas Flow)			0.104	Lbm/ft3
Air Mass Flow (Gas Flow)			4.61	Lbm/min
Pulse Frequency			0.00	Hz
Temperature into Blade			205.4	oF
Temperature out of Blade			290.0	oF
Specific Heat			0.242	BTU/LboF
Cooling Heat Transfer			2.13	BTU/min
Temperature Gas In			830.8	oF
Temperature, Gas Out			779.6	oF
Specific Heat			0.257	BTU/LboF
Gas Heat Loss			60.50	BTU/min
Thermal Effectiveness			13.5	%

Run Number 9

Data Point			Description
11	6.43	PSI	Pressure,Orifice, Hot Side
10	0.17	PSI	Pressure,Orifice,Cooling
9	86.8	oF	Temperature,Ambient
8	73.6	oF	Temperature,Orifice,Cooling
7	205.4	oF	Temperature,Cooling,In
6	290	oF	Temperature,Cooling,Out
5	82.3	oF	Temperature,Orifice,Gas
4	830.8	oF	Temperature,Gas,In
3	779.6	oF	Temperature,Gas,Out
2	82.3	oF	Temperature,Air Supply
1	305.4	oF	Temperature,Cooling,Control
Time	1645		
Date	61		
Pulse Rate	0	Hz	
Barometer	29.58	in Hg	
Orifice,Cool	2.00	in H2O	
Orifice, Gas	1.00	in H2O	

Test Data Date 61 Time 1648 Run No. 10

Barometer	29.58	in Hg
Ambient Temperature	86.4	oF
Relative Pressure into Flowmeter (Cooling Air)	0.18	PSI
Absolute Pressure into Flowmeter (Cooling Air)	14.70	PSI
Delta Pressure across Flowmeter (Cooling Air)	4.8	in H2O
Temperature into Flowmeter (Cooling Air)	73.6	oF
Air Flow from Calibration Curve (Cooling Air)	1.4	CFM
Air Density (Cooling Air)	0.075	Lbm/ft3
Air Mass Flow (Cooling Air)	0.104	Lb/min
Relative Pressure into Flowmeter (Gas Flow)	6.4	PSI
Absolute Pressure into Flowmeter (Gas Flow)	20.9	PSI
Delta Pressure Across Flowmeter (Gas Flow)	2.4	in H2O
Temperature into Flowmeter (Gas Flow)	81.8	oF
Air Flow from Calibration Curve (Gas Flow)	44.1	CFM
Air Density (Gas Flow)	0.105	Lbm/ft3
Air Mass Flow (Gas Flow)	4.61	Lbm/min
Pulse Frequency	380.00	Hz
Temperature into Blade	202.4	oF
Temperature out of Blade	306.9	oF
Specific Heat	0.242	BTU/LboF
Cooling Heat Transfer	2.63	BTU/min
Temperature Gas In	829.3	oF
Temperature, Gas Out	771.9	oF
Specific Heat	0.256	BTU/LboF
Gas Heat Loss	67.81	BTU/min
Thermal Effectiveness	16.7	%

Run Number 10

Data Point			Description
11	6.42	PSI	Pressure,Orifice, Hot Side
10	0.18	PSI	Pressure,Orifice,Cooling
9	86.4	oF	Temperature,Ambient
8	73.6	oF	Temperature,Orifice,Cooling
7	202.4	oF	Temperature,Cooling,In
6	306.9	oF	Temperature,Cooling,Out
5	81.8	oF	Temperature,Orifice,Gas
4	829.3	oF	Temperature,Gas,In
3	771.9	oF	Temperature,Gas,Out
2	82	oF	Temperature,Air Supply
1	305.4	oF	Temperature,Cooling,Control
Time	1648		
Date	61		
Pulse Rate	380	Hz	
Barometer	29.58	in Hg	
Orifice,Cool	2.00	in H2O	
Orifice, Gas	1.00	in H2O	

Test Data	Date	61	Time	165Ø	Run No.	11

Barometer	29.58	in Hg
Ambient Temperature	86.9	oF
Relative Pressure into Flowmeter (Cooling Air)	Ø.19	PSI
Absolute Pressure into Flowmeter (Cooling Air)	14.71	PSI
Delta Pressure across Flowmeter (Cooling Air)	4.8	in H2O
Temperature into Flowmeter (Cooling Air)	73.5	oF
Air Flow from Calibration Curve (Cooling Air)	1.4	CFM
Air Density (Cooling Air)	Ø.Ø75	Lbm/ft3
Air Mass Flow (Cooling Air)	Ø.1Ø4	Lb/min
Relative Pressure into Flowmeter (Gas Flow)	6.4	PSI
Absolute Pressure into Flowmeter (Gas Flow)	2Ø.9	PSI
Delta Pressure Across Flowmeter (Gas Flow)	2.4	in H2O
Temperature into Flowmeter (Gas Flow)	81.9	oF
Air Flow from Calibration Curve (Gas Flow)	44.1	CFM
Air Density (Gas Flow)	Ø.1Ø4	Lbm/ft3
Air Mass Flow (Gas Flow)	4.6Ø	Lbm/min
Pulse Frequency	Ø.ØØ	Hz
Temperature into Blade	2Ø5.Ø	oF
Temperature out of Blade	284.8	oF
Specific Heat	Ø.242	BTU/LboF
Cooling Heat Transfer	2.Ø1	BTU/min
Temperature Gas In	83Ø.7	oF
Temperature, Gas Out	777.4	oF
Specific Heat	Ø.257	BTU/LboF
Gas Heat Loss	62.91	BTU/min
Thermal Effectiveness	12.8	%

Run Number	11		
Data Point			Description
11	6.37	PSI	Pressure,Orifice, Hot Side
10	0.19	PSI	Pressure,Orifice,Cooling
9	86.9	oF	Temperature,Ambient
8	73.5	oF	Temperature,Orifice,Cooling
7	205	oF	Temperature,Cooling,In
6	284.8	oF	Temperature,Cooling,Out
5	81.9	oF	Temperature,Orifice,Gas
4	830.7	oF	Temperature,Gas,In
3	777.4	oF	Temperature,Gas,Out
2	82	oF	Temperature,Air Supply
1	305.7	oF	Temperature,Cooling,Control
Time	1650		
Date	61		
Pulse Rate	0	Hz	
Barometer	29.58	in Hg	
Orifice,Cool	2.00	in H2O	
Orifice, Gas	1.00	in H2O	

Test Data	Date	61	Time	1653	Run No.	12

Barometer	29.58	in Hg
Ambient Temperature	87.9	oF
Relative Pressure into Flowmeter (Cooling Air)	0.18	PSI
Absolute Pressure into Flowmeter (Cooling Air)	14.70	PSI
Delta Pressure across Flowmeter (Cooling Air)	4.8	in H2O
Temperature into Flowmeter (Cooling Air)	72.5	oF
Air Flow from Calibration Curve (Cooling Air)	1.4	CFM
Air Density (Cooling Air)	0.075	Lbm/ft3
Air Mass Flow (Cooling Air)	0.104	Lb/min
Relative Pressure into Flowmeter (Gas Flow)	6.5	PSI
Absolute Pressure into Flowmeter (Gas Flow)	21.0	PSI
Delta Pressure Across Flowmeter (Gas Flow)	2.4	in H2O
Temperature into Flowmeter (Gas Flow)	82.6	oF
Air Flow from Calibration Curve (Gas Flow)	44.1	CFM
Air Density (Gas Flow)	0.105	Lbm/ft3
Air Mass Flow (Gas Flow)	4.61	Lbm/min
Pulse Frequency	400.00	Hz
Temperature into Blade	203.6	oF
Temperature out of Blade	310.1	oF
Specific Heat	0.243	BTU/LboF
Cooling Heat Transfer	2.69	BTU/min
Temperature Gas In	827.9	oF
Temperature, Gas Out	771.3	oF
Specific Heat	0.256	BTU/LboF
Gas Heat Loss	66.86	BTU/min
Thermal Effectiveness	17.1	%

Run Number	12		
Data Point			Description
11	6.45	PSI	Pressure,Orifice, Hot Side
10	0.18	PSI	Pressure,Orifice,Cooling
9	87.9	oF	Temperature,Ambient
8	72.5	oF	Temperature,Orifice,Cooling
7	203.6	oF	Temperature,Cooling,In
6	310.1	oF	Temperature,Cooling,Out
5	82.6	oF	Temperature,Orifice,Gas
4	827.9	oF	Temperature,Gas,In
3	771.3	oF	Temperature,Gas,Out
2	83.2	oF	Temperature,Air Supply
1	303.9	oF	Temperature,Cooling,Control
Time	1653		
Date	61		
Pulse Rate	400	Hz	
Barometer	29.58	in Hg	
Orifice,Cool	2.00	in H2O	
Orifice, Gas	1.00	in H2O	

Test Data	Date 61	Time 1655	Run No. 13
Barometer		29.58	in Hg
Ambient Temperature		88.1	oF
Relative Pressure into Flowmeter (Cooling Air)		0.19	PSI
Absolute Pressure into Flowmeter (Cooling Air)		14.71	PSI
Delta Pressure across Flowmeter (Cooling Air)		4.8	in H2O
Temperature into Flowmeter (Cooling Air)		73.2	oF
Air Flow from Calibration Curve (Cooling Air)		1.4	CFM
Air Density (Cooling Air)		0.075	Lbm/ft3
Air Mass Flow (Cooling Air)		0.104	Lb/min
Relative Pressure into Flowmeter (Gas Flow)		6.4	PSI
Absolute Pressure into Flowmeter (Gas Flow)		20.9	PSI
Delta Pressure Across Flowmeter (Gas Flow)		2.4	in H2O
Temperature into Flowmeter (Gas Flow)		82.5	oF
Air Flow from Calibration Curve (Gas Flow)		44.1	CFM
Air Density (Gas Flow)		0.104	Lbm/ft3
Air Mass Flow (Gas Flow)		4.60	Lbm/min
Pulse Frequency		0.00	Hz
Temperature into Blade		207.3	oF
Temperature out of Blade		288.7	oF
Specific Heat		0.242	BTU/LboF
Cooling Heat Transfer		2.05	BTU/min
Temperature Gas In		831.0	oF
Temperature, Gas Out		777.7	oF
Specific Heat		0.257	BTU/LboF
Gas Heat Loss		62.91	BTU/min
Thermal Effectiveness		13.1	%

Run Number	13		
Data Point			Description
11	6.39	PSI	Pressure,Orifice, Hot Side
10	0.19	PSI	Pressure,Orifice,Cooling
9	88.1	oF	Temperature,Ambient
8	73.2	oF	Temperature,Orifice,Cooling
7	207.3	oF	Temperature,Cooling,In
6	288.7	oF	Temperature,Cooling,Out
5	82.5	oF	Temperature,Orifice,Gas
4	831	oF	Temperature,Gas,In
3	777.7	oF	Temperature,Gas,Out
2	82.1	oF	Temperature,Air Supply
1	303.8	oF	Temperature,Cooling,Control
Time	1655		
Date	61		
Pulse Rate	0	Hz	
Barometer	29.58	in Hg	
Orifice,Cool	2.00	in H2O	
Orifice, Gas	1.00	in H2O	

APPENDIX C

CALCULATION OF BSFC

Calculation of Engine Brake Specific Fuel Consumption as a Function of 1st Stage Turbine Cooling Air

HP	% POWER	SPEED	% BLEED	lb/sec	BSFC
1500	100	22500	3.00	0.456	0.4766
1500	100	22500	2.80	0.432	0.4754
1500	100	22500	2.60	0.409	0.4742
1500	100	22500	2.40	0.386	0.4730
1500	100	22500	2.20	0.362	0.4717
1500	100	22500	2.00	0.339	0.4706

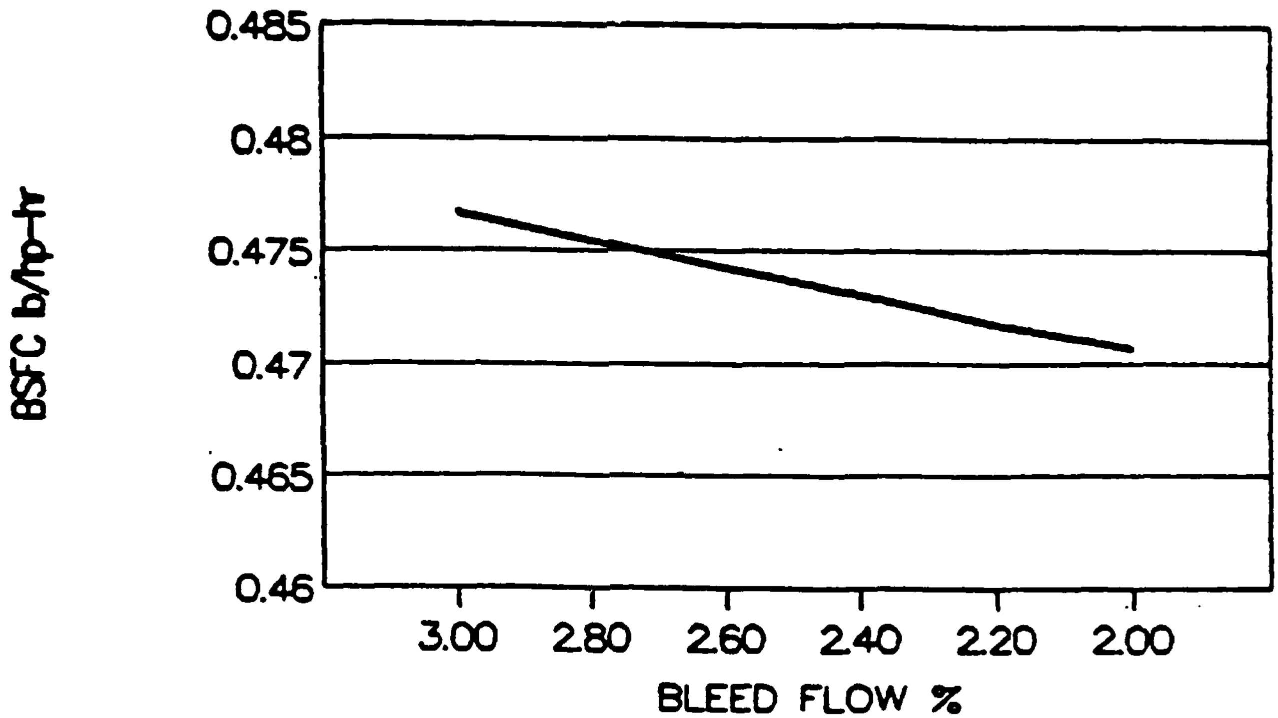

Figure C-1, BSFC vs Bleed Flow

100% Power

APPENDIX D

DERIVATION OF THE VELOCITY OF PROPAGATION OF THE FINITE WAVE

From the continuity equation,

$$\rho_1 \omega A = \rho_2(\omega - v_2)A \qquad (33)$$

The duct is straight and has a constant cross section, A. The effects of wall friction are neglected.

The momentum equation is

$$P_1 + \rho_1 \omega^2 = P_2 + \rho_2(\omega - v_2)^2 \qquad (34)$$

Using the continuity equation to eliminate (w-v2)

$$P_1 + \rho_1 \omega^2 = P_2 + \rho_2 \left(\frac{\rho_1 \omega}{P_2}\right)^2 \qquad (35)$$

$$\omega = \sqrt{\frac{P_2}{\rho_1}\left(\frac{P_2 - P_1}{\rho_2 - \rho_1}\right)} \qquad (36)$$

$$\omega = \sqrt{\frac{P_2}{\rho_1}\left(\frac{\Delta P}{\Delta \rho}\right)} \qquad (37)$$

$$\omega = \sqrt{\frac{P_1}{\rho_1}\left(\frac{\frac{P_2}{P_1} - 1}{1 - P_1/P_2}\right)} \qquad (38)$$

ΔP and $\Delta \rho$ denote changes due to the pressure wave.

It can be seen that the velocity of the compression wave depends on both the state of the fluid and the strength of the wave (ΔP, $\Delta \rho$)

An assumption must be made of the thermodynamic process to go any further with this equation (isothermal, adiabatic, etc).

By assuming an adiabatic process

$$h_2 + \frac{v_2^2}{2} = h_1 + \frac{v_1^2}{2} \tag{39}$$

then

$$\frac{\omega^2}{2} + h_1 = \frac{(\omega - v_2)^2}{2} + h_2 \tag{40}$$

If the fluid is considered an ideal gas

If the fluid is considered an ideal gas

$$h = \left(\frac{k}{k-1}\right)\frac{P}{\rho} \tag{41}$$

then

$$\frac{\omega^2}{2} + \frac{k}{k-1}\left(\frac{P_1}{\rho_1}\right) = \frac{(\omega - v_2)^2}{2} + \left(\frac{k}{k+1}\right)\frac{P_2}{\rho_2} \tag{42}$$

Again using continuity to eliminate w-v2

$$\omega^2 + \frac{2k}{k-1}\left(\frac{P_1}{\rho_1}\right) = \omega^2\left(\frac{\rho_1}{\rho_2}\right)^2 + \left(2k/k-1\right)\left(\frac{P_2}{P_1}\right)\left(\frac{P_1}{\rho_1}\right)\left(\frac{\rho_1}{\rho_2}\right) \tag{43}$$

$$\omega^2 = \frac{k-1}{2}\left(\frac{P_1}{\rho_1}\right) + \frac{k+1}{2}\left(\frac{P_1}{\rho_1}\right)\left(\frac{P_2}{P_1}\right) \tag{44}$$

This gives the propagation of a finite wave with strength P2/P1 into an ideal gas at rest with properties P1 and

This can be related to the velocity of the infinitely small disturbance commonly called "acoustic velocity" or "speed of sound".

As shown,

$$\omega = \sqrt{\frac{P_2}{\rho_1}\left(\frac{\Delta P}{\Delta \rho}\right)} \qquad (45)$$

for the infinitely small disturbance,

$$c = \lim_{\substack{P_2 \Rightarrow P_1 \\ \rho_2 \Rightarrow \rho_1}} \omega \qquad (46)$$

$$c = \lim_{\substack{\Delta P \Rightarrow 0 \\ \Delta \rho \Rightarrow 0}} \sqrt{\frac{\rho_2}{\rho_1}\left(\frac{\Delta P}{\Delta \rho}\right)} \qquad (47)$$

$$c = \sqrt{\frac{dP}{d\rho}} \qquad (48)$$

Since the pressure of a gas is dependent on two other properties, the derivative dP/d is meaningless unless the thermodynamic path is known. Experiments with air have shown that the process is closer to isentropic than isothermal, probably because of the speed that the wave propogates. (46)

$$c = \sqrt{\left(\frac{dP}{d\rho}\right)_S} = \sqrt{k\left(\frac{dP}{d\rho}\right)_T} \qquad (49)$$

For an ideal gas, P= RT

$$c = \sqrt{kRT} = \sqrt{\frac{kP}{\rho}} \qquad (5Ø)$$

We can now show the relationship between the finite wave and the speed of the infinitely small wave under the same fluid conditions.

$$\omega^2 = \frac{k-1}{2}\left(\frac{P_1}{\rho_1}\right) + \frac{k+1}{2}\left(\frac{P_1}{\rho_1}\right)\left(\frac{P_2}{\rho_1}\right) \qquad (51)$$

$$c_1^2 = k\frac{P_1}{\rho_1} \qquad (52)$$

$$\frac{\omega}{c_1} = \sqrt{\frac{k-1}{2k} + \frac{k+1}{2k}\left(\frac{P_2}{P_1}\right)} \qquad (53)$$

It is evident that as $P2/P1 \rightarrow 1$, $w/c1 \rightarrow 1$

List of Abbreviations, Acronyms, and Symbols

q	Heat Flux, BTU/hr
h	Convective Heat Transfer Coefficient BTU/hr-sq ft-°F
A	Area, sq ft
G	Mass Flux, lbm/sec-sq ft
T	Temperature, °F
DT	Temperature Difference, °F
k	Conduction Heat Transfer Coefficient BTU/hr-ft-°F
ρ	Density, lbm/cu ft
c_p	Specific Heat at Constant Pressure BTU/lbm-°F
E_h	Mechanical Diffusivity, cu ft/hr
α	Thermal Diffusivity, $k/\rho c_p$
f	Frequency, Hz
P	Pressure, lbf/ sq ft
l,L,D	Length, ft
V	Mean Fluid Velocity, ft/sec
μ	Viscosity, lbf/sec-ft
β	Temperature Coefficient of Volume Expansion
Str	Strouhal Number, fl/V
Re	Reynolds Number, $\rho dV/\mu$
Nu	Nusselt Number, hD/k
Pr	Prandtl Number, $c_p \cdot \mu/k$
St	Stanton Number, $h/c_p \cdot V \cdot \rho$
Gr	Grashof Number, $D^3 \beta g \Delta t \rho^2/\mu^2$

BSFC	Brake Specific Fuel Consumption, lb/HP-hr

Subscripts

b	bulk
w	wall
f	film

DISTRIBUTION LIST

	Copies
Commander Defense Technical Information Center Bldg 5, Cameron Station ATTN: DDAC Alexandria, VA 22304-9990	12
Manager Defense Logistics Studies Information Exchange ATTN: AMXMC-D Fort Lee, VA 23801-6044	2
Commander U.S. Army Tank-Automotive Command ATTN: ASQNC-TAC-DIT (Technical Library) Bldg 203 Warren, MI 48397-5000	2
Commander U.S. Army Tank-Automotive Command ATTN: AMSTA-CF (Dr. K. Oscar) Warren, MI 48397-5000	1
Director U.S. Army Materiel Systems Analysis Activity ATTN: AMXSY-MP (Mr. Cohen) Aberdeen Proving Ground, MD 21005-5071	1